Université de Paris – École doctorale de sciences mathématiques de Paris centre (ED 386)

Mémoire d'habilitation à diriger des recherches

Spécialité Informatique

Maps: At the interface between Combinatorics and Probability.

Mémoire d'habilitation à diriger des recherches présenté et soutenu publiquement par

Marie Albenque

le 16 décembre 2020

Rapporteuses et rapporteur :

Valérie Berthé,	CNRS – Université de Paris
Mireille Bousquet-Mélou,	CNRS – Université de Bordeaux
Jason Miller,	Cambridge University

Jury :

Valérie Berthé,	CNRS – Université de Paris
Mireille Bousquet-Mélou,	CNRS – Université de Bordeaux
Béatrice de Tilière,	Université Paris Dauphine
Bertrand Eynard,	CEA, IHES
Jean-François Marckert,	CNRS – Université de Bordeaux
Grégory Miermont,	ENS Lyon
Jason Miller,	Cambridge University
Cyril Nicaud,	Université Gustave Eiffel.

Remerciements

Je tiens d'abord à remercier chaleureusement Valérie Berthé, Mireille Bousquet-Mélou et Jason Miller qui m'ont fait l'honneur et le plaisir d'accepter d'être les rapporteuses et rapporteur de ce mémoire. Je remercie particulièrement Valérie pour son "coaching" positif et son soutien inconditionnel lors de mes déboires administratifs, Mireille pour m'avoir expliqué avec patience tous les secrets des invariants de Tutte, qui ont joué un rôle fondamental dans les résultats présentés au chapitre 4 et Jason pour m'avoir réconciliée avec la théorie quantique de Liouville lors d'un mini-cours en 2017 particulièrement inspirant.

Je veux également remercier Béatrice de Tilière, Bertrand Eynard, Grégory Miermont, Jean-François Marckert et Cyril Nicaud d'avoir accepté de participer au jury. C'est un privilège d'être aussi bien entourée aujourd'hui, par des collègues dont j'admire les résultats, et que j'ai toujours beaucoup de plaisir à retrouver lors des rencontres qui rythment notre vie scientifique.

Maintenant que je vais être officiellement autorisée à diriger des recherches, il me faut remercier Mathias Lepoutre qui a accepté d'"essuyer les plâtres" et m'a accordé sa confiance avant que ce ne soit le cas! Je n'aurai pas pu rêver meilleur début en encadrement que de partager cette responsabilité avec Vincent Pilaud, qui partage avec brio les casquettes de co-encadrant, de co-enseignant et de collègue toujours disponible.

Tous les travaux de ce mémoire n'auraient pas vu le jour sans ma formidable équipe de collaborateurs et de collaboratrices. Merci à Louigi Addario-Berry, à qui ce mémoire doit beaucoup, qui m'a proposé une collaboration alors que je doutais plus que jamais de ma légitimité. Merci à Jérémie Bouttier, pour sa patience et sa pédagogie lors de nos séances de travail au tableau, je n'ai pas fini d'apprendre à ses côtés. Merci à Eric Fusy, dont l'expertise combinatoire n'a d'égal que sa bienveillance et sa générosité mathématique. Merci à Lucas Gerin, pour le groupe de travail du RER C et toutes nos aventures probabilistes. Merci à Christina Goldschmidt pour son soutien constant, ses explications lumineuses et toutes nos discussions. Merci à Nina Holden et Xin Sun d'avoir relevé avec succès le défi de la collaboration à distance. Merci à Kolja Knauer pour toutes nos discussions mathématiques sur les terrasses de la TU. Merci à Laurent Ménard, pour son expertise maple, pour toutes les journées de travail passées ensemble et pour son optimisme indéfectible qui a fini par triompher ! Merci à Dominique Poulalhon, pour sa capacité redoutable à détecter les buds dans mes constructions combinatoires. Merci à Gilles Schaeffer, pour ses conseils avisés et son intuition combinatoire remarquable.

J'espère avoir encore de nombreuses occasions de travailler avec vous.

A ces collaborateurs directs s'ajoutent de nombreuses personnes qui pimentent et égaient ma vie scientifique. Je pense notamment aux habitué.e.s des journées alea avec une pensée particulière pour Guillaume Chapuy, Brigitte Chauvin, Sylvie Corteel, Enrica Duchi, Igor Kortchemski, Cécile Mailler et Nicolas Pouyanne. Je pense également aux participants des journées cartes. Last but not least, je remercie tout le groupe de la Barbade, avec qui les séances de problèmes ouverts sont une aventure. Merci à Omer Angel, Anna Ben Hamou, Nicolas Broutin, Luc Devroye, Vida Dujmovic, Gabor Lugosi et Ralph Neininger.

Je remercie chaleureusement mes collègues du laboratoire et du département d'informatique de l'École Polytechnique qui m'ont accueillie depuis mon recrutement au CNRS. Merci en particulier aux membres de l'équipe combinatoire et à Jean-Christophe Filliâtre dont l'exigence pédagogique est

un modèle. Je n'oublie pas les équipes administratives, qui s'efforcent de lisser toutes les difficultés administratives, malgré le contexte de plus en plus difficile.

Difficile de remercier nommément tous les amies et amis qui m'entourent au quotien. Mais je ne peux pas ne pas mentionner Laura, Juliette, Laure, Nadaya, Christine et Tali. Toutes ces femmes fortes sont un exemple !

Merci à toute à ma famille: mon père, mes soeurs et mon frère et la tribu de neveux et nièces, sans cesse plus nombreux! Merci à Swann et Anna, qui s'étonnent toujours que je sois une scientifique sans microscope dans son bureau, mais sont mes plus fidèles admirateurs. Merci à Julien, qui m'accompagne par monts et par vaux, par beau temps et tempête, et rend le chemin infiniment plus chouette!

À Florence,
À ma mère,
À minouche,

Contents

List of publications

Here is a complete list of publications. For convenience, I removed these publications from the general bibliography and used arabic citations to cite them, whereas I used classical citations such as [FS09] for the general bibliography.

Publications obtained after my PhD

[14] Bivariate rationality of the generating series of maps in higher genus. Chapter 2
M. Albenque and M. Lepoutre. `arXiv:2007.07692`, 2020.

[13] Scaling limit of large triangulations of polygons. Chapter 3
M. Albenque, N. Holden and X. Sun. *Electronic Journal of Probability*, 25 : 1 – 43, 2020.

[12] Convergence of odd-angulations via symmetrization of labeled trees. Chapter 3
L.Addario-Berry and M. Albenque. `arXiv:1904.04786`, accepted in *Annales Henri Lebesgue*.

[11] Local convergence of large random triangulations coupled with an Ising model. Chapter 4
M. Albenque, L.Ménard and G.Schaeffer. `arXiv:1812.03140`, accepted in *Transactions of the American Mathematical Society*, 2020.

[10] Scaling limit for simple random triangulations and quadrangulations. Chapter 3
L.Addario-Berry and M. Albenque. *Annals of Probability*, 45.5 : 2767–2825, 2017.

[9] The Brownian continuum random tree as the unique solution to a fixed-point equation. /
M. Albenque and C.Goldschmidt. *Electronic Communications in Probability*, 20.61 : 1-14, 2015.

[8] Convexity in partial cubes: the hull number. /
M. Albenque and K. Knauer. Discrete Mathematics, 39:2 : 866–876, 2016.

[7] Generic method for bijections between blossoming trees and planar maps. Chapter 2
M. Albenque and D.Poulalhon. *Electronic Journal of Combinatorics*, 22.2, P2.38, 2015.

[6] On symmetric quadrangulations and triangulations. /
M. Albenque, É.Fusy and D.Poulalhon. *European Journal of Combinatorics*, 35 : 13 – 31, 2014.

[5] On the algebraic numbers computable by some generalized Ehrenfest urns. /
M. Albenque and L.Gerin. *Discrete Mathematics and Theoretical Computer Science*, 14.2 : 271 – 284, 2012.

[4] Constellations and multicontinued fractions: application to Eulerian triangulations. Chapter 4
M. Albenque and J.Bouttier. Proceedings of *FPSAC'12*. DMTCS Proceedings, vol.AR : 805 – 816, 2012.

Short versions of [6] and [8] appear respectively in the proceedings of the conferences Eurocomb 2011 and Latin 2014.

Publications obtained during my PhD.

[3] A note on the enumeration of directed animals via gas considerations. /
M. Albenque. *Annals of Applied Probability*, 19:1860 –1 979, 2009.

[2] Growth function for a class of monoid. /
M. Albenque and Ph. Nadeau. Proceedings of *FPSAC'09*. DMTCS Proceedings : 25 – 38, 2009.

[1] Some families of increasing planar maps. /
M. Albenque and J.-F. Marckert. *Electronic Journal of Probability*, 13 : 1624 – 1671, 2008.

A short version of [2] appears in the proceedings of the conference Eurocomb 2007.

Introduction

I present in this habilitation a part of the results I obtained since my PhD Thesis. While focusing on planar maps, that are planar graphs embedded in the sphere, my research lies in the realm of combinatorics and probability theory. On the combinatorics side, I enumerate families of maps either "plain ones" or enriched with a statistical physics model (such as the Ising model). On the probabilistic side, I study the behavior of large random maps, either sampled uniformly from a given family, or sampled with a probability distribution given by a statistical physics model. Of course, these two sides have some strong connections: a good understanding of the combinatorics of maps is a necessary first step in the study of random maps but reciprocally universality results established for families of random maps and for their limits give some combinatorial corollaries. I hope that this survey of my work will be a convincing illustration of this general principle.

After an introduction presenting my main results, this document is structured in four chapters. Chapter 1 gathers some general terminology and presents Tutte's method for enumerating maps as well as the general theory of orientations as developed independently by Propp and Felsner. Chapter 2 is devoted to the presentation of bijections between blossoming trees and maps. Chapter 3 focuses on the scaling limit of maps sampled from a uniform distribution, and which are shown to converge either to the Brownian map or to the Brownian disk. Lastly, I present in Chapter 4 some results about maps "with matter", and discuss some aspects of their enumerative properties and of their local limit. Except for the notions presented in Chapter 1, each chapter is self-contained.

The exposition is intentionally informal: proofs are sketched at best. I focus on intuitions and ideas underlying the proofs and refer any interested reader to the publications for details. To keep this habilitation consistent and reasonably short, I chose to include only works related to maps in this document. I present very briefly at the end of this introduction my other works. The numbering of theorems cited in this introduction coincides with their numbering in the main body of the document.

Chapter 2: Around blossoming bijections [7], [14]

Joint works with Mathias Lepoutre (LIX, École Polytechnique) and Dominique Poulalhon (IRIF, Paris)

The study of planar maps was initiated by Tutte in the sixties, who obtained in a remarkable series of articles [Tut62b, Tut62a, Tut63] some closed enumerative formulae for different families of planar maps (triangulations, quadrangulations, general maps,...). The particularly simple form of those formulae was quite striking given that the methodology developed by Tutte (and presented in Section 1.2) is technical and does not give any *a priori* explanation for this simplicity. It was the beginning of the (unended) quest for combinatorial explanations and bijective proofs !

The first bijection between planar maps and some trees (which gives as an immediate enumerative corollary one of Tutte's formulae) was obtained by Cori and Vauquelin in [CV81]. But, the real breakthrough came with major results obtained by Schaeffer [Sch97, Sch98] who obtained different families of bijections between planar maps and some decorated trees.

I focus for now on the results obtained in [Sch97] (and will come back to [Sch98], and the differences between the two approaches in the next section). In this work, Schaeffer obtained a bijection between planar maps and a family of trees, which he named *blossoming trees*. These trees

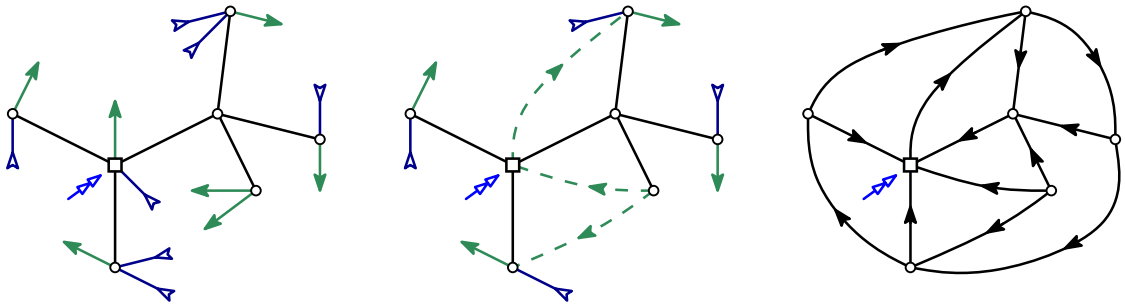

(a) A blossoming tree, (b) some matching of its stems, (c) and the corresponding map

Figure 1. From a blossoming tree to a planar map. Opening stems are represented by plain green arrows, and closing stems by reverse blue arrows.

carry some decorations – called opening stems and closing stems – that can be matched as in a parenthesis word. The tree together with the matching of its stems corresponds naturally to a planar map as illustrated in Figure 1.

Following the work of Schaeffer, other "bossoming bijections" were obtained for different models of maps, for instance in [BDFG02a], [BMS02], [Ber07] and [PS06]. Even if they rely on ad-hoc proofs, all these bijections present some strong similarities, which suggests that there is a hidden structure underneath. In [7], together with Dominique Poulalhon, we obtain a very general bijective scheme, which both enables to obtain many previous constructions as special cases and also *new blossoming bijections*. In particular, it yields a new and unified proof of *all the bijections cited above*. Let me note that this work is complementary to previous similar results obtained by Bernardi and Fusy in [BF12a, BF12b]. It captures different bijections and yields different new bijections.

The generic framework is stated in Theorem 2.2.4. For illustration purposes, I give here one of the new bijection obtained:

Theorem 2.2.7 (*Theorems 5.6 and 6.5 of [7]*)

Fix $d \geq 3$, and let $M_{d;n}$ be the family of d-angulations with n vertices and of girth d (i.e. without cycles shorter than d). Then there exists an explicit bijection between $M_{d;n}$ and a family of blossoming forests with n vertices (easy to describe and to enumerate).

Moreover, the blossoming forest associated to a d-angulation can be computed in linear time.

With these generic bijective schemes, blossoming bijections for planar maps are now well-understood. However, before the PhD thesis of my student Mathias Lepoutre, the situation was much different for maps of genus g (which are maps embedded on a torus with g holes). Apart for one result in genus 1 (see [DGL17]) there was no blossoming bijection available. Yet, enumerative results similar to those of Tutte were also obtained for maps of genus g, see [BC86, BC91]. In the latter article, Bender and Canfield obtained closed formulas for the generating series of maps of genus 1, 2 and 3. But, more importantly, they exhibited a *rationality scheme*; they proved that there exists a function T such that, for any fixed g, the generating series of maps of genus g can be expressed as a rational function of T, see Theorem 2.3.1.

In [CMS09], a (non-blossoming) bijection was obtained for maps of genus g, which unfortunately did not give a combinatorial proof of the rationality scheme obtained in [BC91], but only of a weaker version of it. During his PhD, Lepoutre managed to both *extend Schaeffer's blossoming bijection to any genus* and *give the first combinatorial explanation for the rationality scheme* of Bender and Canfield in [Lep19].

In [BCR93], Bender, Canfield and Richmond obtained a refined rationality scheme, which tackles the enumeration of maps with respect to both their number of faces and of vertices. This result was still lacking a combinatorial proof and with the approach developed in [CMS09], this bivariate

enumeration of maps was out of reach. In the joint work [14] with Lepoutre, we obtained the *first bijective proof* of it, thus answering a question opened for more than 25 years:

Theorem 2.3.2 (*[BCR93], bijective proof in [14]*)

For any fixed $g \geq 1$, let $M_g(z_\bullet, z_\circ)$ be the generating series of rooted maps of genus g enumerated by vertices (by the variable $z_\bullet$) and faces (by the variable $z_\circ$).

Define $T_\bullet(z_\bullet, z_\circ)$ and $T_\circ(z_\bullet, z_\circ)$ as the unique formal power series defined by $T_\bullet = z_\bullet + T_\bullet^2 + 2T_\circ T_\bullet$ and $T_\circ = z_\circ + T_\circ^2 + 2T_\circ T_\bullet$. Then, $M_g(z_\bullet, z_\circ)$ is a rational function of $T_\bullet$ and $T_\circ$.

Chapter 3: Scaling limit of random planar maps

Joint works with Louigi Addario-Berry (McGill University, Montréal), Nina Holden (ETH, Zürich) and Xin Sun (Columbia University, New York)

In 2013, Miermont [Mie13] and Le Gall [LG13] proved that the scaling limit of quadrangulations is the Brownian map after 15 years of research punctuated by many major results, see [CS04, MM06, LGP08, Mie08b, LG10]. In his article, Le Gall also studied the scaling limit of triangulations and of p-angulations for $p \in 2\mathbb{N}$. He raised two open problems: to extend this result first to p-angulations for odd values of p and secondly, to triangulations without loops nor multiple edges (also called simple triangulations[1]). With Louigi Addario-Berry, we answered both these problems in the respective publications [12] and [10].

I start with the publication [10] dealing with simple triangulations. To explain the main difficulty in extending Miermont and Le Gall's result, I give first a brief description of existing bijections for planar maps. In his two pioneering works [Sch97, Sch98], Schaeffer introduced two paradigms to obtain bijections between maps and decorated trees (see the discussion in [Sch15] for a recent account on this topic):

- In [Sch97], he introduced blossoming bijections that I already described at length in the previous section. However, I want to emphasize here, that blossoming bijections turn out to be particularly well-suited when studying maps with connectivity constraints. By that, I mean for instance maps with a lower bound on their girth (i.e. the length of their shortest cycle). And, for simple triangulations (which are triangulations with girth at least 3) such a bijection was indeed obtained by Poulalhon and Schaeffer in [PS06].
- In [Sch98], Schaeffer exhibited a bijection between quadrangulations and some labeled trees (I present it in details in Section 3.1.3). One of the key features of this bijection is that the labels in the tree encode some distances in the associated quadrangulation. Both the results of Miermont and Le Gall rely deeply on this bijection and on this metric property.
  This bijection was successfully extended to other families of maps (including p-angulations for any value of p) by Bouttier, Di Francesco and Guitter in [BDFG04] and to other models, see [Mie09, AB13, BFG14]. The trees obtained in the latter works are colored in black and white, hence they were named *mobiles* after Calder's famous mobiles. By extension, all these bijections are called *mobile-type* bijections. They are especially well-suited to study maps with faces of fixed degree. However, until now there exists no example of a mobile-type bijection for a family of maps with connectivity constraints.

The absence of a bijection with nice metric properties for simple triangulations was hence the main challenge to face. Our main contribution in [10] is to prove that in fact the *blossoming bijection of [PS06] encodes some distance information*. Indeed, a simple functional of the blossoming tree gives an approximation of some metric properties up to an error which turns out to be negligible in the scaling limit. The proof of this result interlaces some combinatorial arguments together with some probabilistic limit theorems. This was an (unexpected) major development, which was key in the proof of the following main result of [10]:

[1] The motivation behind the study of this particular model is briefly described in Section 3.1.5.

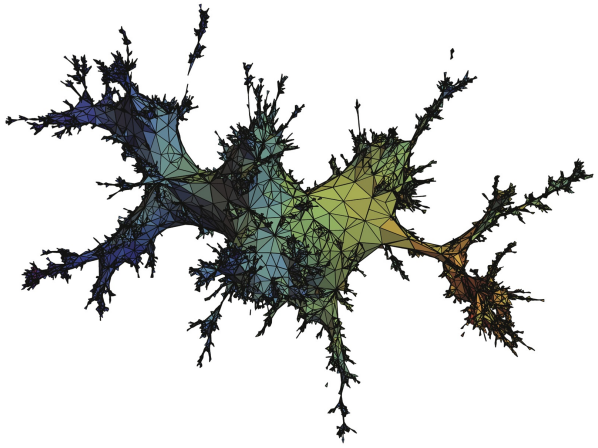

Figure 2. A simulation by Igor Kortchemski of a large random simple triangulation, which gives an approximation of the Brownian map.

Theorem 3.2.1 (*Theorem 1 of [10]*)

For $n \geq 3$, let M_n be a uniformly random simple rooted triangulation with n vertices. Then, as $n \to \infty$, we have:

$$\left(V(M_n), \left(\frac{3}{4n}\right)^{1/4} \mathrm{dist}_{M_n}\right) \xrightarrow{(\mathrm{d})} (M, d^*),$$

for the Gromov–Hausdorff distance, where (M, d^*) is the Brownian map (see Figure 2).

This idea that *blossoming bijections can track distances* is not yet understood to its full extent. However, our result for simple triangulations has already been extended to other models of maps, see [BCF14, BHL19]. In [13], in a joint work with Nina Holden and Xin Sun, we also use this paradigm to establish the convergence of simple triangulations and loopless triangulations with a boundary as stated in Theorem 3.4.2. The latter result is one of the many steps on which relies the recent major breakthrough of Holden and Sun [HS19]. In this paper, they proved that the Cardy embedding of loopless random triangulations converges to the Liouville Quantum Gravity, see Section 3.1.5.

To obtain the main result of [12] about the scaling limit of p-angulations, our strategy was less of a surprise. Indeed, in this case, the Bouttier-Di Francesco-Guitter bijection was available. But, when applied to p-angulations for odd values of p, it yields some labeled multitype trees, whose scaling limit was not understood (even if some partial results were available in [Mie06, Mie08a]). With Addario-Berry, we designed a general *bootstrapping principle*, which allows us to *get rid of a regularity assumption*, on which rely most results about scaling limit of labeled trees. This allows us to obtain the scaling limit of the aforementioned trees, and then the following answer to Le Gall's question:

Theorem 3.3.1

Let $p \geq 5$ be an odd *integer and let (M_n) be a sequence of random maps, such that for any $n \geq 1$, M_n is a uniform p-angulation with n vertices. Then, there exists a constant C_p such that, as n goes to infinity,*

$$\left(V(M_n), \left(\frac{C_p}{n}\right)^{1/4} \mathrm{dist}_{M_n}\right) \xrightarrow{(\mathrm{d})} (M, d^*),$$

for the Gromov–Hausdorff topology and where (M, d^*) is the Brownian map.

Chapter 4: Random triangulations with matter

Joint works with Jérémie Bouttier (IPhT, Saclay), Laurent Ménard (Modal'X, Nanterre) and Gilles Schaeffer (LIX, École Polytechnique)

In this last chapter, the changes in my point of view are twofold. First, I study *local limits* of maps rather than scaling limits as was the case in the previous chapter. Secondly, and more importantly, I consider random maps that are not sampled uniformly from a given family but are sampled with a distribution biased by the weight of an Ising configuration, a typical statistical physics model.

The study of the Ising model on random maps is strongly related to the enumeration of Eulerian maps. In [4], together with Jérémie Bouttier, we studied the combinatorics of Eulerian maps, via the approach of "slices" introduced in [BG12]. We first obtained a combinatorial proof of the generating series of Eulerian triangulations with two marked vertices at a fixed distance (the so-called *2-point function*). Then, we generalized previous results obtained in [BG12] and proved that the 2-point function of planar constellations can be expressed as a quotient of some Hankel determinants. In the case of Eulerian triangulations, we were able to compute these determinants by a bijective proof. For other models of constellations, some enumeration formulas were guessed by Di Francesco [DF05] and it is still an open problem to find bijective proofs of these formulas.

In [11], together with Laurent Ménard and Gilles Schaeffer, we study the local limit of large random triangulations endowed with an Ising configuration and sampled with a weight given by the energy of this configuration. In a more combinatorial setting, it boils down to coloring the vertices of the triangulation in black and white and the weight of the configuration is given by a function (indexed by a parameter ν) of the number of monochromatic edges in this coloring.

The first local limit result for random maps was obtained in the setting of uniform triangulations by Angel and Schramm in the pioneering work [AS03]. Their result relies strongly on the fact that, since the early work of Tutte, many closed enumerative formulas are available for triangulations. However, this is not anymore the case for triangulations with an Ising configuration. The first step in our proof is to extend and refine the deep combinatorial results obtained by Bernardi and Bousquet-Mélou in [BBM11] by a computational *tour de force*. The proof of this extension, stated in Theorem 4.2.1, relies on some elaborate and technical machinery, on some subtle inductive steps and as well as on combinatorial interpretation of a rational parametrization obtained in [BBM11].

Then, some results with a more probabilistic flavor, such as the *tightness of the root degree*, are needed to obtain the main result of this work, which is the following theorem:

Theorem 4.1.2

For any $\nu > 0$ and $n \geq 0$, denote by $\mathbb{P}_n^\nu$ the probability distribution supported on the set of triangulations with $3n$ edges and induced by the energy an Ising configuration with parameter ν. Then, for any $\nu > 0$, there exists a probability distribution $\mathbb{P}_\infty^\nu$ supported on infinite one-ended triangulations endowed with a spin configuration, such that:

$$\mathbb{P}_n^\nu \xrightarrow{(\mathrm{d})} \mathbb{P}_\infty^\nu, \text{ for the local topology.}$$

We call a random triangulation distributed according to this limiting law the Infinite Ising Planar Triangulation with parameter ν *or* ν-IIPT.

This result opens a large and promising area of research: indeed, a lot remains to be understood about the ν-IIPT. Natural questions include the typical size of the *clusters* (i.e. the monochromatic connected components) and of their boundary, and the volume of the balls of fixed radius in the ν-IIPT. All these quantities are expected to depend drastically on the value of ν. It has indeed been known since [BK87], that there exists a critical value of ν at $1 + 1/\sqrt{7}$, where this model exhibits a phase transition.

Angel proved in [Ang03] that the volume of balls of radius R in the local limit of uniform triangulations is of order R^4. Today, one of the major open problems in this field is to extend this

result to the local limit of maps endowed with a (critical) statistical physics model, and the ν-IIPT when ν is critical provides a perfectly typical example of such a model. Even if this kind of result seems out of reach for the moment, by proving that this limiting object does exist, our work is a first essential step, which I hope will be followed by many others.

Other works: [5], [6], [8] and [9]

These four articles do not my belong to my main area of research and I present them only briefly here:

- In [5], together with Lucas Gerin, we study a urn model, which appears naturally in a problem of distributed computing. We rely on some combinatorial arguments and on approximations based on stochastic diffusions to give a characterization of the numbers which are "computable" in this framework.
- In [6], together with Éric Fusy and Dominique Poulalhon, we study families of planar maps which admit non trivial automorphisms. We introduce a new "quotienting" operation, which enables to give a new bijective proof of the enumeration formulae for simple triangulations and quadrangulations.
- In [8], together with Kolja Knauer, we prove that the combinatorial optimization problem of determining the hull number of a partial cube is NP-complete, improving earlier results in the literature. We also provide a polynomial-time algorithm to determine the hull number of planar partial cube quadrangulations.
- In [9], together with Christina Goldschmidt, we provide a new characterization of Aldous' Brownian continuum random tree (defined in Section 3.1.2) as the unique fixed point of a certain natural operation on continuum trees (which gives rise to a recursive distributional equation). We also show that this fixed point is attractive.

Chapter 1

Maps and Orientations

In this chapter, I present some definitions and results about enumerative properties of maps and orientations.

Section 1.1 I gather general terminology about planar maps and define classical families of maps, as well as some standard constructions.

Section 1.2 The modern study of maps started with the work of Tutte in the 60's, who proved particularly nice closed enumerative formulas for many families of maps. I present in this section his method on the archetype example of quadrangulations with a boundary.

Section 1.3 and 1.4 Since orientations of maps have appeared to be a guiding thread of most of my research activity in the last years, I give a succinct presentation of the general theory due to Propp [Pro02] and Felsner [Fel04]. This is the purpose of Section 1.3. To illustrate the variety of combinatorial structures encapsulated by this framework, I present in Section 1.4 some particular cases of interest. Most of these examples reappear later in this document.

1.1 Planar maps

1.1.1 Definition of planar maps

Vertices, edges, faces and Euler's formula. A *planar map* is a proper embedding of a connected (planar) graph in the sphere, where *proper* means that edges are smooth simple arcs which meet only at their endpoints. Two planar maps are identified if they can be mapped one onto another by a homeomorphism that preserves the orientation of the sphere. I emphasize that different embeddings of the same planar graph can yield different maps, see Figure 1.1.

Edges and *vertices* of a map are the natural counterparts of edges and vertices of the underlying graph. The *faces* of a map are the connected components of the complement of the embedded graph. The sets of vertices, edges and faces of M are respectively denoted by $V(M)$, $E(M)$ and $F(M)$. Euler's formula states that the number of edges, faces and vertices of a planar map are linked by the following relation:

$$|V(M)| + |F(M)| = 2 + |E(M)|. \tag{1.1}$$

A planar map is usually represented in the plane via a stereographic projection, by distinguishing an *outer infinite face*, see Figure 1.1.

We can also consider embeddings of graphs on surfaces other than the sphere, such as surfaces of higher genus or even non-orientable surfaces. I will only consider maps of higher genus in Section 2.2.1 and so, unless explicitly mentioned, all maps considered in the following are assumed to be planar.

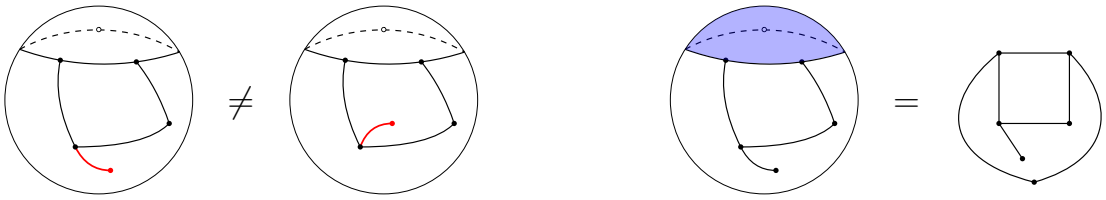

Figure 1.1. (Left) Two different embeddings of the same planar graph. (Right) The equivalence between an embedding on the sphere with a marked face (represented in blue) and an embedding on the plane.

Corners and degree The embedding fixes the cyclical order of edges around each vertex, which defines readily a *corner* as a couple of consecutive edges around a vertex. Corners may also be viewed as incidences between vertices and faces. The *degree* of a vertex or a face is defined as the number of its corners. In other words, it counts incident edges, with multiplicity 2 for each loop (in the case of vertex degree) or for each bridge (in the case of face degree). The set of corners of M is denoted by $C(M)$.

An equivalent definition of maps via gluing of polygons Let me now give another (equivalent and more combinatorial) definition of planar maps, see also [LZ04, Section 1.3]. A *cellular decomposition* of the sphere is a decomposition of the sphere as a family of polygons glued along their sides. More precisely, in a cellular decomposition, we are given a family of polygons with labeled sides and a set of pairwise identifications of sides of polygons, such that the resulting surface is homeomorphic to the sphere, see Figure 1.2.

Then, a *planar map* is a cellular decomposition of the sphere, seen up to a relabeling of its edges. The equivalence between this definition and the aforementioned one follows from standard results in topology, see e.g.[MT01].

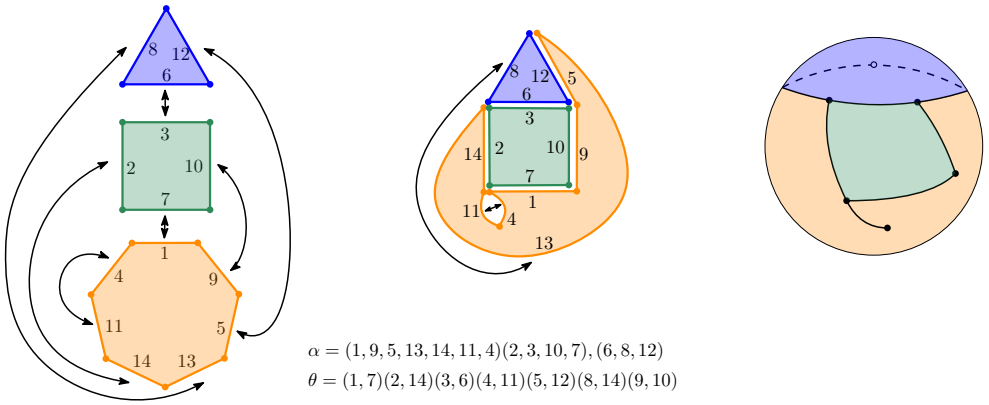

Figure 1.2. An equivalent definition of the map of Figure 1.1 (right) as a gluing of polygons, together with the associated rotation system.

As illustrated on Figure 1.2, a cellular decomposition can naturally be encoded by two permutations. The first one, denoted σ, gives the cyclic ordering of the edges around each polygon (and the cycles of σ are hence in bijection with the polygons). The second one, denoted θ, is a fixed-point-free involution, which gives the matching of the sides of polygons[1]. This point of view will not be used in the rest of the document, but explains why maps have direct links with the algebra of the symmetric group. I refer the interested reader to [Cha18, Chap.2] for a nice introduction on this subject.

[1]Denote by n the total number of sides of the polygons of a cellular decomposition. Then, it is easy to see that the group $\langle \sigma, \theta \rangle$ generated by σ and θ acts transitively on $\{1, \dots, n\}$. Hence, the pair (σ, θ) is a so-called *rotation system*. Conversely, we can define from each rotation system a unique map on an orientable closed surface (which is not necessarily the sphere but might be a torus of genus g for any $g \geq 1$).

1.1.2 Classical terminology

Rooting and pointing To avoid dealing with non-trivial automorphisms of maps, we usually consider *rooted* maps. A rooting consists in the choice of a *root corner* (an equivalent rooting convention frequently used in the literature consists in distinguishing an oriented edge). The root corner will always be represented by a double arrow. The vertex and the face incident to the root corner are respectively called the *root vertex* and the *root face*, and the *root edge* is the edge that follows the root corner in clockwise order around the root vertex. The root corner and the root vertex of a rooted planar map M will be denoted respectively by ξ_M and ρ_M. The subset of vertices not incident to the root face will be denoted by $\mathring{V}(M)$

In the planar representation of a rooted planar map, it is customary to choose the root face as the outer face. However, we will sometimes consider rooted planar maps with an additional marked face. In that case, its planar representation is canonically defined with the marked face as the outer face. For this reason, we will define *plane maps*, as maps with a marked outer face.

A *pointed map* is a map with a marked vertex. A *rooted pointed map* $(M, v^\star)$ has hence two distinguished vertices (which may coincide): its marked vertex $v^\star$, and its root vertex.

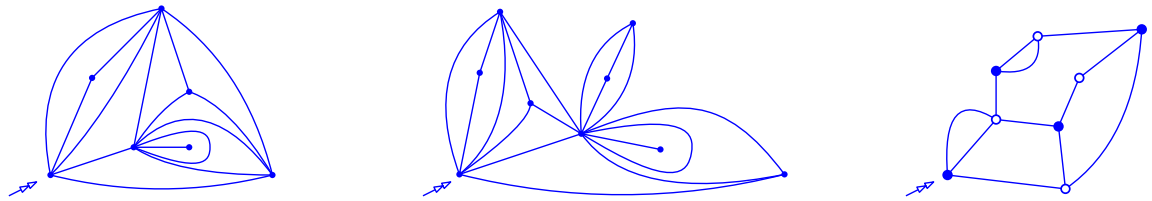

(a) A rooted triangulation

(b) A rooted triangulation with a (non-simple) boundary

(c) A bipartite map

Figure 1.3. Examples of families of maps with constraints.

Some classical families of maps A *plane tree* is a plane map with only one face. Since trees have only one face, there is no distinction between plane trees and planar trees. Note also, that Euler's formula and the definition of planar maps imply immediately that a plane tree is the proper embedding of a connected graph without cycles. Hence, it coincides with the classical graph-theoretical definition of trees.

A map is said to be d-*regular* if all its vertices have degree d. Dually, a map is called a d-*angulation* if all its faces have degree d; the terms *triangulation*, *quadrangulation* and *pentagulation* correspond respectively to the cases where $d = 3, 4, 5$. Next, a d-*angulation with a boundary* is a rooted d-angulation, except that the constraint of face degree is relaxed for its root face, which is allowed to be of arbitrary degree, see Figures 1.3(a) and 1.3(b). A d-*angulation of a* p-*gon* is a d-angulation with a boundary, where we assume additionally that the contour of the boundary is a simple cycle of p edges.

A map is called *Eulerian* (see Section 1.4.2) if all its vertices have even degree. A map is called *bicolorable*, if its faces can be bicolored in black and white, such that every edge separates a black and a white faces. A planar map is Eulerian if and only if it is bicolorable. Note that this equivalence only holds in the *planar case*: in positive genus, some Eulerian maps may not be bicolorable, see also Section 2.2.1. Dually, a map is said to be *bipartite* if its vertices can be partitioned into two subsets B and W such that every edge connects a vertex of B and a vertex of W. It is easy to see that a planar map is bipartite if and only if all its faces have even degree. Again this equivalence only holds for planar maps: in positive genus, a map with only even face degrees may not be bipartite.

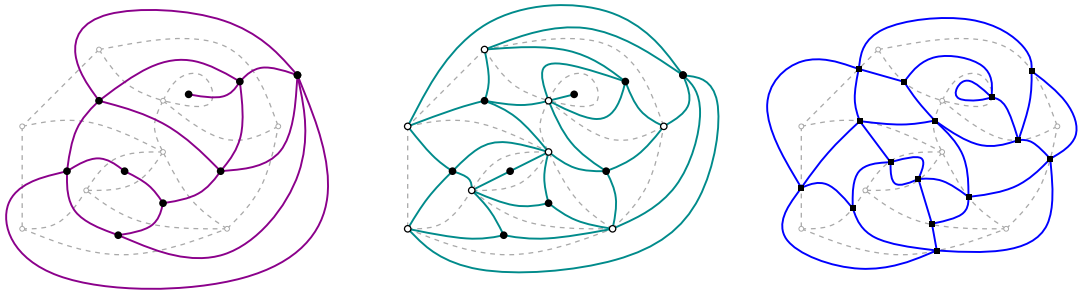

(a) Dualization, (b) quadrangulation, (c) and radialization.

Figure 1.4. Example of classical constructions on a map. The original map is drawn in dashed gray lines with white vertices. Its dual map, quadrangulation and radial map are drawn in plain colored lines.

Simple maps and connectedness In our definition of maps, loops and multiple edges are *a priori* allowed. When loops are forbidden, maps are called *loopless* and when both loops and multiple edges are forbidden, maps are called *simple*. For $d \geq 3$, *irreducible* d-angulations are such that each cycle of length d is the boundary of a face.

The *girth* of a map is the length of one of its shortest cycles. In particular, d-angulations have girth at most d. Note that triangulations of girth 3 and quadrangulations of girth 4 correspond respectively to simple triangulations and simple quadrangulations.

A map is said to be k-*connected*, if at least k vertices have to be removed to disconnect it. Maps are by definition connected, hence 1-connected. We can see that general triangulations, loopless triangulations, simple triangulations and irreducible triangulations correspond respectively to 1, 2, 3 and 4-connected triangulations.

The set of 3-connected planar maps holds special interest since by a theorem of Whitney [Whi33], a 3-connected graph admits a unique planar embedding. Hence, the application that maps a 3-connected graph to its unique planar embedding is clearly a bijection between the set of 3-connected planar graphs and of 3-connected planar maps.

Paths and cycles A *path* is a sequence of directed edges $(e_1, e_2, \dots, e_\ell)$ such that, if we write $e_i = u_i v_i$ for each $i \in \{1, \dots, \ell\}$, then $v_i = u_{i+1}$ for $i \in \{1, \dots, \ell - 1\}$. A *self-avoiding path* is a path in which $u_i \neq u_j$ for $i \neq j$. A *cycle* is a path whose first and last vertices coincide. A *simple cycle* is a self-avoiding path except for its first and last vertices.

1.1.3 Classical constructions for maps

Dualization For a planar map M, its *dual* – denoted $M^\dagger$ – is a planar map, whose vertices correspond to faces of M and faces to vertices of M. Edges are somehow unchanged: each edge e of M corresponds to an edge of $M^\dagger$ that is incident to the same vertices and faces as e, see Figure 1.4(a). Similarly, since a corner in M is an incidence between a vertex and a face, each corner in M corresponds naturally to the corner in $M^\dagger$ incident to the corresponding face and vertex. This gives a canonical way to root $M^\dagger$ if M is rooted.

Tutte's bijection and radialization The following classical and useful construction associates a quadrangulation to each planar map M. Color the vertices of M in white, add a black vertex in each face of M, and for each corner of M, add an edge between the corresponding white and black vertices. This produces a triangulation. Keeping only the edges between black and white vertices leads to a quadrangulation which is called *the quadrangulation* of M, see Figure 1.4(b). This is a bijection between general maps and quadrangulations, called *Tutte's bijection* [Tut63]. The dual map of the quadrangulation of M is called the *radial map* of M, see Figure 1.4(c).

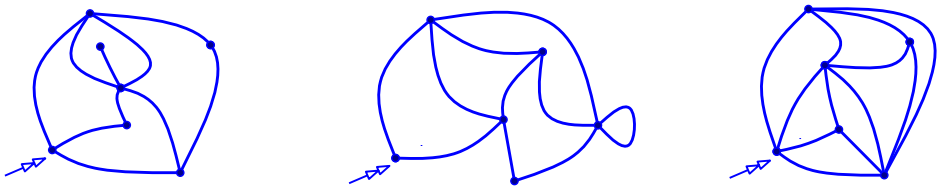

Quadrangulations with n faces

$$\frac{2\cdot 3^n}{(n+1)(n+2)}\binom{2n}{n}$$

general maps with n edges

$$\frac{2\cdot 3^n}{(n+1)(n+2)}\binom{2n}{n}$$

Simple triangulations with $n+2$ vertices

$$\frac{2(4n-3)!}{n!(3n-1)!}$$

Figure 1.5. Illustration of some families of maps, with their enumerative formulae. The fact that quadrangulations with n faces are equinumerous with general maps with n edges, can be explained bijectively by Tutte's bijection [Tut63], defined in Section 1.1.3. A bijective proof of the formula for simple triangulations was given in [PS06], and the corresponding bijection is presented in Section 3.2.

1.2 Enumeration of planar maps via generatingfunctionology

The enumeration of planar maps was initiated in the 60's with the pioneering work of Tutte [Tut62b, Tut63]. To obtain enumeration formulas for planar maps, Tutte translates some combinatorial decompositions into equations satisfied by their generating functions. The equations thus obtained are quite complicated, in particular some additional parameters (known as *catalytic variables*) have usually to be introduced to write them, see below for a concrete example. The work of Tutte is a computational *tour de force*. Indeed, he managed to solve these equations and to obtain closed (and particularly simple) formulas for numerous families of maps. Some examples are given in Figure 1.5. The method he introduced was later generalized and systematized, and the resolution of equations with catalytic variables is still an active area of research, as illustrated for instance by [BMJ06, BM11, BBM11]

To illustrate Tutte's methodology, I will deal with the enumeration of rooted quadrangulations. It turns out that we cannot write directly an equation for the generating series of rooted quadrangulations, but we have to consider instead the more general class $\mathcal{Q}$ of rooted quadrangulations with a boundary. Let us introduce the bivariate generating series $Q(z,x)$ of elements of $\mathcal{Q}$, enumerated by their number of non-root faces and half the degree of their root face (the length of the boundary of an element of $\mathcal{Q}$ is indeed necessarily even). Namely, for $q\in\mathcal{Q}$, let us denote $\mathsf{df}(q)$, the degree of its root face and $|q|$ the number of its non-root faces, then we set:

$$Q(z,x)=\sum_{q\in\mathcal{Q}} z^{|q|}x^{\mathsf{df}(q)/2}=\sum_{p\geq 0}x^pQ_p(z),$$

where $Q_p(z)$ is the (univariate) generating series of quadrangulations with a boundary of length $2p$ enumerated by their number of non-root faces. We adopt the convention that $Q_0=1$, which corresponds to the map reduced to a single vertex. Observe that Q_1 is equal to the generating series of rooted quadrangulations enumerated by their number of faces. Indeed, for q a quadrangulation with a boundary of length 2, if we glue together the two edges of its root face, we obtain a quadrangulation of the sphere with $|q|$ faces, see the figure just below.

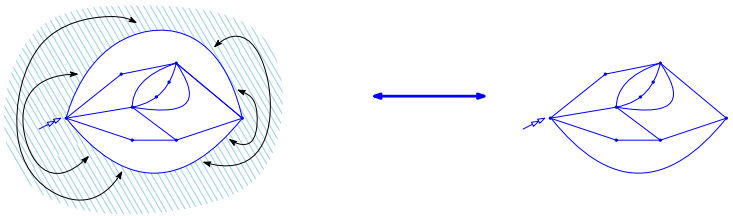

To write an equation for $Q(z,x)$, we want to decompose elements of $\mathcal{Q}$. Fix $q \in \mathcal{Q}$ such that q has at least one edge and consider the deletion of its root edge. Two possibilities can occur, see Figure 1.6:

- Either, the root edge of q is a bridge, and its deletion disconnects q. In that case, we obtain two elements q_1 and q_2 of $\mathcal{Q}$, such that $|q_1| + |q_2| = |q|$, and $\mathsf{df}(q_1) + \mathsf{df}(q_2) = \mathsf{df}(q) - 1$.
- Or, it is not a bridge. Its deletion does not disconnect q, but produces an element $\tilde{q}$ of $\mathcal{Q}$, such that $|\tilde{q}| = |q| - 1$ and $\mathsf{df}(\tilde{q}) = \mathsf{df}(q) + 1$. In particular, the boundary of $\tilde{q}$ has length at least 4.

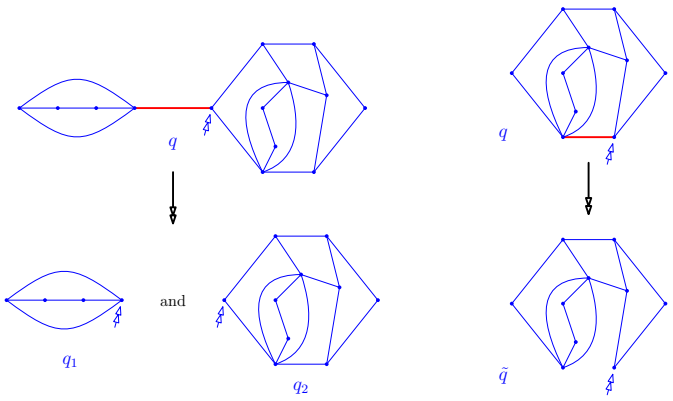

Figure 1.6. Illustration of the two possible cases that can occur when removing the root edge of a quadrangulation with a boundary. On the left, the root edge is a bridge. On the right, it is not.

Since $Q(z,x) - 1 - xQ_1$ is the generating series of quadrangulations with a boundary of length at least 4, this operation can be translated into the following equation for $Q(z,x)$:

$$Q(z,x) = 1 + x\big(Q(z,x)\big)^2 + z\frac{Q(z,x) - 1 - xQ_1(z)}{x}. \tag{1.2}$$

In this equation, we say that the variable x is catalytic, a term first coined by Zeilberger, which traduces the fact that this variable needs to be introduced to write a non-trivial equation.

To solve (1.2), Tutte used a guess-and-check approach and obtained the following rational parametrization of Q_1. Define $T(z)$ to be the unique generating series in z defined by $T(z) = 1 + 3zT(z)^2$ and set:

$$Q_1 = \frac{T(4-T)}{3} \quad \text{and} \quad Q = \frac{1 - T + 3xT^2 - (1 - T + 2xT + xT^2)\sqrt{1-4xT}}{6x^2T^2}.$$

We can check by a simple computation that this is a solution of (1.2). Combined with the fact that $Q(z,x)$ is a power series with nonnegative coefficients, it implies that this indeed gives the expression of the generating series Q and Q_1. From this expression, a direct application of Lagrange's inversion formula (see e.g. [FS09, p.732]) yields the following expression for the number q_n of rooted quadrangulations with n faces (and of the number m_n of rooted general maps with n edges by Tutte's bijection):

$$m_n = q_n = \frac{2}{n+2} \cdot \frac{3^n}{n+1}\binom{2n}{n}, \tag{1.3}$$

For equations with one catalytic variable (and some equations with two catalytic variables, see Chapter 4), we fortunately do not need to guess-and-check anymore! Since the work of Tutte, methods to solve such equations have been developed and systematized, and we refer the interested reader to the survey [BM11] for a thorough and modern presentation of those.

From this computation, it is a priori not clear why the enumeration results should be so simple and in particular why a rational parameterization involving the generating series of some decorated

trees[2] exists. Moreover, similar simple expressions and nice rational parameterizations also exist for many other families of maps. Some bijective explanations have been developed in the last 20 years, and I will present them in both Chapters 2 and 3. I also refer the reader to [Sch15] and references therein for a more exhaustive presentation of the existing literature.

Let me conclude this section by mentioning that the enumeration of maps has also been studied extensively in various fields of mathematics and mathematical physics. I will not discuss them here, but other classical techniques to enumerate maps include matrix integrals, topological recursion and connections with KP-hierarchy (see for instance [LZ04] and [Eyn11]).

1.3 Orientations

I present in this section the lattice structure of orientations. Apart from Definitions 1.3.4 and 1.3.7, the material covered here will not be used in the following. However, since orientations play such a central work in my research, I decided that introducing a little bit of context will be helpful, especially because it may not be the area of expertise of the reader. Last but not least, this is a very elegant theory, at least from my biased perspective !

1.3.1 c-orientations and push

I quit for a section the realm of maps and consider instead graphs. Let G be a (non-necessarily planar) graph. An *orientation* O of G is the choice of an orientation for each of its edges. In other words, for each $e = \{u, v\} \in E(G)$, either the edge e oriented from u to v belongs to O or the edge e oriented from v to u.

For G endowed with an orientation O, we say that the directed edge e is *forward* if e belongs to O and *backward* otherwise. Similarly, a path or a cycle are said to be *forward* (respectively *backward*) if all their edges are *forward* (respectively *backward*). Given two vertices v and w of G, we say that w is *accessible* from v if there exists a forward path from v to w.

Let C be a directed cycle of G. Then, the *circulation* of O around C is the difference between the number of forward edges in C and the number of backward edges. More generally, the circulation c_O of O is the function that associates to each cycle of G its circulation.

Definition 1.3.1

Let G be a graph and c be a function that maps each cycle of G to an integer. A c-orientation *– as introduced by Propp [Pro02] – is an orientation O such that $c_O = c$. If such an orientation exists, c is called a* feasible circulation.

An *accessibility class* of (G, O) is a subset $A \subset V(G)$ such that all vertices of A are pairwise mutually accessible; in other words, for any couple (u, v), with $v, u \in A$, there exists a forward path from u to v and another one from v to u, see Figure 1.7. An accessibility class A is moreover called *maximal* (respectively *minimal*) if all the edges between A and its complement A^c point towards A (respectively towards A^c). Maximal and minimal accessibility classes are in particular inclusion-wise maximal among accessibility classes.

The *push-down* of a maximal accessibility class A consists in reversing the orientation in O of all the edges between A and A^c. The *push-up* of a minimal accessibility class is defined similarly. It is easy to check that pushing down or pushing up an accessibility class produces a new orientation with the same circulation as O, and the same accessibility classes.

[2] Indeed, the "dictionary" between generating series and combinatorial structures (see [FS09, Chapter 1]) ensures that the unique formal power series $A(z)$ solution of the equation $A(z) = 1 + zA(z)^2$ is the generating series of plane binary trees enumerated by their number of non-leaf vertices or equivalently of plane trees enumerated by their number of edges. Hence, $T(z)$ can be seen for instance as the generating series of either binary trees where the vertices are decorated in 3 possible ways or of plane trees where the edges are decorated in 3 possible ways. Two bijections due to Schaeffer and presented respectively in Sections 2.1.2 and 3.1.3 give bijective explanations of these two facts.

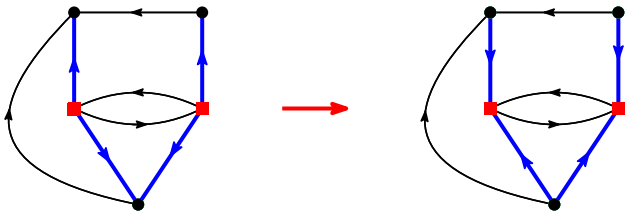

Figure 1.7. Illustration of the push-up of a minimal accessibility class (represented by red squared vertices).

Propp proved in [Pro02] that any c-orientation can be obtained from another c-orientation by a finite sequence of push-downs and push-ups of accessibility classes. In fact, he proved a much stronger structural result which I describe in the next section.

1.3.2 The lattice of c-orientations

I assume some familiarity with the notions of partially ordered sets, lattices and distributive lattices and refer to [Sta11, Chapter 3] for a thorough introduction to these concepts[3]. I only remind here the following two definitions essential for our purposes.

Definition 1.3.2

- *For x, y two elements of a partially-ordered set $(P, \leq)$, we say that y* covers *x if and only if $x < y$ and if for all z in P such that $x \leq z \leq y$, then either $x = z$ or $z = y$.*
- *Let $(P, \leq)$ be a partially-ordered set, then P is a* lattice *if and only every two elements of P have a unique supremum and a unique infimum.*

The main result of [Pro02], illustrated in Figure 1.9, is the following theorem:

Theorem 1.3.3 (*Theorem 1 of [Pro02]*)

Let G be a finite connected graph, let c be a feasible circulation of G. Fix A^* an accessibility class of G. For two c-orientations O_1 and O_2, we say that O_2 covers O_1 if and only if O_1 is obtained from O_2 by pushing-down a maximal accessibility class different from A^*.
Then, endowed with this covering relation, the set $\mathcal{O}_c$ of c-orientations of G is a finite distributive lattice.

Since a finite distributive lattice admits a unique minimum and a unique maximum, an important consequence of this theorem is the following definition:

Definition 1.3.4

Let G be a finite connected graph, let c be a feasible circulation of G (as defined in Definition 1.3.1). Fix A^* an accessibility class of G. Then the minimum (respectively maximum) of $\mathcal{O}_c$ is called the c-minimal orientation *(respectively the* c-maximal orientation*). Equivalently, it is the unique c-orientation whose only maximal (respectively minimal) accessibility class is A^*.*

1.3.3 α-orientations and c-orientations on planar maps: two dual points of view

The theory developed by Propp and summarized in the two previous sections is very powerful. Since c-orientations are defined for graphs, they can be applied directly to graphs embedded on any given surface: sphere, disk, torus of genus g or even non-orientable surfaces. But, since this habilitation focuses mostly on planar maps[4], let me come back to planar maps. It turns out that in [Fel04], Felsner

[3] With a little hint of nostalgia, I also refer the francophone reader to the Section 1.2 of my PhD thesis [Alb08] for a quick recap of those

[4] However, the application of Propp's theory for maps on surfaces other than the sphere will play a crucial role in Section 2.2.1

developed quite independently from the work of Propp a dual definition of orientations, called α-orientations. He obtained in this work a result equivalent to Theorem 1.3.3 for α-orientations on *planar* maps. Even though the result of Felsner does not have the same level of generality as the one of Propp's, the formalism of α-orientations appears to be often better suited for applications. That is the reason why I now introduce α-orientations.

Let M be a planar map endowed with an orientation O of its edges. The *indegree* and *outdegree* of a vertex v, denoted respectively by $\mathrm{in}(v)$ and by $\mathrm{out}(v)$, are respectively the number of edges oriented inwards v and outwards v in O.

Definition 1.3.5

Fix $\alpha : V(M) \to \mathbb{N}$. An α-orientation *is an orientation of M such that for each $v \in V(M)$, $\mathrm{out}(v) = \alpha(v)$. If such an orientation exists, α is said to be* feasible.

From now on, we assume that M is a plane map, i.e. that M has a marked face and is embedded in the plane with this face as its outer face. A forward directed cycle is called a *clockwise cycle* if the outer face of M lies on its left and a *counterclockwise cycle* otherwise. A *flip* (respectively a *flop*) consists in reversing the orientation of all the edges of a clockwise (respectively *counterclockwise*) cycle, see Figure 1.8. It is easy to check that a flip or a flop produces a new orientation – say O' – with the same outdegree at each vertex. Hence it transforms an α-orientation into another α-orientation.

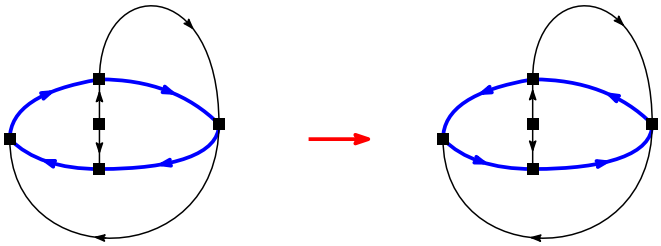

Figure 1.8. Illustration of the flip of a clockwise cycle (represented by fat blue edges).

Felsner proved the following result dual to Theorem 1.3.3.

Theorem 1.3.6 (*Theorem 1 of [Fel04]*)

Let M be a rooted plane map and let $\alpha : V(M) \to \mathbb{N}$ be a feasible function. Then the flips and flops turn the set of α-orientations into a distributive lattice.

It enables in particular to state the following counterpart of Definition 1.3.4:

Definition 1.3.7

Let M be a rooted plane map, and let α be a feasible function (as defined in Definition 1.3.5). Then there exists a unique α-orientation without counterclockwise (respectively clockwise) cycle. It is called the minimal α-orientation *(respectively the* maximal α-orientation*).*

Let me elaborate on the fact that for planar maps c-orientations and α-orientations are dual notions. Recall that $M^\dagger$ denotes the dual map of M. Any orientation O on M gives a canonical dual orientation $O^\dagger$ of $M^\dagger$, by adopting the following construction. An edge of $M^\dagger$ is oriented in such a way that, when we follow it, its dual edge is oriented from its right to its left, see Figure 1.9(b).

It is easy to see that, that if we start with a c-orientation of M, then the circulation of each of its facial cycles is prescribed. Hence, if we perform the construction above starting, it implies that the indegree and outdegree of any $v \in V(M^\dagger)$ is fixed. Conversely, if $M^\dagger$ is endowed with an α-orientation, then it uniquely determines the circulation of each facial cycle of M. Since, in a planar map, the facial cycles form a cycle-basis of the maps, M is in fact endowed with a c-orientation,

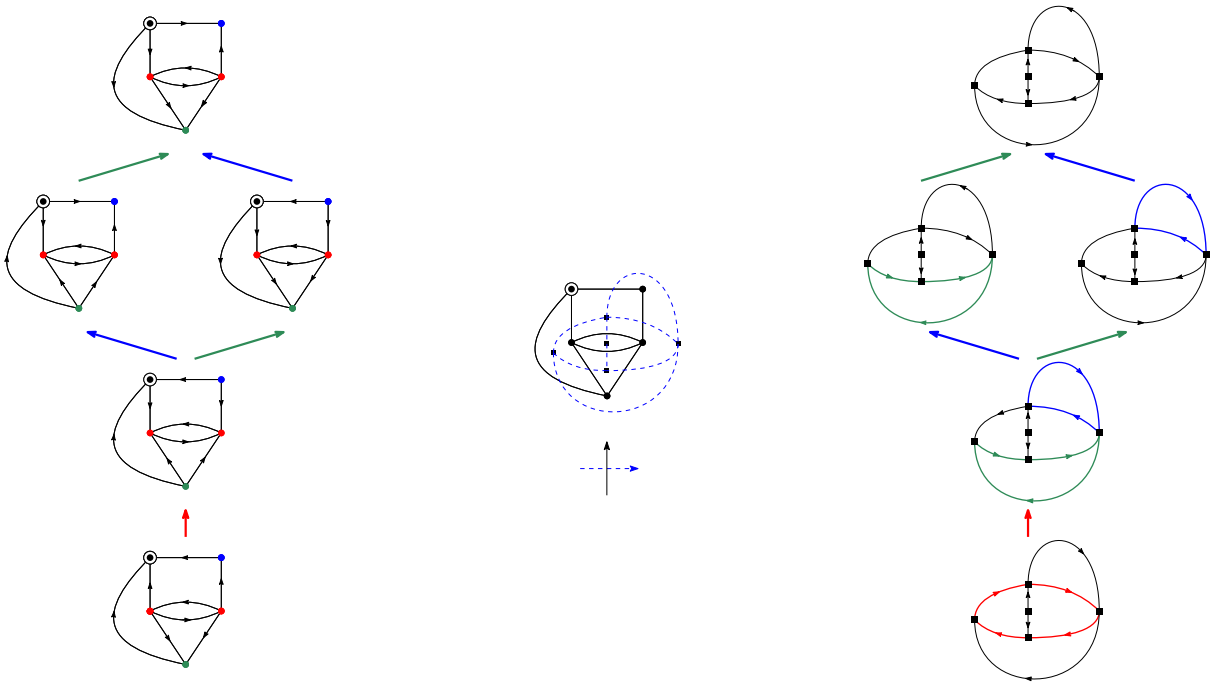

(a) The lattice of c-orientations,

(b) the convention for orienting edges of the dual, represented in dashed blue edges,

(c) and the corresponding lattice of α-orientations on the dual map.

Figure 1.9. In (a), an example of lattice of c-orientations is given. Inclusion-wise maximal accessibility classes are represented by vertices of the same color and $A^\star$ is the vertex circled. The convention given in (b) enables to orient edges from the dual map and to get the dual α-orientations represented in (c).
The color of the arrows illustrate which accessibility class (in (a)) or which directed cycle (in (c)) is flipped to switch from one orientation to the one above.

where c if fully characterized by α[5,6].

With a bit more work, we can see that, in the planar case, the lattice structures exhibited by Propp and Felsner coincide. For instance, in the setting of Theorem 1.3.3, if A^* is reduced to a single vertex, then this gives a natural plane embedding of the dual map by choosing the face corresponding to A^* as the outer face. In that case, it is easy to see that the dual of the c-minimal orientation is the α-minimal orientation, see Figure 1.9(c).

1.4 Some particular cases of α-orientations

The purpose of this section is to convince the reader that the formalism of α-orientation has a large expressive power and to demonstrate how some classical or less classical combinatorial structures on maps can be encoded by α-orientations. Most of these examples already appear in the works of Propp and Felsner.

[5]Be aware, that the duality on oriented planar maps is *not* an involution, but a transformation of order 4. In particular, if we start with a c-orientation of M and applies twice the duality, we will obtain a $(-c)$-orientation of M.

[6]When considering maps on surfaces of higher genus, such as the torus, the dual of a c-orientation is no longer an α-orientation. Indeed, the fact that the circulation around a non-contractible cycle is fixed gives an additional constraint, which cannot be expressed in the α-orientation formalism.

1.4.1 Matchings of bipartite maps

Let M be a bipartite planar map. Consider the partition – as defined in Section 1.1.2 – of the vertices of M into W and B. A *perfect matching* of M is a subset S of its edges such that each vertex of M is incident to exactly one edge of S.

Now define α as follows, $\alpha(v) = \deg(v) - 1$ for $v \in B$ and $\alpha(v) = 1$ for $v \in W$. Given an α-orientation O, define S_O as the set of edges outgoing from vertices of W. The set S_O is clearly a perfect matching of M, and we claim that this construction is a bijection between perfect matchings of M and its α-orientations, see Figure 1.10. In particular, α is feasible if and only if M admits a perfect matching, which can easily and efficiently be checked by Hall's theorem.

Theorem 1.3.6 hence implies that the set of perfect matchings of M is endowed with a lattice structure. By the bijection between orientations and matchings, a flip on the orientation corresponds to the following operation on matchings. Let O be an orientation and S_O be its associated matching. A forward directed cycle $C = (e_1, \dots, e_{2\ell})$ of O corresponds to an alternating cycle of S_O (that is a cycle, such that $e_i \in S_O$ if and only if i is even). Then the flip of C in O consists in replacing e_{2i} by e_{2i-1} for any $1 \leq i \leq \ell$ in S_O.

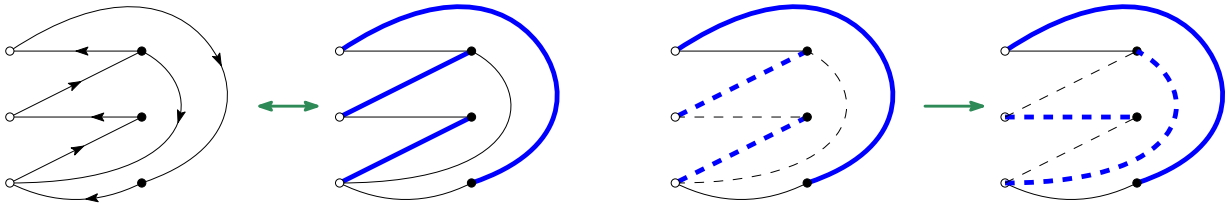

Figure 1.10. The correspondence between perfect matchings and α-orientations (left) and an example of flip of an alternating cycle of the matching (right).

1.4.2 Eulerian orientations

Recall that a map is *Eulerian* if and only all its vertices have even degree. An *Eulerian orientation* of an Eulerian map M is an α-orientation, with $\alpha(v) = \deg(v)/2$ for any $v \in V(M)$. Equivalently it is an orientation in which $\mathrm{in}(v) = \mathrm{out}(v)$, for any $v \in V(M)$.

An *Eulerian tour* of M is a cycle C on M such that each edge of M belongs exactly once to C. By Euler's theorem – proved by Hierholzer in 1873 – a map admits an Eulerian tour if and only if it is Eulerian. Orienting the edges of an Eulerian tour in the direction they are followed, yields an Eulerian orientation of the underlying graph. This application is clearly not injective, see Figure 1.11, but implies that α is feasible on any Eulerian map.

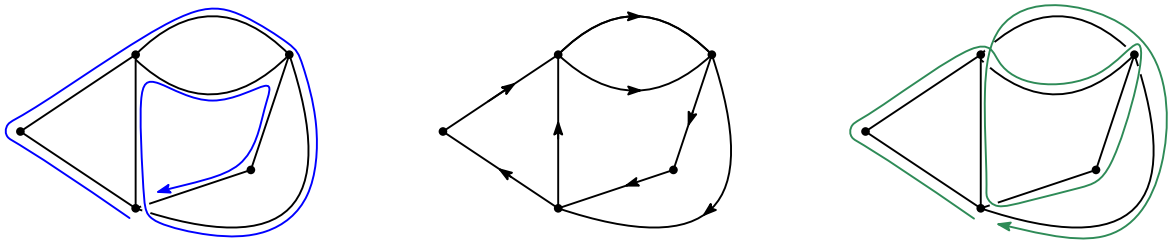

Figure 1.11. Two different Eulerian tours can yield the same Eulerian orientation (which turns out to be the minimal one in this example).

Remark 1.4.1

In this survey of my work, I will mostly use Eulerian orientations (or more precisely the *minimal Eulerian orientation) as a tool to study planar maps. For instance, in order to enumerate some families of maps, I will enumerate them decorated by their* unique *minimal Eulerian orientation. In terms of enumeration, the two problems are of course completely equivalent, but the structure of the orientation proves useful when designing some combinatorial constructions. I will come back at length to this idea in Chapter 2.*

Another completely different problem is to enumerate Eulerian orientations on planar maps (see also Chapter 4 for related models). This question is natural and interesting in its own right, and has also some deep connections with models from theoretical physics such as the so-called ice-model. *Very recent results have been obtained for this problem. Following some earlier works [BBMDP17] and [EPG18], Bousquet-Mélou and Elvey-Price managed to write in [BMEP] a system of equations for the generating series of Eulerian orientations, and, quite remarkably, they were able to solve it explicitly. In particular, they proved that the number of Eulerian orientations of 4-valent maps with n vertices behaves asymptotically like $(4\sqrt{3}\pi)^{n+2}/(18n^2(\log(n))^2)$.*

This asymptotic result implies that the generating series is not D-finite, i.e. that it is not the solution of a linear differential equation with polynomial coefficients. Whereas, as proved in Section 1.2, the generating series of quadrangulations (or equivalently of 4-valent maps) is known to be algebraic, and is hence a much simpler object.

1.4.3 Orientations for simple triangulations and quadrangulations

Let T be a rooted triangulation and Q be a rooted quadrangulation. For a rooted map M, recall that $\mathring{V}(M)$ denotes the set of its vertices not incident to its root face. Define $\alpha_3 : V(T) \to \mathbb{N}$ and $\alpha_4 : V(Q) \to \mathbb{N}$ as follows:

$$\alpha_3(v) = \begin{cases} 3 & \text{if } v \in \mathring{V}(T) \\ 1 & \text{otherwise,} \end{cases} \quad \text{and} \quad \alpha_4(v) = \begin{cases} 2 & \text{if } v \in \mathring{V}(Q) \\ 1 & \text{otherwise.} \end{cases}$$

Schnyder [Sch89] (for triangulations) and Fusy [Fus07] (for quadrangulations) proved that α_3 and α_4 are feasible if and only if the underlying map is simple, see Figure 1.12.

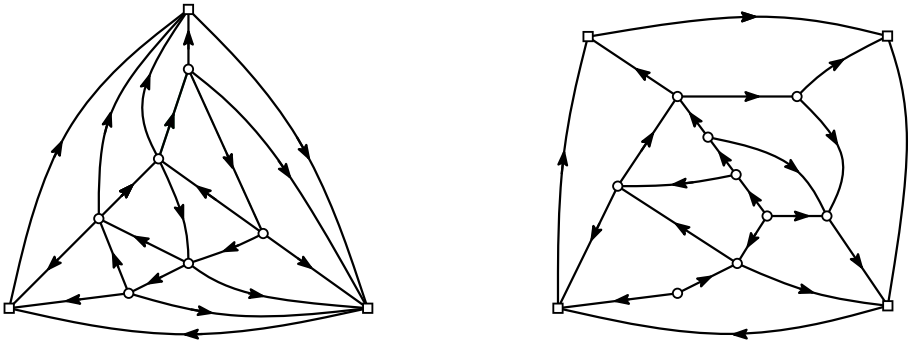

Figure 1.12. A simple triangulation (left) and a simple quadrangulation (right) endowed respectively with their minimal α_3 and α_4-orientation. Vertices of $\mathring{V}$ are represented by circles and other vertices by squares.

Historically, α_3-orientations were introduced by Schnyder to study what is now known as *Schnyder woods*, a combinatorial structure defined on simple triangulations. Schnyder proved that the set of Schnyder woods can be endowed with a lattice structure. This can now be seen as a particular case of the general theory of α-orientations but was in fact the example that triggered Felsner's work. His original motivation was indeed to generalize Schnyder woods (and their lattice structure) to any 3-connected planar graph, and he realized that this setting could in fact be made much more general.

1.4.4 Two generalizations: fractional and pseudo-orientations

In this last section, I present two natural generalizations of α-orientations: fractional orientations and pseudo α-orientations. Both were introduced formally in [BF12a], but pseudo-orientations already made some earlier appearance in [PS06].

Fractional orientations The k-expanded version of a planar map M is defined as the planar map where each edge of M has been replaced by k copies. A *k-fractional orientation* of M is defined in [BF12a] as an orientation of the k-expanded map of M, with the additional property that two copies of the same edge cannot create a counterclockwise cycle. It is conveniently considered as an orientation of M in which edges can be partially oriented in both directions and the in- or out-degree of a vertex v (that can now be fractional) is defined as the in- or out-degree of v in the k-expanded map, divided by k, see Figure 1.13. In this setting, a *forward path* is a path in which each edge is at least partially oriented in the considered direction. The notions of clockwise or counterclockwise cycles, of minimality and of accessibility follow.

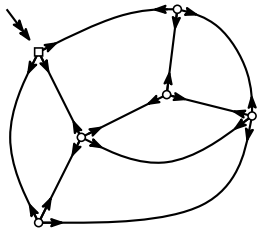

(a) A 2-fractional quasi-Eulerian oriented map,

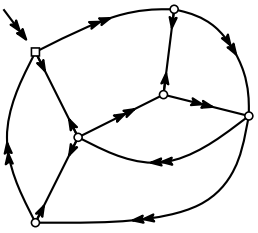

(b) the minimal orientation with same in- and out-degrees,

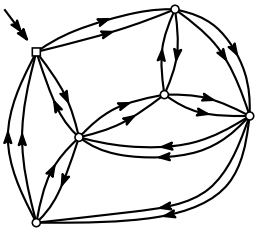

(c) and the representation of the minimal orientation as an oriented 2-expanded map.

Figure 1.13. A rooted planar map endowed with quasi-Eulerian 2-fractional orientations.

Let me mention two particularly nice examples of fractional orientations:

- For a general map M, a *quasi-Eulerian orientation* is a 2-fractional orientation in which $\alpha(v) = \deg(v)/2$ for any $v \in V(M)$. Such an orientation is easily seen to exist for any map. It suffices to partially orient in both directions every edge in the map, see Figure 1.13(a).
- Fix M a rooted map and for $k \geq 1$, define α_{2k} and α_{2k+1} as follows:

$$\alpha_{2k}(v) = \begin{cases} \dfrac{k}{k-1} & \text{if } v \in \mathring{V}(M) \\ 1 & \text{otherwise,} \end{cases} \quad \text{and} \quad \alpha_{2k+1}(v) = \begin{cases} \dfrac{2k+1}{2k-1} & \text{if } v \in \mathring{V}(M) \\ 1 & \text{otherwise.} \end{cases}$$

Bernardi and Fusy [BF12a] proved that, for any $d \geq 3$, a rooted d-angulation has girth d if and only if it admits a $(d-1)$-fractional α_d-orientation if d is or and a $(d/2-1)$-fractional α_d-orientation if d is even, see Figure 1.14. Note that the cases $d = 3$ and $d = 4$ correspond respectively to the cases of simple triangulations and quadrangulations described in the previous section.

Pseudo α-orientations *Pseudo α-orientations* are introduced in [BF12a] to deal with d-angulations with a boundary. They are generally well-suited to study maps in which the root face plays a special role. For M a rooted planar map, fix $k \in \mathbb{N}$ and $\alpha : \mathring{V}(M) \to \mathbb{N}$, then a pseudo (α, k)-orientation (or a pseudo α-orientation when k is implicit) of M is an orientation O such that:

$$\mathrm{out}(v) = \alpha(v) \text{ for } v \in \mathring{V}(M), \qquad \sum_{v \in V(M) \setminus \mathring{V}(M)} \mathrm{out}(v) = k,$$

and such that the boundary of the root face is a forward or a backward cycle. Theorem 1.3.6 can easily be generalized to endow the set of pseudo (α, k)-orientations with a lattice structure.

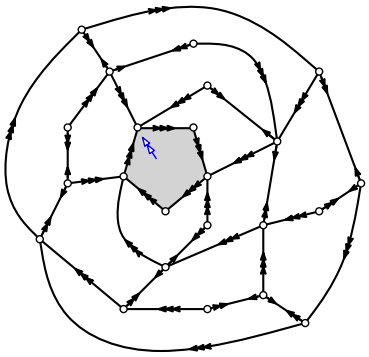

Figure 1.14. A pentagulation of girth 5 endowed with its minimal 5/3-orientation.

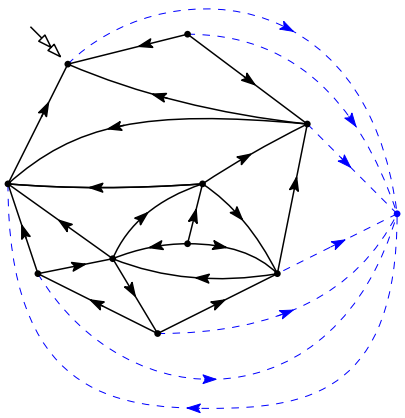

(a) A simple triangulation with a "star" outer vertex endowed with its minimal α_3-orientation,

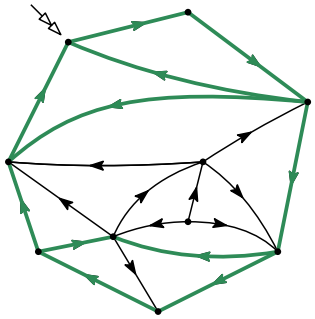

(b) and the corresponding triangulation of the 7-gon, endowed with its minimal $(\alpha_3, 11)$-orientation.

Figure 1.15. Construction of a pseudo α_3-orientation for a simple triangulation of the 7-gon. In (a), we add an additional vertex in its root face, triangulate the resulting face (by adding the dashed blue edges), and consider the minimal α_3-orientation of this simple triangulation. Then, up to reorienting the boundary of the p-gon, this yields the minimal pseudo $(\alpha_3, 2p-3)$-orientation of the original map as represented in (b). The 11 edges outgoing from vertices incident to the p-gon are represented by fat green edges.

We can go one step further and combine k-fractional and pseudo-orientations. A special case of interest is the family of d-angulations of a p-gon, which admit fractional pseudo $(\alpha_d, 2p-3)$-orientation if and only if they have girth d, as proved in [BF12a, Lemma 18]. An illustration of the construction of a pseudo α_3-orientation for a simple triangulation of a p-gon is given in Figure 1.15.

1.5 Comments

As I already mentioned at the beginning of Section 1.3, I do not make much use of the whole lattice theory of c- or α-orientations. What I *do* use a lot is the existence of a unique minimal c- or α-orientation. Indeed, much of the work presented in Chapters 2 and 3 relies on the fact that a planar map (or a map in higher genus in Section 2.2.1) can be endowed canonically with an orientation. The choice of the appropriate c or α depends on the family of maps of interest, and Section 1.4 gives an exhaustive list of the orientations considered in the rest of this document.

Let me also mention that the study of maps endowed with a (non-necessarily minimal) orientation is also a whole area of research, which has regained an interest recently, both in combinatorics (see for instance [BMEP, BMFR19]), and in probability theory (see for instance [KMSW19, LSW17]).

Chapter 2

Around blossoming bijections

The purpose of this chapter is to present some of my contributions to the study of blossoming bijections. It presents the results of the publications [7] and [14].

Section 2.1 I start by a short introduction, in which I introduce blossoming bijections, relying on Schaeffer's original bijection between 4-valent maps and some so-called "blossoming trees". I further present the existing literature related to blossoming bijections.

Section 2.2 I describe the results of the publication [7] obtained in collaboration with Dominique Poulalhon. In this work, we construct a generic framework to obtain blossoming bijections for maps endowed with some canonical orientations. Combined with the general theory of α-orientations developed by Felsner and presented in Section 1.3.3, it enables to retrieve many known bijections and to construct new ones. In particular, I emphasize how our framework enables to get nice enumerative corollaries by getting rid of the classical "balance" assumption and to obtain bijections for maps with a boundary.

Section 2.2.1 I present the publication [14] obtained in a joint work with my PhD student Mathias Lepoutre. In this section, I leave the realm of planar maps and consider some maps on the torus of genus g. Building on previous results obtained in [Lep19] and in particular on a bijection between bicolorable 4-valent maps and blossoming unicellular maps, we obtain the first bijective proof of a rationality scheme for the bivariate enumeration of general maps with respect to their number of faces and of vertices.

Section 2.4 I conclude this chapter with some research perspectives, which I hope will convince the reader that much remains to be understood and explored in the fascinating world of blossoming bijections.

2.1 Blossoming trees and maps

2.1.1 Bijective proofs

In Section 1.2 of Chapter 1, I concluded the presentation of Tutte's method by mentioning that such nice closed formulas call for a bijective explanation. More explicitly, what I call a *bijective explanation* or a *bijective proof* is the following. In Section 1.2, we obtained that the number q_n of quadrangulations with n faces (or equivalently of general maps with n edges or of 4-valent maps with n vertices) is equal to:

$$q_n = \frac{2 \cdot 3^n}{n+2} \frac{1}{n+1} \binom{2n}{n} = \frac{2 \cdot 3^n}{n+2} \mathtt{Cat}_n, \tag{2.1}$$

where $\texttt{Cat}_n$ denotes the n-th Catalan number, which is well-known to enumerate families of trees. It is therefore tempting to look for an encoding of maps as some colored trees, or a *bijection* between maps and such trees (see also the footnote on page 23).

Such a bijection was indeed obtained by Cori and Vauquelin in [CV81] for general maps and was later simplified and reformulated by Schaeffer [Sch98] for quadrangulations (I present the latter bijection in Section 3.1.3). A direct corollary of this bijection is of course to give a new proof of the enumeration formula obtained by Tutte, but it also sheds some light about deep combinatorial properties of maps. In particular, the bijection obtained by Schaeffer is quintessential to the study of random planar maps, a very active field of research which I will revisit in more details in Section 3.1. Because of this role, the so-called "Cori–Vauquelin–Schaeffer bijection" has become quite famous. In this introduction, I want do discuss another (in fact earlier) bijection by Schaeffer [Sch97] between 4-valent maps and some decorated trees.

Before doing so, let me mention that there exist numerous bijections between maps and some families of decorated trees. Two main trends emerge in these bijections:

- Either the trees are decorated by some integers that capture some metric properties of the maps, this is the case of Schaeffer's bijection [Sch98] mentioned above, which was generalized to maps of arbitrary degrees by Bouttier, Di Francesco and Guitter [BDFG04] (see also Section 3.3.1) and to other families of maps, see [Mie09, BFG14]. Because the trees that appear in those bijections are called *mobiles*, I will later refer to this family of bijection as the "mobile-type" bijections.
- Or, the trees are some spanning trees of the maps with some decorations that allow to reconstruct the facial cycles, see for instance [CV81, Sch97, BDFG02a, PS06]). This is this type of so-called "blossoming bijections" that I want to investigate further in this chapter.

2.1.2 Blossoming trees and 4-valent maps, following [Sch97]

Blossoming trees Let T be a plane tree such that all its vertices have either degree 3 or degree 1, and with a pointed vertex of degree 1. (These trees are sometimes called *planted binary trees*. They are clearly in bijection with the more classical family of rooted binary trees and hence are also enumerated by the Catalan numbers). Then, decorate T in the following way, see Figure 2.1(a).

- For each $v \in V(T)$ with $\deg(v) = 3$, add an *outgoing half-edge* in one of the corners incident to v.
- For each $v \in V(T)$ with $\deg(v) = 1$ (i.e. for each leaf of T), replace v and its unique incident edge by an *incoming half-edge* incident to the only neighbor of v[1]. If v was the pointed vertex, mark the corresponding half-edge.

Trees thus obtained are called *4-valent blossoming trees*. We denote respectively $\mathcal{T}^\times$ and $\mathcal{T}_n^\times$ the sets of 4-valent blossoming trees and of blossoming trees with n vertices. Note that by construction, an element of $\mathcal{T}^\times$ with n outgoing half-edges has $n+2$ incoming half-edges.

Closure and bijection For $t \in \mathcal{T}^\times$, the *closure* of t is defined as follows[2]. Perform a clockwise contour of t starting from its marked half-edge. Each time an outgoing half-edge is followed by an incoming half-edge, merge these two half-edges, orient the resulting edge in the direction given by the orientation of the two half-edges and draw the new edge such that the outer face lies on its left, see Figure 2.1(b). This operation is called a *local closure* and the edge created a *closure edge*. When all possible local closures are done (it may require to do the contour of the tree several times), two incoming half-edges remain unmatched, see Figure 2.1(c). If one of them is the marked half-edge, the tree is called *balanced* and the set of balanced blossoming trees is denoted $\mathcal{T}^{\times,b}$. In that case, finish the construction by changing the orientation of the marked half-edge, and perform the last

[1] Outgoing and incoming half-edges were respectively called *buds* and *leaves* in the original paper.
[2] A more formal definition of the closure is given in Section 2.2.1.

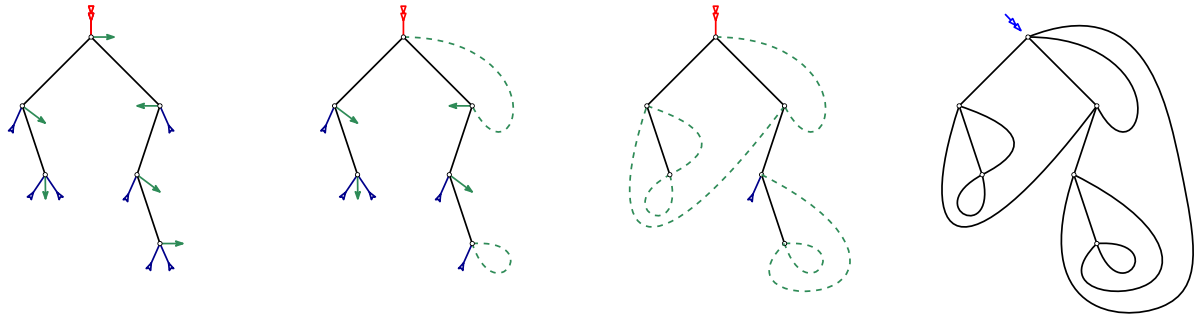

(a) A balanced 4-valent blossoming tree,

(b) after 2 local closures,

(c) all possible local closures have been performed,

(d) the resulting 4-valent map.

Figure 2.1. Illustration of Schaeffer's bijection between balanced 4-valent blossoming trees and rooted 4-valent maps. The marked ingoing half-edge is represented by the red double arrow.

possible local closure. Finally root the resulting map at the corner preceding the marked half-edge (in clockwise order), see Figure 2.1(d). The main result of [Sch97] is the following:

Theorem 2.1.1

The closure operation is a bijection between the set of balanced 4-valent blossoming trees with n vertices and rooted 4-valent maps with n vertices.

Re-rooting and enumeration A direct consequence of Theorem 2.1.1 is that the number of rooted 4-valent maps with n vertices is equal to the number of balanced blossoming trees with n vertices. However, enumerating balanced blossoming trees is not trivial. A much easier problem consists in the enumeration of (non necessarily balanced) blossoming trees. Indeed, in the construction of an element of $\mathcal{T}_n^\times$ from a planted binary tree with n vertices, there are 3 possible choices for the position of each outgoing half-edge. It follows immediately that $|\mathcal{T}_n^\times| = 3^n \cdot \mathtt{Cat}_n$.

To relate $|\mathcal{T}_n^\times|$ and $|\mathcal{T}_n^{\times,b}|$, Schaeffer made the following key observation. For $t \in \mathcal{T}_n^\times$, after performing all local closures, t has exactly two unmatched incoming half-edges. Marking one of them and forgetting the marked half-edge of t produces a *balanced* blossoming tree. Since t has $n+2$ incoming half-edges, it follows that:

$$|\mathcal{T}_n^{\times,b}| = \frac{2}{n+2}|\mathcal{T}_n^\times| = \frac{2 \cdot 3^n}{n+2}\mathtt{Cat}_n.$$

Combined with Theorem 2.1.1, it concludes the bijective proof of the enumerative formula (**2.1**).

2.1.3 Other blossoming bijections

There are (at least) two ways to generalize this initial "blossoming bijection". The first possible extension is to consider different families of planar maps, such as the ones defined in Chapter 1. The second possible extension is to consider 4-valent maps on other surfaces than the sphere, for instance on orientable surfaces of higher genus or on non-orientable surfaces.

The former extension has been much studied. The bijection for 4-valent maps was followed by some variants and extensions dealing with various families of maps (in fact, already in his paper, Schaeffer studies more generally Eulerian maps with prescribed degree sequence). A non-exhaustive list includes (non-Eulerian) maps with prescribed degree sequence [BDFG02a], maps endowed with a physical model [BMS02] or with a spanning tree [Ber07] and maps with connectivity constraints [PS06]. Each of these bijections appears as an ad-hoc explanation of the known enumeration formula, but they present strong similarities, which calls for a unified bijective theory.

With Dominique Poulalhon, we obtained in [7] a generic framework, which both enable to obtain many previous constructions as special cases (and in particular all the aforementioned ones) and to obtain new bijections. I present this work in the next section. Note that another generic framework was developed before our work in [BF12a, BF12b], where a "master bijection" is introduced in order to see many constructions as special cases of a common construction. Our approach and the one obtained by Bernardi and Fusy are complementary: they do not capture the same subsets of existing bijections and when applied to the same family of maps, they do not necessarily yield the same bijective construction.

The latter extension was only carried out recently by my PhD student Mathias Lepoutre, who managed to extend the bijective construction of Schaeffer to 4-valent *bicolorable* maps on any surface of higher genus [Lep19]. As a byproduct of his construction, he obtained the first bijective proof of some enumerative results (previously obtained by Bender and Canfield [BC91]) for maps on surfaces of higher genus. I will briefly discuss his result in Section 2.2.1. Then, I will present an extension that we obtained in a joint work [14], which gives the first bijective proof of a bivariate enumerative result in higher genus.

2.2 Generic framework for blossoming bijections, [7]

In [7], with Dominique Poulalhon, we construct a unified bijective scheme between planar maps and blossoming trees, where a blossoming tree is defined as a spanning tree of the map decorated with some dangling half-edges that enable to reconstruct its faces. Our method generalizes a previous construction of Bernardi [Ber07] by loosening its conditions of application.

The benefits of this generalization are twofold. On the one hand, our construction includes *plane maps*, that is maps embedded in the plane with a root face different from the outer face. In particular, it is well-suited for families of maps with a boundary, in which the root face plays a special role (see Section 1.4.4). On the other hand, our scheme produces naturally blossoming trees which are not necessarily *balanced*, and therefore whose enumeration is much simpler than the one of their balanced counterparts.

Most of the previous bijective constructions that involve a spanning tree of the map – apart from the notable exception of the bijection for irreducible quadrangulations of the hexagon [FPS08] – are captured by our generic scheme. Moreover, we obtained new bijections for plane bipolar orientations and d-angulations of a p-gon with girth d.

As mentioned above, bijective proofs appear often as an *a posteriori* enlightening explanation of a simple enumerative formula. In fact, the formula is used as a guide to construct the "simplest" objects that it enumerates. Here, remarkably, the orientations on which the construction relies are often natural enough so that they can be guessed even if a formula is not available.

I start by introducing the material needed to state our main theorem in Section 2.2.1. In Section 2.2.2, I will then illustrate some of its applications on two examples.

2.2.1 Accessible orientations and blossoming bijections

Blossoming maps and closure I start by the formal definition of blossoming maps and of the closure operation, which were only sketched in Section 2.1.

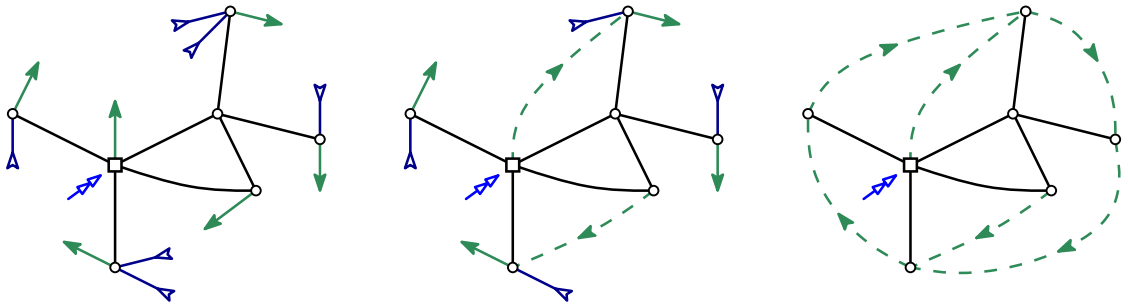

(a) A blossoming map, with cyclic contour word $e\bar{b}be\underline{bee}\bar{b}\underline{\bar{b}}bee\bar{b}bee\underline{bee}\bar{b}\underline{\bar{b}}be$,

(b) a local closure, which yields a new cyclic contour word $\underline{e\bar{b}}\,\underline{bee\bar{b}}\,\underline{bee\bar{b}}\,\underline{beee\bar{b}}\,\underline{be}$,

(c) and the total closure, with cyclic contour word $eeee$.

Figure 2.2. Closure of a blossoming map. Opening stems are represented by plain green arrows, and closing stems by reverse blue arrows. Factors to be substituted by e are underlined in the contour word.

Definition 2.2.1

A blossoming map *is a plane map, in which each corner incident to the outer face can carry a sequence of opening or closing* stems *(i.e. opening or closing* half-edges*), such that the number of opening stems is equal to the number of closing stems.*

A blossoming tree *is a blossoming map with only one face.*

The cyclic contour word *of a blossoming map is the word on $\{e, b, \bar{b}\}$, which encodes the cyclic clockwise order of edges and stems along the border of the outer face with e coding for an edge and b and $\bar{b}$ for opening and closing stems, see Figure 2.2(a).*

A *local closure* of a blossoming map is a substitution of a factor $be^\star\bar{b}$ by the letter e in its contour word, where $e^\star$ denotes any (possibly empty) sequence of e, see Figure 2.2(b). In terms of maps, it corresponds to the creation of a new edge (and hence a new face) by merging an opening stem with the following closing stem (provided that there is no other stem in between) in clockwise order around the border of the outer face. The new edge is canonically oriented from the opening vertex to the closing vertex, with the new bounded face on its right. If several local closure operations are possible on a blossoming map, performing all of them in any order yields the same result. Hence iterating such local closures produces eventually a unique object:

Definition 2.2.2

The closure *of a blossoming map M is the (non-blossoming) map obtained after iterating all possible local closure operations, see Figure 2.2(c). The edges created during local closures operations are called* closure edges.

Since closure edges are canonically oriented, if a blossoming map is endowed with an orientation, so is its closure. Moreover, considering opening and closing stems respectively as outgoing and incoming (half-)edges (as in Section 2.1), in- and out-degrees are preserved. Since all the closures are performed in clockwise direction around the map, no counterclockwise cycle can be created during a local closure operation. Consequently if the initial blossoming map is endowed with a minimal α-orientation, then so is its closure.

The last definition I need is the following one[3]:

[3]For the sake of simplicity, I restrict here my attention to classical orientations. All results are in fact stated in [7] for fractional orientations, as defined in Section 1.4.4.

Definition 2.2.3

Let M be a rooted plane map, and let $\alpha : V(M) \to \mathbb{N}$ be a feasible function. Let O be an α-orientation. Then, O is said to be accessible *if, for any $v \in V(M)$, there exists a forward path from v to to the root vertex of M.*

Since two α-orientations differ from one another by a sequence of flips and flops of forward cycles, this implies that either all or no α-orientations of M are accessible. In the former case, α is said to be accessibly feasible.

Note that a rooted plane tree only admits one accessible orientation, in which all edges are oriented from a child to its parent. An example of a blossoming tree and its closure is given in Figures 2.3(c) and 2.3(a).

Orientations and opening The main contribution of our work is to provide an inverse construction of the closure, stated in the following theorem and illustrated in Figure 2.3.

Theorem 2.2.4 (*Theorem 2.3 of [7]*)

Let M be a plane rooted map, and suppose that M is endowed with an accessible orientation O without counterclockwise cycle. Then, there exists a unique rooted blossoming plane tree, endowed with its unique accessible orientation, such that its closure is M oriented with O.

Equivalently, M admits a unique partition of its edges $(\mathcal{T}_M, \mathcal{C}_M)$ such that:

- *Edges in $\mathcal{T}_M$ (called* tree edges*) form a spanning tree of M, endowed with its unique accessible orientation.*
- *Any edge in $\mathcal{C}_M$ (called a* closure edge*) is a clockwise edge in the unique cycle it forms with edges in $\mathcal{T}_M$.*

Let us call such a partition the tree-and-closure partition *of M.*

It might not be immediate to see why Theorem 2.2.4 gives a generic bijective scheme. Its strength comes from its combination with the general theory of α-orientations presented in Section 1.3. Indeed, as an immediate corollary, we obtain the following result:

Theorem 2.2.5

Let $\mathcal{M}$ be a family of plane maps, whose elements can be characterized by the existence of an accessible α-orientation. Then, there exists a bijection between $\mathcal{M}$ and a family of blossoming trees (which admits a simple description in terms of α).

This theorem can for instance be applied to any family of maps described in Section 1.4 and enables to retrieve Schaeffer's original bijection for Eulerian maps (see Section 1.4.2), and the bijections for simple triangulations and quadrangulations obtained respectively by Poulalhon and Schaeffer [PS06] and Fusy [Fus07] (see Section 1.4.3).

Before stating some other applications, let me comment on the algorithmic complexity of these constructions. Given a blossoming tree, its closure can be computed in linear time. Reciprocally given a map endowed with an appropriate orientation, it follows directly from the proof of Theorem 2.2.4 that the corresponding blossoming tree can be computed in quadratic time by a generic algorithm. As mentioned above, for the maps considered in [Ber07], the opening can in fact be computed in linear time. It turns out that for many families of maps, ad-hoc algorithms can be designed to compute the blossoming tree in linear time. One of the main contribution of [7] is in fact to design a linear-time algorithm that computes the blossoming tree associated to a d-angulation of the p-gon (see Theorem 2.2.7).

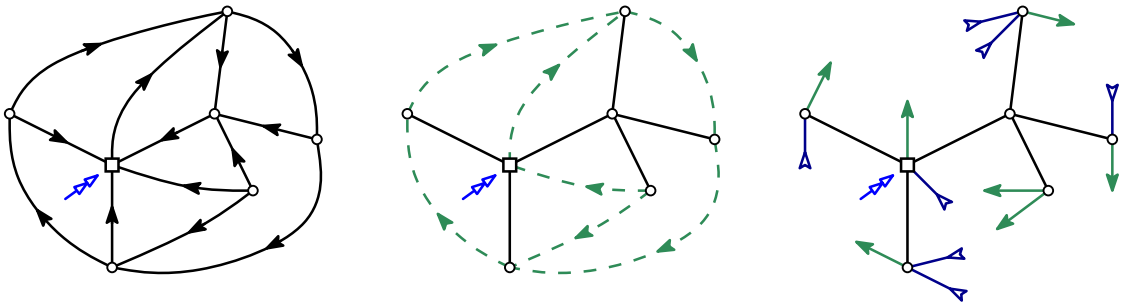

(a) A minimal accessible orientation, (b) the corresponding tree-and-closure partition, (c) and the corresponding blossoming tree.

Figure 2.3. From a minimal accessible orientation to a blossoming tree.

2.2.2 New application of the bijective scheme

In [Ber07] obtained a result similar to Theorem 2.2.4. However, in his work, the outer infinite face of a rooted plane map is required to be the root face. The proof of his result relies deeply on the fact that *both* the accessibility and the minimality of the orientation are defined according to the root face. Theorem 2.2.4 shows that this hypothesis is unnecessary. For illustration purposes, I now present two specializations of Theorem 2.2.4, which require this stronger result.

Getting rid of the balancing constraint: Schaeffer's bijection revisited To see how our setting enables to get rid of the balancing constraint, let me apply it to the family of 4-valent maps already introduced in Section 2.1.

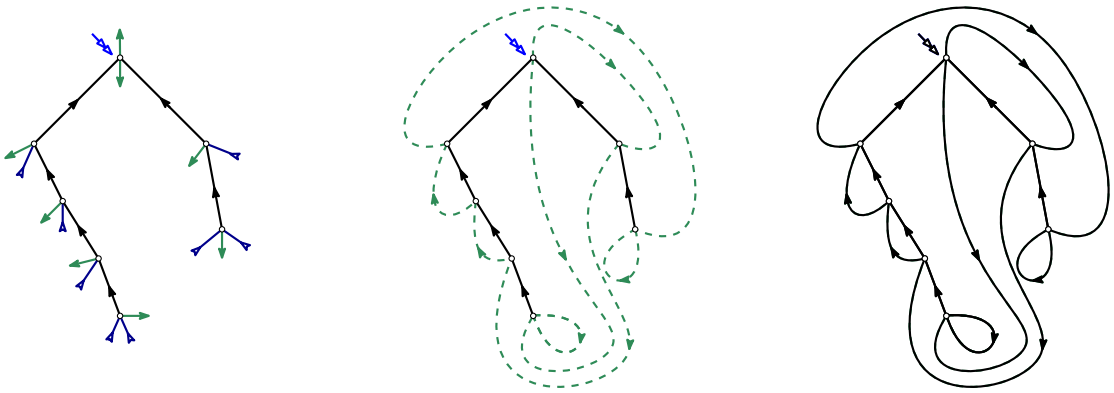

(a) A blossoming 4-valent tree, (b) its closure, (c) and the corresponding plane 4-valent map.

Figure 2.4. Example of Schaeffer's bijection, starting from a non-balanced tree. The resulting map is a rooted 4-valent *plane* map endowed with its minimal Eulerian orientation.

Consider a (non-necessarily balanced) blossoming tree $t \in \mathcal{T}_n^{\times}$. Flip its marked ingoing half-edge into an outgoing half-edge, and orient canonically any edge of t from a child to its parent. It follows that for each $v \in V(t)$, $\mathrm{out}(v) = \mathrm{in}(v) = 2$. Then, the closure is a 4-valent plane map endowed with its unique minimal Eulerian orientation, and rooted at a corner that precedes (in clockwise order) an outgoing edge, see Figure 2.4.

Theorem 2.2.4 implies that this operation is a bijection between $\mathcal{T}_n^{\times}$ and 4-valent plane maps with n vertices, rooted at a corner that precedes (in clockwise order) an outgoing edge. Exactly half of the rooted 4-valent plane maps are rooted at a corner that precedes an outgoing edge, and, by Euler's formula, a 4-valent map with n vertices has $n+2$ faces. Hence, there are $q_n(n+2)/2$ such

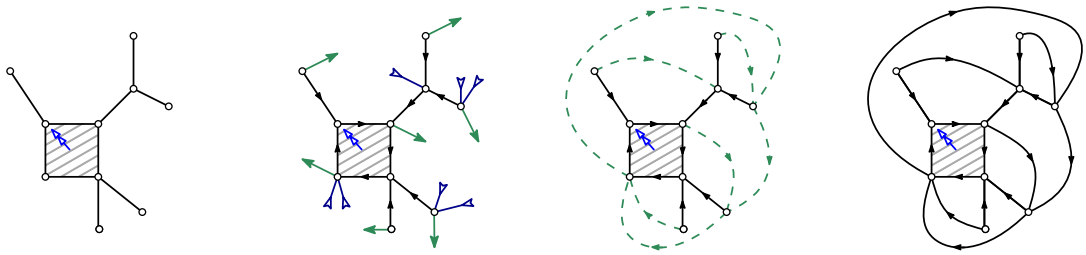

(a) A 4-cyclic forest, (b) with opening and closing stems, (c) the matching of its stems, (d) and its closure.

Figure 2.5. Closure of a blossoming cyclic forest. The root face is dashed.
Reciprocally, the map represented in (d) satisfies the hypotheses of Proposition 2.2.6, its edge partition is represented in (c), and its (unique) corresponding blossoming forest in (b).

maps, which yields:

$$q_n \cdot \frac{n+2}{2} = |\mathcal{T}_n^{\times}| = 3^n \cdot \mathtt{Cat}_n,$$

and thus, we obtain directly the enumeration formula for q_n.

Of course, in this case, the rerooting procedure gives another way to get rid of the balancing constraint. But, there are classes of trees (for instance, those introduced in [BMS02] or in [BDFG02a]), for which the rerooting operation does not behave as nicely, and where the enumeration of balanced trees is much more complicated.

I want to emphasize that, in particular, the reinterpretation of the bijection of [BMS02] in our setting (without the balancing constraint) is instrumental in the work [11]. Indeed, thanks to this reinterpretation we obtain directly that the (non-necessarily balanced) trees obtained in [BMS02] are in bijection with bipartite planar maps *with a marked face* (i.e. plane maps), see also the discussion in the last paragraph of Section 4.3.

Bijection for maps with a boundary When we consider families of maps with boundary, or more generally families of maps in which the root face plays a special role, it can be useful to consider a variant of our result. Let me first introduce the following family of planar maps akin to forests of trees. A *p-cyclic forest* is a plane rooted map with two faces, the root one and the outer one, such that the border of the root face is a simple cycle of length p. Observe that a cyclic forest is nothing else but a sequence of rooted trees grafted on a p-gon, see Figure 2.5(a). Hence, it admits a canonical orientation obtained by orienting the p-gon clockwise and any edge of the rooted trees from a child to its parent. This orientation is the unique accessible minimal orientation for which the boundary of the root is a clockwise cycle.

Next, a *blossoming cyclic forest* is a cyclic forest, whose vertices can carry opening and closing stems, which lie in the outer face, and such that the numbers of opening and closing stems are equal. We give in Figure 2.5(b) an example of a blossoming cyclic forest, endowed with its canonical orientation, and represent its closure in Figure 2.5(d). Theorem 2.2.4 can be extended to give a bijection between plane maps and blossoming cyclic forests as follows:

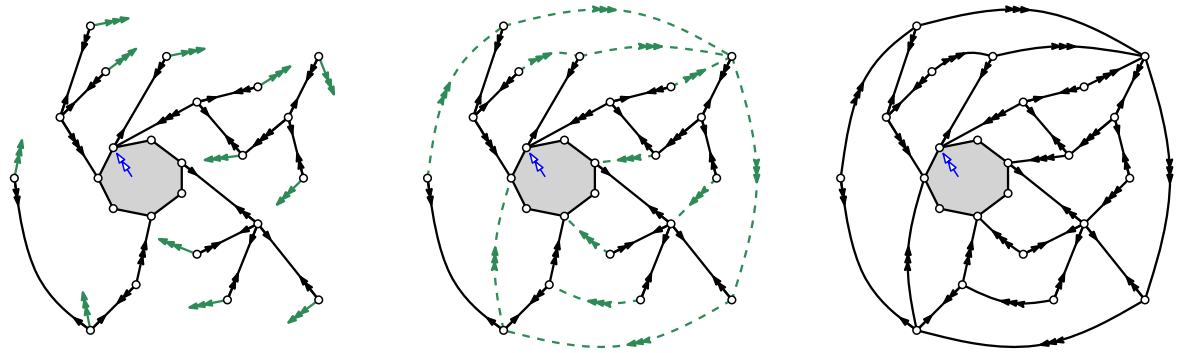

(a) A blossoming cyclic forest, (the closing stems are omitted)

(b) how to close the opening stems to form pentagons,

(c) and the corresponding pentagulation with girth $d = 5$ of the 7-gon.

Figure 2.6. From a blossoming cyclic forest to a pentagulation with girth $d = 5$ of the 7-gon endowed with its canonical fractional pseudo-$5/3$-orientation.

Proposition 2.2.6 (*Corollary 5.5 of [7]*)

Let M be a plane rooted map with distinct root and outer faces, and such that the boundary of the root face is a simple cycle. Assume that M is endowed with a minimal accessible orientation O, in which the boundary of the root face is a directed cycle. Then, there exists a unique rooted blossoming cyclic forest, endowed with its canonical orientation, such that its closure is M oriented with O.

Equivalently, M admits a unique edge-partition $(\mathcal{T}_M, \mathcal{C}_M)$ such that:

- *Edges in $\mathcal{T}_M$ form a spanning cyclic forest of M with same root as M, on which the restriction of O is accessible;*
- *Any edge in $\mathcal{C}_M$ turns clockwise around the unique cycle it forms with edges in $\mathcal{T}_M$.*

For any $k \in \mathbb{N}$, Proposition 2.2.6 can be applied to the k-expanded version of a map M (see Section 1.4.4) and hence, can also deal with fractional orientation. With that in mind, it allows us in particular to obtain new blossoming bijections for d-angulations of girth d with or without a boundary, illustrated on Figure 2.6.

Theorem 2.2.7 (*Theorems 5.6 and 6.5 of [7]*)

Fix $p \geq d \geq 3$, and let $M_{d;p}$ be the family of d-angulations with girth d of a p-gon. Then there exists an explicit bijection between $M_{d;p}$ and a family of blossoming cyclic forests (easy to describe and to enumerate).

Moreover, the cyclic blossoming forest associated to a d-angulation can be computed in linear time.

Let me comment the result of this theorem, starting with the bijective part. It follows from the results stated in Sections 1.4.3 and 1.4.4 that elements of $M_{d;p}$ can canonically be endowed with a pseudo-orientation (which is a fractional orientation if $d \geq 5$).

It can be checked, that in the *plane* embedding of an element of $M_{d,p}$ in which the outer infinite face is different from its root face, then its canonical orientation without counterclockwise cycle is accessible. For this accessibility property to hold, it is crucial that we consider accessibility towards the root vertex and not towards the outer face. In other words, it is crucial that *we allow accessibility and minimality to be defined relatively to two different faces* (the root face and the outer face)[4].

By applying Proposition 2.2.6, we then obtain directly the first part of Theorem 2.2.7, which

[4] In [BF12a], accessibility and minimality are both defined relatively to the outer face. In that case, the existence of a minimal suitable orientation is conditioned on the map being non-separated (*i.e.* there cannot exist a cycle of girth length that separates the root face and the outer face).

is illustrated in Figure 2.6. In this particular case where the degree of faces is prescribed, closing stems are redundant. Hence, blossoming forests only carry opening stems, and a local closure is then defined as the transformation of an opening stem into an edge to create a face of a degree d, see Figure 2.6(b).

Let me now comment on the algorithmic result. As mentioned above, computing the map from a blossoming forest can be easily performed in linear time, so let me focus on the *opening part*. The generic scheme provided in Theorem 2.2.4 (and in its extension stated in Proposition 2.2.6) only yields *a priori* an algorithm whose complexity is quadratic in the size of a map. In [7], we prove that an exploration starting from the outer infinite face enables to decide efficiently whether a subset of edges belongs or not to the closure. Then, a careful and quite subtle recursion scheme allows to apply the same idea on a smaller submap. This can then be turned in a linear-time algorithm. I refer the interested reader to Figure 19 and Section 6 of [7], for the complete description of this algorithm.

As an enumerative byproduct, we obtain a *bijective proof* of the following formula (first obtained by Brown [Bro64], via manipulation of generating series) for the number $T_{n,p}$ of simple triangulations of a p-gon with n vertices:

$$T_{n,p} = \frac{2 \cdot (2p-3)!}{(p-1)!(p-3)!} \frac{(4n-2p-5)!}{(n-p)!(3n-p-3)!}.$$

For d-angulations of girth d of a p-gon, no closed formulas are available, but the generating series of maps are solutions of a polynomial system of equations, which enables to compute recursively and efficiently their coefficients, see Section 5.3 of [7] and Propositions 25 and 26 of [BF12a].

Let me also note that for simple triangulations of the p-gon, this bijection has been previously obtained by Poulalhon and Schaeffer [PS06], but their proof relied on the existing enumerative result obtained by Brown and did not constitute a bijective proof of it. Moreover, since no closed formulas are available for d-angulations of girth d, a direct extension of their argument was not possible.

2.3 Blossoming bijection for 4-valent maps in higher genus, [14]

The purpose of this section is to present the results of [14]. For once, I consider graphs which are not embedded on the plane or on the sphere but rather on a compact orientable surface without boundaries. By the classification's theorem (see for instance [MT01]), any such surface is in fact homeomorphic to the torus with g holes for a fixed $g \in \mathbb{N}$, called the *genus* of the surface.

A *map of genus* g is then a proper *cellular* embedding of a graph on the g-torus, where cellular means that the faces of the map are all topologically equivalent to disks, see Figure 2.7. Note that since the embedding is cellular, the underlying graph is necessarily connected. Two maps of genus g are identified if they can be mapped one onto the other by an homeomorphism that preserves the orientation of the torus, see [LZ04, Section 3.1] for a pedagogical introduction to this subject.

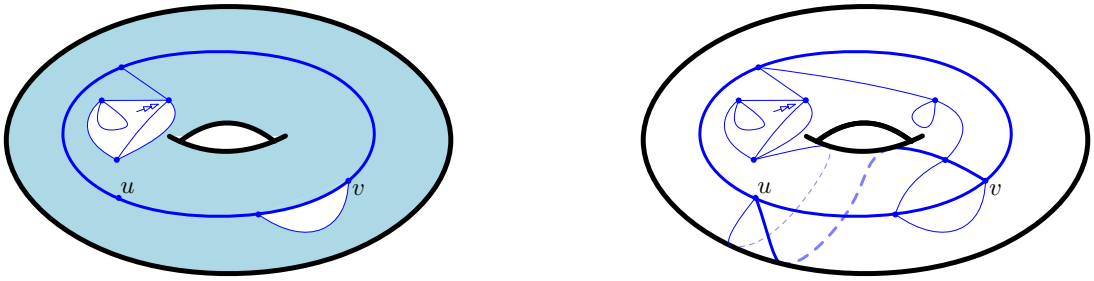

Figure 2.7. Two embeddings of a connected graph on the torus of genus 1. On the left, the embedding is not cellular: the shaded face is indeed not homeomorphic to a disk. On the right, the embedding is cellular and defines a map of genus 1.

2.3.1 Enumeration of maps of higher genus by edges

The first enumerative results for maps on surfaces of positive genus were obtained by Lehman and Walsh [WL72a, WL72b], who gave expressions for the generating series of maps with fixed excess (the excess is the difference between the number of edges and the number of vertices minus 1). In [BC91], Bender and Canfield obtained closed expressions for the generating series of rooted maps of genus 1, 2 and 3, thus generalizing the work of Tutte, presented in Section 1.2. More generally, they proved the following rationality result:

Theorem 2.3.1 (*Tutte [Tut63] for $g = 0$, Bender and Canfield [BC91] for $g \geq 1$*)

For any $g \geq 0$, let $M_g(z)$ be the generating series of rooted planar maps of genus g enumerated by their number of edges. Then, $M_g(z)$ is a rational function of $T(z)$, where $T(z)$ is the unique generating series in z that satisfies $T(z) = z + 3\Big(T(z)\Big)^2$.

As in the planar case, this result calls for a bijective explanation. But until the recent work (presented below) of my PhD student Mathias Lepoutre [Lep19], no bijective explanation of this result was known for $g \geq 2$. In positive genus, rather than considering bijections between maps and decorated trees, it is instead more natural to consider bijections between maps and decorated unicellular maps (i.e. maps with only one face) of genus g[5]. As in the planar case, two trends emerge for bijections in positive genus.

Bijections of the mobile-type have been successfully extended to higher genus [CMS09, Cha09, Mie09], and to non-orientable surfaces [CD17, Bet15a]. With these techniques (in particular, see [CMS09]), it is possible to show that the generating series of maps satisfies a rationality scheme. But in this scheme, the auxiliary function (that plays a role analogous to $T(z)$ in Theorem 2.3.1) is solution of a polynomial equation of degree 4 instead of degree 2.

The situation is much different in the case of bijections with blossoming trees, and apart from [DGL17] which presents a bijection between simple triangulations of genus 1 (with some additional constraints) and a family of blossoming unicellular maps, there was, previously to Lepoutre's work, no other extension of the existing planar bijections. The main difficulty in higher genus is to come up with a good notion of canonical orientation. Indeed, because of the presence of non-contractible cycles, Felsner's theory fails to be extended and Propp's formalism is harder to manipulate. In [BC11], Bernardi and Chapuy proposed a generalization of the minimal and accessible assumption for orientations in the planar case and defined so-called *left-accessible orientations*. They designed a bijection between a map endowed with a spanning unicellular embedded graph (whose genus can be smaller than the genus of the initial surface) and a map endowed with a left-accessible orientation, thus obtaining a generalization of [Ber07] to higher genus. I will come back to this work in Section 2.4.

Let me now present briefly the bijective proof of [Lep19]. The first point is the classical result that, for any $g \geq 0$, the radial construction presented in Section 1.1.3 is a bijection between rooted planar maps of genus g with n edges and rooted *bicolorable* 4-valent maps with n vertices. Then, Lepoutre generalized Schaeffer's bijection for 4-valent maps presented in Section 2.1.2, see Figure 2.9. His proof can be decomposed into four main steps:

- He first constructs explicitly a canonical Eulerian orientation for bicolorable 4-valent maps, the so-called "dual-geodesic orientation", obtained as follows. Label the faces of the map by their distance to the root in the dual map. Since the map is bicolorable, the labels of two adjacent faces differ exactly by one. Orient then every edge such that the face with minimal label lies on its right, see 2.8(a). One nice property of this orientation is that it can also be characterized as a minimal c-orientation.

[5] Since unicellular maps in genus 0 exactly correspond to plane trees, unicellular maps in genus g are indeed a natural generalization of plane trees in genus g.

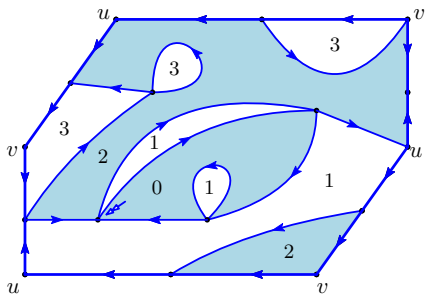

(a) Construction of the dual-geodesic orientation based on the labeling of the faces.

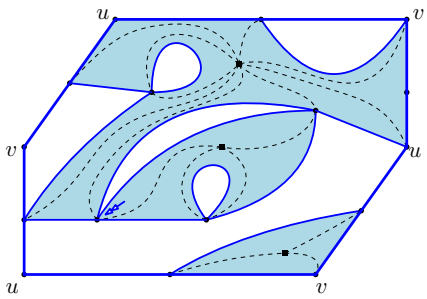

(b) A map of genus 1 (dashed edges) and its radial map (full edges). .

Figure 2.8. In (a), I construct the dual-geodesic orientation of the 4-valent bicolorable map represented in Figure 2.7(right). We use an hexagonal representation, from which we can retrieve the classical representation by gluing the opposite sides of the hexagon. The edges between the vertices u and v glued together are represented by bold edges in Figure 2.7(right).
On (b), I illustrate the radial construction. Note that faces with even (respectively odd) labels in the 4-valent map correspond to vertices (respectively faces) of the original map.

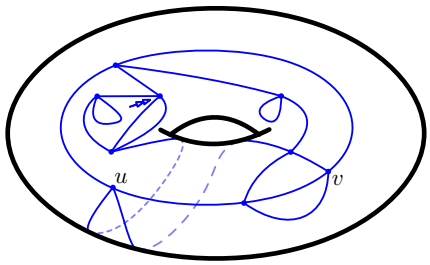

(a) A map 4-valent map of genus 1,

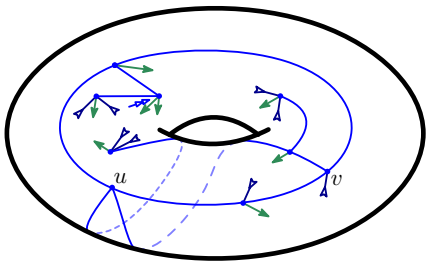

(b) and its corresponding blossoming unicellular map.

Figure 2.9. Illustration of Lepoutre's bijection for 4-valent maps on higher genus.

- Then, Lepoutre shows that, for this specific orientation, the bijection of [BC11] always gives a spanning unicellular map of the same genus as the original map. Hence, it yields a bijection between bicolorable 4-valent maps endowed with their (canonical) dual-geodesic orientation and a family of *balanced* blossoming unicellular maps[6]. Moreover, this family of maps admits a nice description thanks to the characterization of the dual-geodesic orientation as a minimal c-orientation.
- Thanks to a rerooting argument (significantly more involved than in the planar case), the enumeration of balanced blossoming unicellular maps can be deduced from the enumeration of blossoming unicellular maps.
- Last but not least, following an approach originally developed in [CMS09], he proves that the generating series of blossoming unicellular maps is a rational series in terms of the series T, defined in Theorem 2.3.1. This computation requires a very subtle analysis of the structure of the blossoming unicellular maps, and is one of the main difficulties of this proof.

To explain why the blossoming approach developed in [Lep19] gives a bijective proof of Theorem 2.3.1, whereas the mobile-type bijections would not, let me be slightly more precise. To enumerate unicellular maps in positive genus, we classically consider their canonical decomposition into a collection of forests of trees grafted on a unicellular map where all the vertices have degree at least 3, see Figure 2.10(a). These are the so-called *reduced schemes*. In [Lep19], it is proven that for any given

[6]The terminology in [Lep19] is actually slightly different. The analogue of *balanced* blossoming maps as defined in [Sch97], are called *well-rooted* blossoming maps. For sake of consistency with the rest of this chapter, I stick however to the balancing terminology.

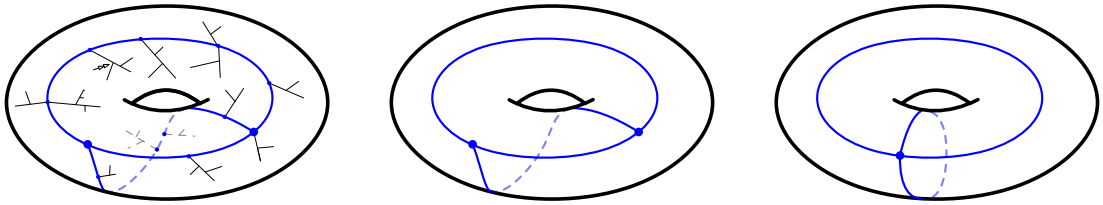

(a) Canonical decomposition of a unicellular map in genus 1.

(b) One reduced scheme in genus 1,

(c) and the other reduced scheme.

Figure 2.10. In (a), we represent the "tree parts" of a unicellular map of genus 1 in black and its reduced scheme in blue. In (b) and (c), I represent the only two reduced schemes of genus 1.

reduced scheme s, the generating series of the blossoming unicellular maps which admits s as a reduced scheme is a rational function of the generating series T. Since the number of schemes of a fixed genus is finite, summing over all possible schemes gives the desired rationality result.

This scheme-by-scheme rationality result is not true for the mobile-type bijection obtained in [CMS09]. It is still quite mysterious that it does hold for the blossoming bijection, but seems to indicate that blossoming bijections are better-suited to obtain rationality results in higher genus. This is also confirmed by the extension of Lepoutre's work, that we obtain in a joint work and which I present in the next section.

2.3.2 Enumeration of maps of higher genus by vertices and faces

In view of Euler's formula, which states that for any map M of genus g:

$$|V(M)| + |F(M)| = 2 - 2g(M) + |E(M)|,$$

a natural way to refine the result of Bender and Canfield is to count maps by both their number of vertices and their number of faces. Arquès obtained the first results in that direction and gave explicit formulae for the bivariate generating functions of maps in the sphere or in the torus [Arq85, Arq87]. In 1993, Bender, Canfield and Richmond [BCR93] then generalized Theorem 2.3.1 and gave a rational parametrization for the bivariate generating function enumerating rooted maps of genus g counted by vertices and faces.

Theorem 2.3.2 (*Bender, Canfield and Richmond [BCR93], bijective proof in [14]*)

For any fixed $g \geq 1$, let $M_g(z_\bullet, z_\circ)$ be the generating series of rooted maps of genus g enumerated by vertices (by the variable $z_\bullet$) and faces (by the variable $z_\circ$).

Define $T_\bullet(z_\bullet, z_\circ)$ and $T_\circ(z_\bullet, z_\circ)$ as the unique formal power series defined by $T_\bullet = z_\bullet + T_\bullet^2 + 2T_\circ T_\bullet$ and $T_\circ = z_\circ + T_\circ^2 + 2T_\circ T_\bullet$. Then $M_g(z_\bullet, z_\circ)$ is a rational function of $T_\bullet$ and $T_\circ$.

The original proof of Theorem 2.3.2 relies on some *generatingfunctionology*, extending the method originally developed by Tutte and presented in Section 1.2. In particular, it is not clear at all from the work of Bender, Canfield and Richmond, why some generating series of decorated trees ($T_\bullet$ and $T_\circ$) appear. Finding a combinatorial proof of this result was hence a natural question and it has been an open question for quite a few years. In a joint work with Mathias Lepoutre [14], we obtained a bijective proof of the rationality statement of Theorem 2.3.2. (Note that for $g = 0$, a combinatorial proof was given by Schaeffer based on his bijection presented in Section 2.1.2).

The reason why the original result of Lepoutre can be extended to a bivariate enumeration result is that a scheme-by-scheme rationality result (as described in the end of the previous section) also holds for the bivariate enumeration. It hence confirms that, in higher genus, blossoming bijections produce the right "elementary objects". This extension is also a success demonstrating the robustness of blossoming bijections. In contrast, the mobile-type bijections constructed in [Sch98] for the planar case and in [CMS09] for the higher genus fail to provide bivariate enumerative results.

Let me sketch very briefly our proof, which is articulated as follows. We first proceed as in the work of [Lep19] and use the same bijection. In the construction of the radial of a map, it is easy to see that the faces labeled by an even integer (respectively an odd integer) in the construction of the dual–geodesic orientation correspond to vertices (respectively faces) of the original map, see Figure 2.8(b). Hence, the bivariate enumeration of general maps boils down to the bivariate enumeration of 4-valent bicolorable maps with one variable for the even faces and one variable for the odd faces.

Two additional difficulties appear. First, the rerooting steps must be analyzed with more details to keep track of the number of even and odd opening and closing stems. Second, the analysis of the blossoming unicellular maps then obtained is much more elaborate than in [Lep19]. It does not seem possible to generalize directly the method used there. Fortunately, as mentioned above, the scheme-by-scheme rationality result also holds for the bivariate enumeration. To carry out the enumeration, we developed a new method, which very roughly speaking consists in grouping in a careful way the contribution of some unicellular maps that admits the same reduced scheme. As a corollary, we obtain a new (and easier) proof of the original result of Lepoutre.

2.4 Perspectives

In this last section, I survey three directions of research based on the results obtained in this chapter, that I would like to explore in more details.

Blossoming bijections in higher genus As emphasized in Section 2.2, a map endowed with a minimal and accessible orientation can also be viewed as a map with a spanning tree. This observation was successfully combined with the general theory of α-orientations developed by Felsner to give general bijective schemes in the planar case, see [BF12b] and [7].

It would be highly desirable to obtain systematic bijective schemes in higher genus by combining Bernardi and Chapuy's result obtained in [BC11] together with Propp's theory of c-orientations, surveyed in Section 1.3.2. The main difficulty to tackle is to characterize the orientations that produces spanning unicellular embedded graphs whose genus matches the genus of the original surface. The orientation constructed in [Lep19] (see also in [DGL17] for orientations of simple triangulations in genus 1) does produce such embedded graphs, and can hence be seen as an important first step in that direction. On a side note, let me mention that Propp's (unpublished) work was somehow overshadowed by Felsner's article, whose setting is easier to manipulate but only holds in the planar case. In [Lep19] and [14], we were the first to try and endow maps in higher genus with canonical c-orientations.

A natural way to continue this work is hence to try and describe generically (for instance as c-orientations) which orientations produce such spanning unicellular maps. A more specific direction of research would be to investigate the generalization in higher genus of existing (planar) bijections. Because of their link with some statistical physics model such as the hard particles model or the Ising model (see also Chapter 4), particularly interesting examples of such bijections are given in [BDFG02b, BMS02] for bipartite maps with prescribed vertex degrees. In particular, there does not seem to exist an equivalent of Theorem 2.3.1 for bipartite cubic (or with more general prescribed vertex degrees) maps in higher genus. Obtaining such a result directly by some bijective arguments would definitely be a consecration of blossoming bijections in higher genus.

Blossoming bijections for non-minimal or non-accessible orientations In contrast to the Cori–Vauquelin–Schaeffer bijection (or more generally to mobile–type bijections, i.e. bijections between maps and labeled trees), for which many generalizations have been constructed (see for instance [Mie09, AB13, BFG14]) blossoming bijections have been somehow neglected! It would be natural to see if the variants available for mobile–type bijections have some counterparts for blossoming bijections. We could for instance consider non-necessarily minimal or non-necessarily accessible orientations.

Some evidence supporting this quest is the mysterious enumerative connection between some blossoming trees and general Eulerian orientations revealed by the recent work of Bousquet–Mélou and Elvey–Price, see [BMEP] and Remark 1.4.1. Explaining combinatorially this connection for 4-valent maps would be quite a bijective success, which would trigger some additional interests for generalizations of blossoming bijections.

Blossoming bijections and metric properties of maps The last perspective has some strong connections with my publications [10] and [13] presented in Chapter 3 and really lies at the interface between bijective combinatorics and probability theory. From their construction, blossoming bijections and the blossoming trees they produce do not seem to carry any metric information of the initial map. However, in some work with Louigi Addario-Berry (detailed in Section 3.2), we proved that blossoming bijections for simple triangulations and simple quadrangulations encode some metric properties of the map. In particular, thanks to these bijections, we were able to prove that the scaling limit of those maps is the Brownian map.

Our approach has then been successfully extended to simple maps [BCF14], to simple triangulations of the torus of genus 1 [BHL19] and to simple triangulations of a p-gon [13] (see also Section 3.4). It hence makes sense to investigate systematically metric properties of blossoming bijections, either in genus 0, following the general framework introduced in [7], or in higher genus, after developing adequate bijections as suggested above. In higher genus, a first step would be to see if the labeling of the faces (which encodes some metric properties of the dual map) can help to study the scaling limit of some families of maps.

When available, mobile–type bijections are perfectly suited to investigate metric properties of the maps. However, contrary to blossoming bijections, they do not behave well for maps with connectedness constraints. For those types of maps, developing a general blossoming scheme with some control on the distances would be a major achievement.

Chapter 3

Scaling limit of random planar maps

In this chapter, I present my publications [10], [12] and [13], which belong to the field of scaling limits of random planar maps. Here is a quick presentation of the different sections of this chapter.

Section 3.1 I introduce in this section some material needed which is common to the rest of the chapter, and survey the existing literature in the field of scaling limits of random maps.

Section 3.2 I describe the scaling limit of simple triangulations and present the main result of the publication [10], obtained in collaboration with Louigi Addario-Berry. As with most results in this field, this work starts with a bijection between maps and decorated trees. In our case, we use the Poulalhon-Schaeffer bijection [PS06] between simple triangulations and blossoming trees, that we rephrased into a bijection between simple triangulations and a class of labeled trees. To establish the convergence of these maps, we follow the now-classical framework developed by Le Gall in [LG13]. The main difficulty here is to see how distances in the map can be tracked through the bijection into a reasonably simple functional of the tree. To do that, we rely heavily on the so-called *leftmost paths* of simple triangulations. On the one hand, we prove that these paths are almost shortest paths between any vertex and the root vertex. On the other hand, we explain how they can be constructed directly on the tree, thus allowing us to express their lengths as simple functionals of the tree. Once this is established, we need to prove that the scaling limit of the labeled trees is the Brownian snake. This will be obtained as a special case of a more general result obtained in Section 3.3.

Section 3.3 I present the main result of the publication [12], also obtained in collaboration with Louigi Addario-Berry. Here, we study the scaling limit of *odd-angulations*, that is p-angulations for p an odd integer such that $p \geq 5$. We focus only on these values of p, since the other values were treated in the original work of Miermont [Mie13] (for $p = 4$) and of Le Gall [LG13]. Again, we rely on a bijection between planar maps and labeled multitype trees: this time, we use the Bouttier–Di Francesco–Guitter bijection [BDFG04]. Thanks to the general approach developed in [LG13], the only new result needed to obtain the scaling limit of odd-angulations is that the encoding functions of the corresponding multitype labeled trees converge to the Brownian snake. To prove the preceding fact, we present a bootstrapping principle for distributional convergence of random labeled plane trees. Thanks to previous results obtained by Miermont [Mie08a], the latter allows to obtain an invariance principle for the scaling limit of labeled multitype Galton-Watson trees, with only a weak assumption on the centering of the label displacements.

Section 3.4 I briefly discuss the results of [13], obtained in collaboration with Nina Holden and Xin Sun about the scaling limit of Boltzmann simple, loopless and general triangulations with a simple boundary. We first obtain the result for simple triangulations and extend it to loopless and general triangulations by a standard core decomposition. To establish the scaling limit for simple triangulations, we rely, on the combinatorics side, on a bijection by Poulalhon and Schaeffer [PS06] between simple

triangulations with a simple boundary and blossoming *forests*. And, on the probabilistic side, we rely on the convergence of rescaled uniform quadrangulations with a boundary towards the Brownian disk as established by Bettinelli and Miermont [BM17]. The Poulalhon–Schaeffer bijection does not encode metric properties directly, but the techniques developed in [10] can be adapted to this setting by changing the definition of leftmost paths. There is also a new difficulty in relating distances in the maps with labels in the trees coming from the presence of the macroscopic boundary. We overcome this new issue by considering a simple triangulations with a certain *random* perimeter.

Section 3.5 I conclude this chapter by presenting some ongoing work and some research perspectives.

3.1 An introduction to the scaling limit of random maps

For (M_n) a sequence of random maps with n edges, the *scaling limit* of (M_n) consists in seeing M_n as a random compact metric space (where the vertices of the map are the points of the metric space and the distance between any two vertices is given by the graph distance between them), and in studying the convergence in distribution of M_n after suitably normalizing its distance. The scaling limit of (M_n) is then a random (non-trivial) distribution on compact metric spaces. This question was first formalized by Schramm for triangulations at the ICM in 2006 [Sch11] and was solved by Miermont [Mie13] and Le Gall [LG13] in 2013.

In this section, I introduce the material needed to state this result together with the main results in this field.

3.1.1 Gromov–Hausdorff and Gromov–Hausdorff–Prokhorov distances

In this chapter, we focus on the limit of random trees and random maps, viewed as *random metric spaces* equipped with the graph distance. Recall that the graph distance is the number of edges on a shortest path between any pair of vertices. For M a planar map, we always denote dist_M the graph distance on M.

To study the convergence of such objects, we need to equip the set of compact metric spaces with a distance. The most natural choice is the *Gromov–Hausdorff distance* defined as follows, and illustrated in Figure 3.1. We follow the presentation of [Mie09]. Let $\mathrm{X} = (X, d)$ and $\mathrm{X}' = (X', d')$ be two compact metric spaces. Given $C \subset X \times X'$, the *distortion* of C, denoted $\mathrm{dis}(C)$, is the quantity

$$\mathrm{dis}(C) = \sup\{|d(x,y) - d'(x',y')| : (x,x') \in C, (y,y') \in C\}.$$

A *correspondence* between X and X' is a set $C \subset X \times X'$ such that for every $x \in X$ there is $x' \in X'$ such that $(x,x') \in C$ and vice versa. We write $C(X, X')$ for the set of correspondences between X and X'. The Gromov–Hausdorff distance $d_{\mathrm{GH}}(\mathrm{X}, \mathrm{X}')$ between the metric spaces $\mathrm{X} = (X, d)$ and $\mathrm{X}' = (X', d')$ (or, rather, between the isometry classes of $\mathrm{X} = (X, d)$ and $\mathrm{X}' = (X', d')$) is:

$$d_{\mathrm{GH}}(\mathrm{X}, \mathrm{X}') = \frac{1}{2} \inf\{\mathrm{dis}(C) : C \in C(X, X')\}.$$

It can indeed be proved that this defines a distance on $\mathbb{K}$, the set of isometry classes of compact metric spaces. Moreover, the metric space $(\mathbb{K}, d_{\mathrm{GH}})$ is a *Polish space*.

The metric space associated to a map is naturally endowed with a measure, which corresponds to the uniform measure on the set of vertices. Hence, it makes sense to consider the scaling limits of maps as measured metric spaces rather than as metric spaces alone. The Gromov–Hausdorff distance can be extended to the *Gromov-Hausdorff-Prokhorov distance*, a distance between measured metric spaces, which roughly speaking coincides with the Gromov–Hausdorff distance for the metric part and with the Prokhorov distance for the measure part. I refer again to [Mie09, Section 6] for precise definitions and details, see also Figure 3.1 for some toy examples. For the sake of conciseness, I

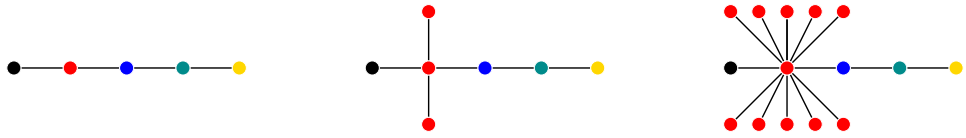

(a) (b) (c)

Figure 3.1. The Gromov–Hausdorff distance between any 2 of these 3 graphs is equal to 1. The colors of the vertices illustrate one correspondence realizing the minimal distortion. However, if we view them as metric spaces endowed with the uniform measure on their vertices, then the Gromov–Hausdorff–Prokhorov distance between (a) and (b) is much smaller than the distance between (a) and (c).

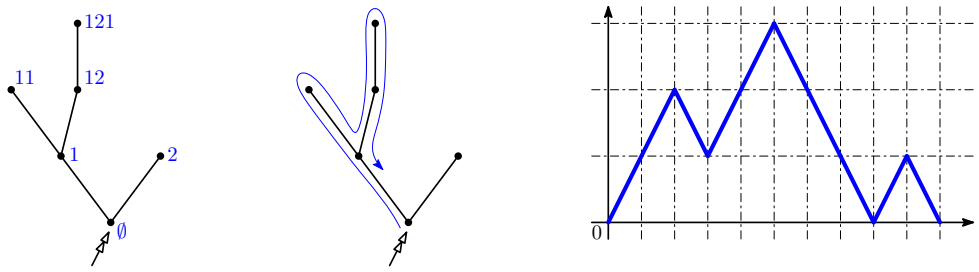

(a) (b) (c)

Figure 3.2. (a) Illustration of the Ulam-Harris-Neveu encoding, (b) the contour exploration and (c) the contour process.

state all convergence results in this chapter for the Gromov–Hausdorff distance, but they could be reinforced without difficulty by considering the Gromov–Hausdorff–Prokhorov distance instead.

3.1.2 Convergence of labeled Galton-Watson trees

Before I get to the scaling limit of maps, I would like to start with the scaling limit of rooted plane trees and of rooted plane labeled trees. I will restrict my attention here to unlabeled and labeled Galton-Watson trees.

Ulam-Harris-Neveu encoding and the contour: two useful ways to encode plane trees Let me start by introducing the Ulam-Harris-Neveu formalism to characterize rooted plane trees. Let $\mathcal{T}$ be the set of rooted plane trees and let $t \in \mathcal{T}$. The size of t, denoted $|t|$, is defined as its number of vertices. For a vertex v of t we write $k_t(v)$ for the number of children of v in t (k stands for "kids"). In the following we identify the vertex set $V(t)$ with the set of words given by the Ulam-Harris-Neveu encoding, see Figure 3.2(a). In this encoding, nodes are labeled by elements of $\bigcup_{n\geq 0} \mathbb{N}^n$, where $\mathbb{N}^0 = \{\emptyset\}$ by convention. Then:

- The root vertex ρ_t receives label $\emptyset$;
- The children of a vertex $v = v_1 v_2 \dots v_h \in \mathbb{N}^h$ receive labels $(vi, 1 \leq i \leq k_t(v))$ in the order given by the plane embedding.

For $v \in V(t)$, the *subtree of t rooted at v* is the subtree spanned by v and its descendants. In other words, if v is labeled $v_1 \dots v_h$, this subtree is the set of vertices whose labels have $v_1 \dots v_h$ as prefix.

It will also be useful to encode plane trees via their contour processes. For $t \in \mathcal{T}$, let us define the *contour exploration* $\beta : [\![0, 2|V(t)| - 2]\!] \to V(t)$, see Figure 3.2(b). We set $\beta(0) = \rho_t$. Then for $1 \leq i \leq 2|V(t)| - 2$, let $\beta(i)$ be the smallest (for the lexicographic order induced by the Ulam-Harris-Neveu encoding) child of $\beta(i-1)$ that has not been explored yet, if such a vertex exists. Otherwise, let $\beta(i)$ be the parent of $\beta(i-1)$. Since t has $2|V(t)| - 2$ "sides of edges", $\beta(2|V(t)| - 2) = \rho_t$.

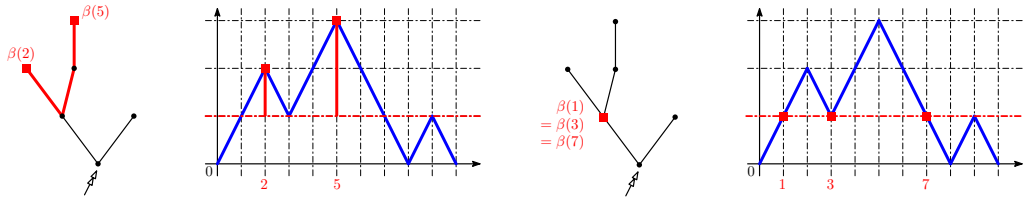

(a) Distances in the tree and in the contour process

(b) Identification of vertices of the tree via the contour process

Figure 3.3. How to retrieve metric properties of the tree via the contour process.

Then, the *contour process* C_t of t is the $\mathcal{C}([0, 2|V(t)|-2], \mathbb{R})$-function defined by (see Figure 3.2(c)):

$$C_t(i) = \mathrm{dist}_t(\beta(i), \rho_t) = |\beta(i)|, \text{ for } i \in [\![0, 2|V(t)| - 2]\!],$$

where $|\beta(i)|$ is the length of the Ulam-Harris-Neveu label of $\beta(i)$. Then, for $x \in [0, 2|V(t)| - 2]\backslash\mathbb{N}$, $C_t(x)$ is defined by linear interpolation.

It is easy to see that the tree can be retrieved from its contour function. In fact, the contour even encodes metric properties of the tree in a simple way. Indeed, one can check that, for $0 \leq i \leq j \leq 2|V(t)| - 2$ (see also Figure 3.3):

$$d_{C_t}(i, j) := C_t(i) + C_t(j) - 2\check{C}_t(i, j) = \mathrm{dist}_t(\beta(i), \beta(j)), \tag{3.1}$$

where for $0 \leq i \leq j \leq 2n - 2$, $\check{C}_t(i, j) = \min\{C_t(k) : k \in [\![i, j]\!]\}$. It follows, that the function d_{C_t} is a pseudo-distance on $[\![0, 2n - 2]\!]$ and that the set $[\![0, 2n - 2]\!]/\{d_{C_t} = 0\}$ is a metric space isometric to t.

This point of view will be fundamental in the rest of this chapter. Fix a positive continuous function f on $[0, 1]$, such that $f(0) = f(1) = 0$. We can define d_f a pseudo-distance on $[0, 1]$ as follows. For $0 \leq s \leq t \leq 1$:

$$d_f(s, t) := f(s) + f(t) - 2\check{f}(s, t), \quad \text{where } \check{f}(s, t) = \min\{f(u) : s \leq u \leq t\}. \tag{3.2}$$

Then the metric space $\mathcal{T}_f = ([0, 1]/\{d_f = 0\}, d_f)$ is a metric space, called a *real tree*. We again refer to [LG05] for more details. Note that $\mathcal{T}_f$ can also naturally be endowed with a measure by considering the push-forward of the Lebesgue measure on [0,1].

Galton-Watson trees and the Brownian Continuum Random Tree Let $\mu = (\mu_i)_{i\geq 0}$ be a probability measure on non-negative integers, called the *offspring distribution*. We assume throughout this section that $\mu_1 < 1$ and that $\sum_{i\geq 1} i\mu_i = 1$. The latter assumption makes μ a *critical* offspring distribution. Then, the law of a *Galton-Watson tree* with offspring distribution μ is the unique probability measure $\mathrm{LGW}(\mu)$ on the set of rooted plane trees such that (we refer to [LG05] for a formal construction):

- The number of children of the root vertex is distributed according to μ, i.e. $\mathrm{LGW}(\mu)(k_t(\emptyset) = i) = \mu_i$,
- Conditionally on $k_t(\emptyset) = i$, the subtrees rooted at $1, \ldots, i$ are independent and distributed according to $\mathrm{LGW}(\mu)$.

For $n \geq 0$, we denote $\mathrm{LGW}(\mu; n)$ the law of a Galton-Watson tree conditioned to have n vertices [1]. It is important to note that many families of classical random trees can be formulated as Galton–Watson trees. For instance, uniform plane trees, uniform Cayley trees, uniform binary trees, are all special cases of conditioned Galton-Watson trees (with μ being respectively the geometric distribution, the Poisson distribution and the distribution $(\delta_0 + \delta_2)/2$, where δ_i is the Dirac measure on $\{i\}$).

[1] I always restrict my attention to values of n for which such a conditioning makes sense, i.e. such that $\mathbf{P}\{|\mathrm{LGW}(\mu)| = n\} \neq 0$.

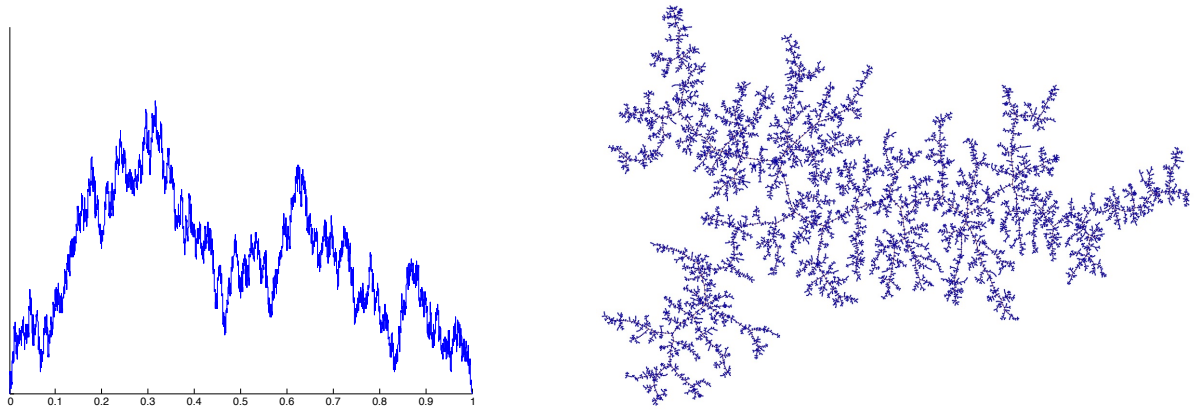

(a) Approximation of a Brownian excursion.

(b) Approximation of a Continuum Brownian tree.

Figure 3.4. A simulation of the contour of a large random tree and of a plane random tree. Both are due to Igor Kortchemski.

The scaling limit of Galton-Watson trees has been well understood since the work of Aldous. Let $\mathbf{e} = (\mathbf{e}(t), 0 \leq t \leq 1)$ be a standard Brownian excursion; that is, informally, a Brownian motion conditioned so that $\mathbf{e}(0) = \mathbf{e}(1) = 0$ and $\mathbf{e}(s) \geq 0$, for $0 \leq s \leq 1$). Then, the *Brownian Continuum Random Tree* (or *Brownian CRT*) $\mathcal{T}_\mathbf{e}$ is the real tree $[0,1]/\{d_\mathbf{e} = 0\}$, where $d_\mathbf{e}$ is defined as in (3.2) (see Figure 3.4 for some simulations). The following result characterizes the scaling limit of Galton-Watson trees with finite variance.

Theorem 3.1.1 (*[Ald93, LG05]*)

Let μ be a critical offspring distribution with finite variance σ^2. Let (T_n) be distributed according to $LGW(\mu; n)$. Then we have the following convergence:

$$\left(V(T_n), \frac{\sigma}{2\sqrt{n}}\mathrm{dist}_{T_n}\right) \xrightarrow{(\mathrm{d})} (\mathcal{T}_\mathbf{e}, d_\mathbf{e}),$$

for the Gromov–Hausdorff distance (I abuse notation and also write $d_\mathbf{e}$ for the projection of $d_\mathbf{e}$ on $\mathcal{T}_\mathbf{e}$).

Labeled Galton-Watson trees and the Brownian Snake A *rooted labeled plane tree* is a pair $\mathrm{t} = (t, \mathrm{d})$ where $t \in \mathcal{T}$ and $\mathrm{d} = (d(e), e \in E(t)) \in \mathbb{R}^{E(t)}$ give the *displacements* of labels along the edges of t. For a vertex $v \in V(\mathrm{t})$, its label $\ell_\mathrm{t}(v)$ is defined as the sum of the displacements along the edges on the unique path between v and ρ_t, see Figure 3.5(b). More formally, if $v = v_1 v_2 \dots v_h$ in the Ulam-Harris-Neveu encoding, then:

$$\ell_\mathrm{t}(v) = \sum_{i=1}^{h} d(\{v_1 \dots v_{i-1}, v_1 \dots v_i\}).$$

Recall the definition of the contour exploration, illustrated in Figure 3.2(b). Then, the label process Z_t of t is the $\mathcal{C}([0, 2|V(t)| - 2], \mathbb{R})$-function defined by:

$$Z_\mathrm{t}(i) = \ell_\mathrm{t}(\beta(i)), \text{ for } i \in [\![0, 2|V(t)| - 2]\!],$$

and by linear interpolation otherwise, see Figure 3.5(b).

A labeled Galton-Watson tree is then defined as follows. Fix an offspring distribution μ and a sequence $\nu = (\nu_k, k \geq 1)$, where for each $k \geq 1$, ν_k is a probability distribution on $\mathbb{R}^k$. Then, the law $\mathrm{LGW}(\mu, \nu)$ is the probability distribution on plane labeled trees $\mathrm{t} = (t, \mathrm{d})$ such that:

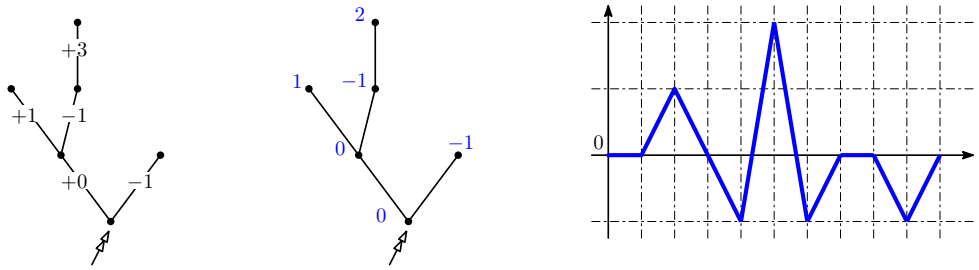

(a) (b) (c)

Figure 3.5. (a) An example of edges displacements, (b) the corresponding labels and (c) the label process.

- t is distributed according to $\mathrm{LGW}(\mu)$.
- Conditionally on t, d has the following law. Independently for each $u \in V(t)$, if u has k children, then the vector of displacements $(d(\{u, u1\}), \dots, d(\{u, uk\}))$ has law ν_k.

For $n \in \mathbb{N}$, we denote additionally $\mathrm{LGW}(\mu, \nu; n)$ the law of a labeled Galton-Watson tree sampled from $\mathrm{LGW}(\mu, \nu)$ and conditioned to have n vertices. To study the scaling limit of labeled Galton-Watson trees, we further require some hypotheses on ν. For $k \geq 1$ and $i \in [\![1, k]\!]$, denote ν_k^i the i-th marginal of ν_k (i.e. the distribution of the i-th component of a vector sampled according to ν_k). Then, we assume that $\mathbf{E}\left[|\nu_k^i|^4\right] < \infty$, for all $k \geq 1$ and all $i \in [\![1, k]\!]$ and additionally that at least one of the two following assumptions holds:

Assumption (A) The marginals of ν are *locally centered*, meaning that:

$$\int_{\mathbb{R}} x \mathrm{d}\nu_k^i(x) = 0 \qquad \text{for all } k \in \mathbb{N} \text{ and for all } 1 \leq i \leq k.$$

Assumption (B) The law μ has *bounded support* and ν is *globally centered*, namely

$$\sum_{k \geq 0} \mu(\{k\}) \sum_{i=1}^{k} \int_{\mathbb{R}} x \mathrm{d}\nu_k^i(x) = 0,$$

Then, we have the following scaling limit for labeled Galton-Watson trees:

Theorem 3.1.2 (*[JM05, Mie08a] for (A) and [Mar08] for (B)*)

Let μ be a critical offspring distribution with finite variance and let (T_n) be a sequence of labeled Galton-Watson trees distributed according to $\mathrm{LGW}(\mu)$ and satisfying either Assumption (A) or (B). Then, there exist explicit constants $a, b \in \mathbb{R}_+$ such that:

$$\left(\frac{a}{n^{1/2}} C_{\mathrm{T}_n}((2n-2)t), \frac{b}{n^{1/4}} Z_{\mathrm{T}_n}((2n-2)t)\right)_{0 \leq t \leq 1} \xrightarrow{(\mathrm{d})} (\mathbf{e}(t), Z(t))_{0 \leq t \leq 1},$$

where $Z(t)$ is the so-called Brownian snake *defined below.*

Conditionally given $\mathbf{e}$, $Z = (Z(t), 0 \leq t \leq 1)$ is a centered Gaussian process such that $Z(0) = 0$ and for $0 \leq s \leq t \leq 1$,

$$\mathrm{Cov}(Z(s), Z(t)) = \check{\mathbf{e}}(s, t), \qquad \text{where } \check{\mathbf{e}}(s, t) := \inf\{\mathbf{e}(u) \,|\, u \in [s, t]\}. \tag{3.3}$$

We may and shall assume that Z is a.s. continuous; see [LG99, Section IV] for a more detailed description of the construction of the pair $(\mathbf{e}, Z)$.

Let $\mathbf{e}$ a Brownian excursion, recall the definition of $d_{\mathbf{e}}$ given in (3.2). Let $0 \leq s \leq t \leq 1$ be such that $d_{\mathbf{e}}(s, t) = 0$, in other words s and t correspond to the same vertex of the continuum random tree $\mathcal{T}_{\mathbf{e}}$ encoded by $\mathbf{e}$.

Let then Z be a Brownian snake indexed by $\mathbf{e}$, it follows from the definition of a centered Gaussian process and from (3.3) that $\mathbb{E}[(Z_s - Z_t)^2] = 0$, which implies that $Z_s = Z_t$ a.s. This implies that Z can really be seen as a random process indexed by the random tree $\mathcal{T}_\mathbf{e}$. Informally, it is a Brownian motion on $\mathcal{T}_\mathbf{e}$.

Multitype Galton-Watson trees Let S be a finite set. A tree t is a S-type tree if each node $v \in V(t)$ has a type $s(v) \in S$. To define a Galton-Watson multitype tree, we need to fix a family of offspring distributions $\mu = (\mu_i)_{i\in S}$, such that for $i \in S$, μ_i is a distribution on $\mathbb{N}^{|S|}$. The process goes as follows: fix $i, j \in S$, for v a vertex of type i, denote $n_j^{(i)}$ the number of children of v of type j, then the vector $(n_1^{(i)}, \dots, n_{|}^{(i)}S|)$ has law μ_i. Furthermore, the ordering of the children of v is chosen uniformly among all the possible orderings and independently of anything else.

Labeled Galton-Watson multitype trees can be defined likewise. For any $i \in S$, any $k \in \mathbb{Z}_{>0}$ and any $\mathrm{s} := (s_1, \dots, s_k) \in S^k$, let ν_s^i be a probability distribution on $\mathbb{R}^k$. The labeling procedure goes as follows. Let v be a vertex of type i with k children and such that the vector of the types of its children is given by s, i.e. $\Big(s(v1), \dots, s(vk)\Big) = \mathrm{s}$. Then, the vector of displacements from v to its children is distributed according to ν_s^i, in other words:

$$\Big(d(\{v, v1\}), \dots, d(\{v, vk\})\Big) \sim \nu_\mathrm{s}^i. \tag{3.4}$$

For labeled Galton-Watson multitype trees conditioned to have a fixed number of vertices of a given type and satisfying Assumption (A), results similar to Theorem 3.1.2 have been obtained in [Mie08a], with slightly stronger assumptions on the moments of the marginals. I do not detail them here and refer the interested reader to the original publication.

3.1.3 Scaling limit of uniform quadrangulations

The Cori-Vauquelin-Schaeffer bijection The starting point of the study of random planar maps is the Cori-Vauquelin-Schaeffer bijection [CV81, Sch98] between rooted quadrangulations and some labeled trees, whose main properties are gathered in the following theorem and illustrated in Figure 3.6.

Theorem 3.1.3 (*Schaeffer's bijection [Sch98]*)

There exists an explicit construction Φ_{CVS} between the set $\mathcal{Q}_{n+1}^\bullet$ of rooted and pointed quadrangulations with $n+1$ vertices and the set $\mathcal{T}_n^{\mathrm{CVS}}$ of rooted labeled plane trees with n vertices satisfying the following properties:

- *The root is labeled 0 and is decorated by $+$ or $-$.*
- *For $v \in V(t)$, let $\ell(v)$ be its label. Then, for any $\{u, v\} \in E(t)$, $\ell(u) - \ell(v) \in \{-1, 0, 1\}$.*

For $\mathrm{q} = (q, v^\bullet) \in \mathcal{Q}_{n+1}^\bullet$, if $\mathrm{t} = \Phi_{\mathrm{CVS}}(\mathrm{q})$, then $V(q)\backslash\{v^\bullet\}$ is in bijection with $V(\mathrm{t})$. Moreover, for any $v \in V(\mathrm{t})$:

$$\mathrm{dist}_\mathrm{q}(v, v^\bullet) = \ell(v) - \min\{\ell(u) \text{ for } u \in V(\mathrm{t})\} + 1,$$

where we identify a vertex of t with its image in q.

We only sketch the construction from a pointed quadrangulation to a well-labeled tree and refer the reader to [Sch98, MM06] for details. We follow here the construction presented in [MM06] which differs slightly from the original construction but is clearly equivalent. The construction is illustrated in Figure 3.6. Fix $\mathrm{q} = (q, v^\bullet) \in \mathcal{Q}^\bullet$. We first label all the vertices of q by their (graph) distance to $v^\bullet$. Then, in each face of q, depending on the configuration of labels of its incident vertices, we add a "green edge", see Figure 3.6(b)-(c). Notice that since a quadrangulation is bipartite, the labels of two incident vertices differ exactly by one, so that each face is of one of the two types displayed in Figure 3.6(b). The set of green edges turns out to form a spanning tree of $V(\mathrm{q})\backslash\{v^\bullet\}$. Its root corner is defined as the image of the root corner of q and its root is decorated by $+$ if the root edge

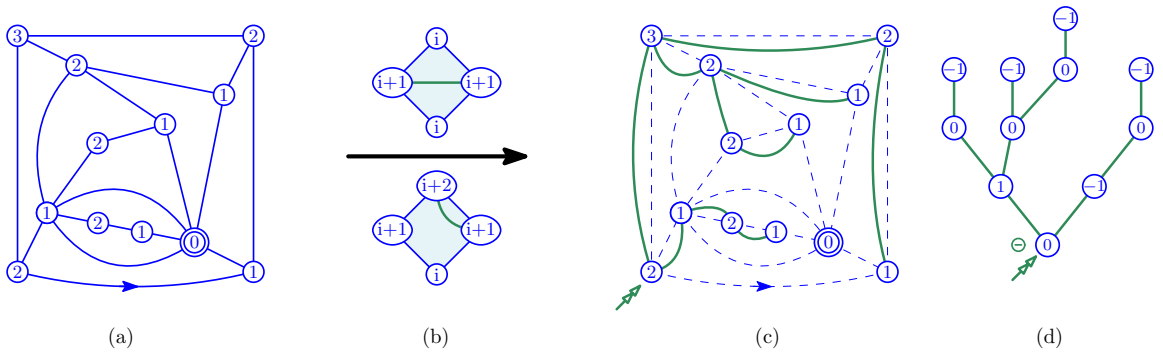

Figure 3.6. Illustration of the Cori-Vauquelin-Schaeffer bijection. (a) A rooted quadrangulation q with a marked vertex (represented by the double disk). Vertices are labeled by their distance to the marked vertex. (b) Description of the local rules: in each face, we add an edge. (c) Construction of Φ_{CVS} on q. (d) The labels of the tree are shifted so that its root is labeled 0.

of q was labeled $(i, i+1)$ for $i \in \mathbb{N}$ and by $-$ otherwise (in Figure 3.6, the root of q being labeled $(2,1)$, the root of $\Phi_{\mathrm{CVS}}(q)$ is decorated by $-$).

Convergence to the Brownian map Chassaing and Schaeffer [CS04] studied the labeled trees obtained via Schaeffer's bijection and proved that the radius[2] of uniform quadrangulations is of order $n^{1/4}$, so that the right scaling to study uniform quadrangulations is $n^{1/4}$. Moreover, they characterized the limiting distribution of the rescaled radius and of the rescaled profile [3] of uniform quadrangulations.

In the following years, uniform quadrangulations were intensely studied. This research activity culminated in the following result by Miermont and Le Gall:

Theorem 3.1.4 (*Miermont [Mie13], Le Gall [LG13]*)

Let (M_n) be a sequence of uniform planar quadrangulations with n vertices. Then:

$$\left(V(M_n), \left(\frac{9}{8n}\right)^{1/4} \mathrm{dist}_{M_n}\right) \xrightarrow{(\mathrm{d})} (M, d^*),$$

where (M, d^*) is the Brownian map*, defined as follows.*

Recall the definition of $(\mathbf{e}, Z)$ of Theorem 3.1.2. Then, for $0 \le s \le t \le 1$, first set:

$$D^\circ(s,t) = Z(s) + Z(t) - 2\max\left(\min_{u\in[s,t]} Z(u), \min_{u\in[t,1]\cup[0,s]} Z(u)\right)$$

Next let D^* be the largest pseudo-distance on $[0,1]$ such that $D^* \le D^\circ$, and such that for all $x, y \in [0,1]$, if $d_{\mathbf{e}}(x,y) = 0$, then $D^*(x,y) = 0$. Then, let $M = [0,1]/\{D^* = 0\}$ and let d^* be the push-forward of D^* to M. The Brownian map *is (the law of) (M, d^*).*

For the proof of this result, I refer the interested reader to the original publications, or to Miermont's Saint Flour lecture notes [Mie], which are a very good entry point to the literature. Let me nonetheless mention that, very roughly speaking, the main difficulty in extending Chassaing and Schaeffer's result to a Gromov–Hausdorff type result is that Schaeffer's bijection does not easily give good approximation of the distance between any two vertices. Indeed, only the distance between any vertex and the root vertex is well-controlled. Major results about geodesics in uniform quadrangulations were obtained by Le Gall in [LG10]. Other works include [MM06], where the term "Brownian map" appears for the first time, [LG07], where it is established that the Hausdorff dimension of the Brownian map is 4, [LGP08] and [Mie08b], which proved that the topology of the Brownian map is

[2] The radius is the maximal distance between a vertex and the root vertex.

[3] The profile is the function that gives the number of vertices at each possible distance from the root

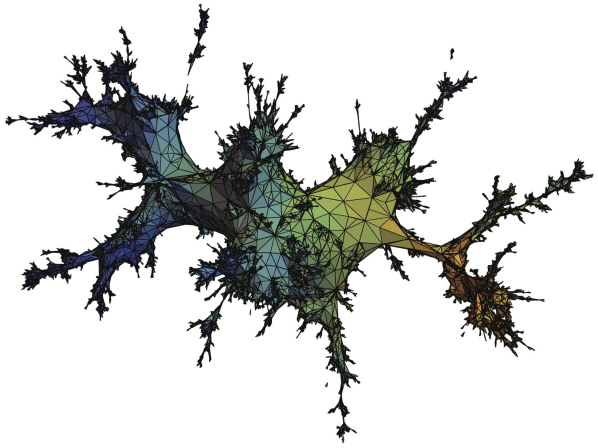

Figure 3.7. A simulation by Igor Kortchemski of a large random simple triangulation, which gives an approximation of the Brownian map.

that of the 2-dimensional sphere. Hence, the Brownian map is really a 2-dimensional analogue of the Brownian motion (which has Hausdorff dimension 2 and the topology of a line) and is a fractal-like surface as illustrated on Figure 3.7.

3.1.4 Universality of the Brownian map

It is widely believed that the scaling limit of any "reasonable" families of maps[4] should also be the Brownian map. In fact, in his original paper, Le Gall studied the scaling limit not only of uniform quadrangulations but also of p-angulations for $p \in \{3\} \cup 2\mathbb{N}$. For $p \neq 4$, the role of the Schaeffer bijection is played by the Bouttier–Di Francesco–Guitter bijection [BDFG04] described in Section 3.3.1.

A key point in the argument of [LG13] to extend the result from quadrangulations to triangulations is the following. Since we know that the distribution on quadrangulations is invariant by rerooting, then by Theorem 3.1.4, a continuum analogue of this result must also be true, and thus the Brownian map is invariant under rerooting. Hence, the law of the distance between the root and a uniform vertex is equal to the law of the distance between any two uniform vertices. By a tricky argument, Le Gall used this observation to prove convergence of uniform triangulations. His argument has become a standard tool to obtain the scaling limit of random maps using the invariance by rerooting of the Brownian map, which has been successfully applied for quadrangulations without vertices of degree one [BLG13], for simple triangulations and quadrangulations [10] (presented in Section 3.2), for general maps [BJM14], for bipartite maps [Abr16], for bipartite maps with prescribed degree sequence [Mar18b] and for p-angulations for other values of p in [12] (presented in Section 3.3).

Very informally (see Section 4 of [10] for a precise statement), in order to prove a result equivalent to Theorem 3.1.4 for another family (M_n) of maps, thanks to Le Gall's argument, it is now enough to prove the following :

(1) The random rooted map M_n must be encoded by a labeled tree T_n such that vertices of the maps are in correspondence with a subset of the vertices of the tree.
(2) The scaling limit of the contour and label process of T_n must be a Brownian excursion and a Brownian snake.

[4] An enumerative way to define a "reasonable family" of maps is to consider a family for which the enumerative coefficients have an asymptotic behavior in $\kappa \rho^n n^{-5/2}$, for some constants κ and ρ. (Details about the asymptotic enumeration of maps will be given in Chapter 4). It is indeed known that some "unreasonable" families of maps, such as the uniform stack-triangulations studied during my PhD [3], admit the Brownian CRT as scaling limit.

(3) The labels on the vertices of the tree must encode certain metric properties of the map (as in Schaeffer's bijection).
In particular the distance *in the map* between a vertex and the root must be equal (up to $o(n^{1/4})$ correction) to the difference of labels *in the tree* between the image of this vertex and the minimum label of the tree.

(4) The vertex with minimum label in the tree must correspond to a vertex in the map whose distribution is asymptotically uniform on $V(M_n)$.

This framework will be instrumental in the proof of convergence of simple triangulations and p-angulations (for odd $p \geq 5$) that I will sketch in the next two sections.

3.1.5 Embedding of the Brownian map and Liouville Quantum Gravity

Studying the scaling limit of uniform maps is in a sense a natural way to endow the sphere with a random metric structure, by first discretizing it and then passing to the limit. However, even if the Brownian map is known to be homeomorphic to the sphere, homeomorphism equivalence is too weak, for example, to deduce conformal information or to prove dimensional scaling relations. For these, a canonical embedding of the Brownian map in $\mathcal{S}^2$ is needed (or at least would be very useful). To conclude this introduction, I would like to briefly survey some results proving that such an embedding can be constructed via the theory of Liouville Quantum Gravity (LQG).

For $\gamma \in [0, 2)$, the γ-Liouville quantum gravity constructed by Duplantier and Sheffield [DS11] (see also [Gar12]) is a measure on a surface which is roughly defined as the exponential of the so-called Gaussian Free Field (GFF). Such a definition does not make rigorous sense, since the Gaussian Free Field is not a function but a distribution, so that one of the main contributions of [DS11] was to prove that the exponential of a sequence of regularized versions of the GFF converges. (I should mention that LQG was introduced in the physics literature by Polyakov [Pol81] in the eighties. There is also another way to define LQG by means of the Gaussian Multiplicative Chaos initially studied by Kahane in [Kah85], and LQG is studied with this perspective by Berestycki, David, Kupiainen, Rhodes and Vargas, among others, see for instance [Ber17, DKRV16, Var17]).

A surface equipped with a γ-LQG measure does not a priori come with a metric structure compatible with this measure. Note that this is somehow the opposite to the Brownian sphere, which comes with a metric but does not come with a measure (since there is no canonical embedding of the Brownian map in the sphere, the measure on the Brownian map cannot be projected onto a measure on the sphere). In an impressive series of papers [MS15, MS16a, MS16b] based on earlier work by Sheffield [She16a] and joint work with Duplantier [DMS14], Miller and Sheffield prove that the Brownian map and $\sqrt{8/3}$-LQG are equivalent. By this we mean that they can couple these two objects naturally enough so that one determines the other. I will not say anything more about this construction, but refer the interested reader to the original papers (or for a soft introduction, to Miller's talk at the ICM 2018, which presents the intuition underlying their construction [Mil]).

However, the construction of Miller and Sheffield lives only in the continuum world. It would be natural to try to obtain an embedding of the Brownian map as the limit of the embeddings of discrete maps. It turns out that a very natural way to embed canonically a map in the sphere is given by the Koebe-Andreev-Thurston theorem (see, e.g., [Ste05], Chapter 7), which guarantees that a map can be represented by the tangency graph of a circle packing, see Figure 3.9. For simple triangulations, this circle packing is unique up to Möbius transformations, and hence gives a canonical embedding of simple triangulations in the sphere, see Figure 3.8.

It is still an open problem to know whether a sequence of "circle-packed" random simple triangulations converges to LQG. But very recently, Holden and Sun [HS19] have proved a result similar in spirit (see also [GHS19] for a survey on the connection between LQG and random planar maps). They established that triangulations embedded via the so-called Cardy embedding converge to $\sqrt{8/3}$-LQG. This significant result builds on many previous results, among them [13], which I will present in Section 3.4.

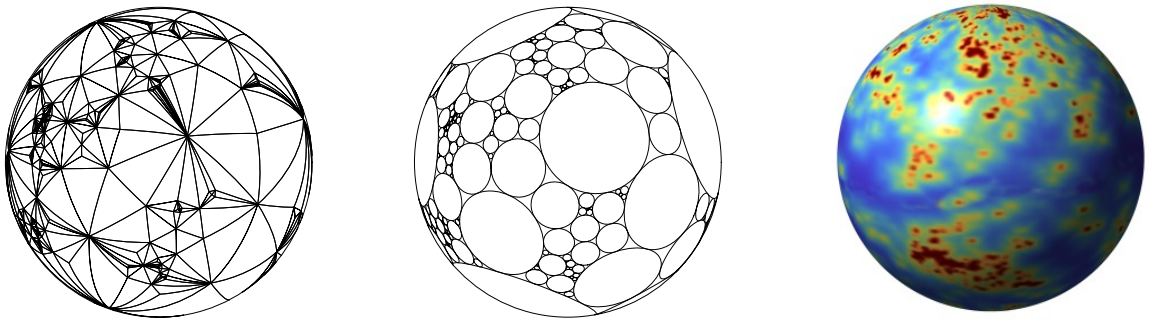

(a) A simple triangulation embedded in the sphere,

(b) the corresponding simple packing,

(c) and a simulation of $\sqrt{8/3}$-LQG (courtesy of Timothy Budd)

Figure 3.8. Simulations to illustrate the conjecture that circle-packed simple triangulations should converge to $\sqrt{8/3}$-LQG. The variation of colors in (c) indicates the intensity of the measure. Figures (a) and (b) are obtained via Ken Stephenson's "Circle Pack" software.

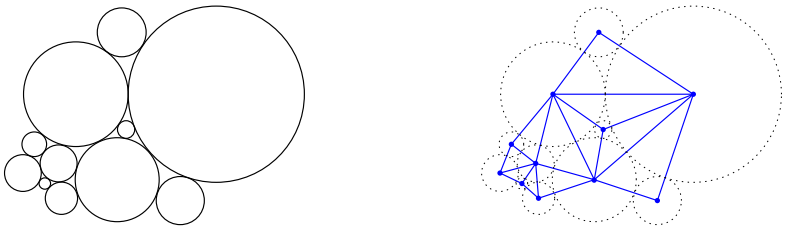

(a) A circle packing,

(b) and, the corresponding simple triangulation (with a boundary).

Figure 3.9. Illustration of the correspondence between circle packings and simple triangulations.

3.2 Scaling limit of simple triangulations

I present in this section the main results of [10] and give some ideas of their proofs. This article is dedicated to the study of the scaling limit of uniform simple planar triangulations and quadrangulations, where we recall that a planar map is *simple* if it has neither loops nor multiple edges. The results and the proofs being similar for triangulations and quadrangulations, I only deal with simple triangulations here and refer the reader interested in quadrangulations to [10].

The motivation for studying simple triangulations was twofold. First, as already mentioned in Section 3.1, it is widely believed that the Brownian map is a universal limiting object. When we started working on this problem, the only models for which the convergence towards the Brownian map had been established were p-angulations for $p \in \{3\} \cup 2\mathbb{N}$. In [LG13], Le Gall asked whether these results could be extended to simple triangulations. It was indeed natural to investigate the scaling limit of models of maps with connectivity constraints, and simple triangulations are, in some sense, the simplest model of such maps. Second, the case of simple triangulations holds additional interest due to the Koebe-Andreev-Thurston theorem, as already discussed in Section 3.1.5 and illustrated in Figures 3.9 and 3.8.

I now head straight to the result.

Theorem 3.2.1 (*Theorem 1 of [10]*)

For $n \geq 3$, let M_n be a uniformly random simple rooted triangulation with n vertices. Then, as $n \to \infty$, we have:

$$\left(V(M_n), \left(\frac{3}{4n}\right)^{1/4} \mathrm{dist}_{M_n}\right) \xrightarrow{(\mathrm{d})} (M, d^*),$$

for the Gromov–Hausdorff distance, where (M, d^*) is the Brownian map introduced in Section 3.1.3.

To prove this theorem, the first idea might be to use Bouttier-di Francesco–Guitter bijection between triangulations and mobiles and to see how its restriction to simple triangulations behaves. This is natural, because this bijection is known to be well-suited to study distances in maps which is exaclty what we need here. Such an approach was carried out for simple quadrangulations by Bouttier and Guitter in [BG10]. In this work, they obtained fine metric properties of large random quadrangulations. But, considering simple rather than general quadrangulations puts many constraints on the labeled trees obtained via Schaeffer's bijection. Hence, studying their scaling limit seems hopeless.

With Addario-Berry, we adopted another strategy and started from a bijection well-suited for simple triangulations (the Poulalhon-Schaeffer bijection [PS06]) but apparently ill-suited to study distances in maps. The main (and unexpected) contribution of [10] is to prove that in fact this bijection encodes some distance information. Indeed, a simple functional of the blossoming tree gives an approximation of some metric properties up to an error which turns out to be negligible in the scaling limit. The proof of this result interlaces some combinatorial arguments together with some probabilistic limit theorems.

I describe in the rest of this section some ideas of the main steps of the proof. As already discussed in Section 3.1.4, the proof relies on the convergence of quadrangulations obtained by Miermont and Le Gall and by the general framework designed by Le Gall. So, I will discuss only how to establish points (1) and (3) of Section 3.1.4 ((4) is immediate in this setting and (2) can be obtained as a special case of Theorem 3.3.5 discussed in the next section). I first present a reformulation of the Poulalhon-Schaeffer bijection [PS06]. This reformulation transforms blossoming trees into labeled trees, more suited for our purposes. I then explain how these labels encode some metric properties of maps via a study of so-called leftmost paths.

3.2.1 A reformulation of the Poulalhon–Schaeffer bijection

Let $\mathcal{T}^{(2)}$ be the set of 2-blossoming trees, that is, planetrees such that each vertex carries two opening stems, and let $\mathcal{T}_n^{(2)}$ be the subset of $\mathcal{T}^{(2)}$ with n vertices. In [PS06], Poulalhon and Schaeffer prove the following result[5]:

Theorem 3.2.2 (*Poulalhon–Schaeffer bijection*)

There exists a $(4n-2)$-to-2 constructive mapping between $\mathcal{T}_n^{(2)}$ and the set of simple triangulations with $n+2$ vertices.

This result is in fact one of the first examples of a blossoming bijection as described in Chapter 2. It is illustrated in Figure 3.10. However, since elements of $\mathcal{T}^{(2)}$ do not carry closing stems, the definition of the closure procedure given in Section 2.2.1 must be adapted, as already described on page 40. Because the resulting map is a triangulation, instead of defining a local closure as a

[5] Their result is in fact not stated in this exact form. They first prove that there exists a bijection between *balanced* 2-blossoming trees and simple triangulations. Then, they prove that given a (not necessarily balanced) 2-blossoming tree T, there exist exactly two corners c_1 and c_2 of T such that re-rooting T at c_1 or c_2 produces a balanced 2-blossoming tree. Since an element of $\mathcal{T}_n^{(2)}$ has $2n-4$ corners, this yields Theorem 3.2.2.

matching between an opening and a closing stem, we define it as a matching between an opening stem and a corner of the tree with the constraint that the face created is triangular.

After performing all possible local closures, some opening stems remain unmatched. To end the construction, two additional vertices are added and the remaining stems are transformed into edges to these vertices. Since the details of the construction are not needed for the rest of this presentation, I refer the interested reader to Figure 3.10 for a general idea of it or to the original paper for details.

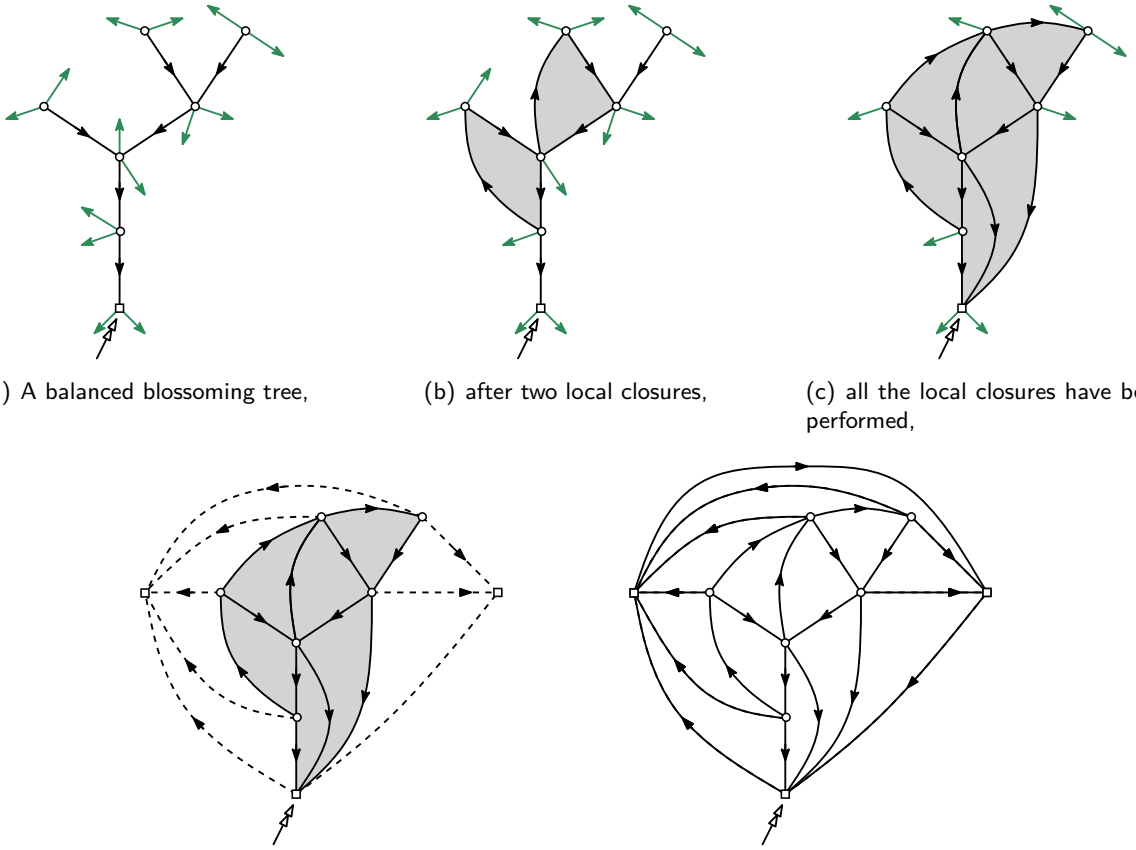

(a) A balanced blossoming tree,

(b) after two local closures,

(c) all the local closures have been performed,

(d) and, the remaining stems are matched to two additional vertices.

(e) The resulting rooted simple triangulation, endowed with its unique minimal 3-orientation

Figure 3.10. The closure of a balanced tree with $n = 7$ vertices into a simple triangulation.

We now reformulate the Poulalhon–Schaeffer bijection as a bijection between simple triangulations and validly-labeled trees, defined below.

Definition 3.2.3

A validly-labeled tree *is a labeled tree* T *such that all displacements along its edges belong to* $\{-1, 0, 1\}$ *and for all* $v \in V(T)$*, listing the children of* v *as* $v_1, \dots, v_k$ *in the lexicographic ordering, the sequence* $d_{\{v,v_1\}}, \dots, d_{\{v,v_k\}}$ *is non-decreasing.*

The set of validly labeled trees with n *vertices is denoted* $\mathcal{T}_n^{\mathrm{vl}}$*.*

Fix an element T of $\mathcal{T}^{(2)}$. First, perform a contour exploration of T starting from its root corner, which is labeled 0, and label its subsequent corners according to the rules displayed in Figure 3.11(a). Then, label each vertex by the minimum label of one of its incident corners and erase both the opening stems and the labels of corners. It is easily seen that this construction is a bijection between $\mathcal{T}_n^{(2)}$ and $\mathcal{T}_n^{\mathrm{vl}}$. Hence Point (1) of Section 3.1.4 is established.

The uniform distribution on validly-labeled trees of fixed size admits an equivalent description as a Galton-Watson process with random displacements as defined in Section 3.1.2. However, for the label

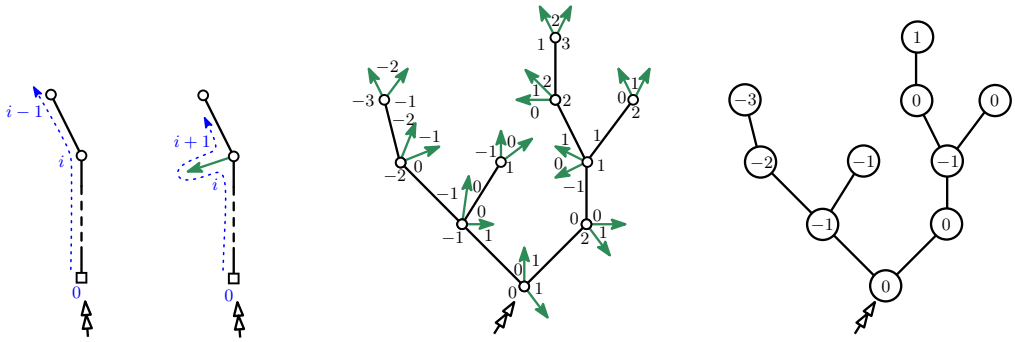

(a) The rules to label the corners of a 2-blossoming tree.

(b) The corner labeling of a 2-blossoming tree

(c) The resulting validly-labeled tree

Figure 3.11. The correspondence between a 2-blossoming tree and a validly-labeled tree.

process, new difficulties arise. Recall the notation ν_k given in the introduction, then in our setting ν_k is the uniform distribution over non-decreasing vectors $(d_1, \dots, d_k) \in \{-1, 0, 1\}^k$. In our setting, neither Assumption (A) nor Assumption (B) preceding Theorem 3.1.2 is satisfied. The marginals of ν are clearly not locally centered: observe, for instance, that $\int_{\mathbb{R}} x \mathrm{d}\nu_2^1(x) = -1/3$. Moreover, ν is globally centered but the support of μ is not finite. Using some "symmetrization techniques" that I will present in Section 3.3, we were nevertheless able to prove the following convergence of the contour and label processes of validly labeled plane trees towards the Brownian excursion and the Brownian snake. The following theorem establishes Point (2) of Section 3.1.4:

Theorem 3.2.4 (*Proposition 6.1 of [10]*)

For $n \geq 1$ let T_n be uniformly random validly labeled tree with n vertices. Then as $n \to \infty$,

$$\Big((3n)^{-1/2} C_{\mathrm{T}_n}((2n-2)t), (4n/3)^{-1/4} Z_{\mathrm{T}_n}((2n-2)t)\Big)_{0 \leq t \leq 1} \xrightarrow{(\mathrm{d})} (\mathbf{e}(t), Z(t))_{0 \leq t \leq 1}, \quad (3.5)$$

for the topology of uniform convergence on $C([0,1], \mathbb{R})^2$.

3.2.2 A study of leftmost paths

In view of Point (3) of Section 3.1.4, a key point to prove is that the label of a vertex of a validly labeled tree approximates the distance between the corresponding vertex in the map and the root vertex. To do that, we use *leftmost paths* extensively.

Fix M a simple triangulation. For the rest of this section, we always assume that M is endowed with its unique minimal α_3-orientation O as defined in Section 1.4.3, see Figures 3.10(e) and 3.12(b). Recall that this means that each edge of M is oriented in such a way that:

- for $v \in V(M)$ not incident to the root face, $\mathrm{out}(v) = 3$,
- for $v \in V(M)$ incident to the root face, $\mathrm{out}(v) = 1$,
- there is no counterclockwise cycle in the embedding of M in the plane such that its root face is the unbounded face.

The following classical definition is illustrated in Figure 3.12.

Definition 3.2.5

For M as above, let $e = uw \in O$, then the leftmost path *from e is the unique oriented path $(u = u_0, w = u_1, \dots, u_k)$ such that for $1 \leq i < k$, $u_i u_{i+1} \in O$ and all the edges between $u_{i-1}u_i$ and $u_i u_{i+1}$ – when turning clockwise around u_i – are oriented towards u_i.*

It follows from a simple counting argument (based on Euler's formula and on the properties of the 3-orientation) that a leftmost path reaches the root vertex ρ_M of M and that a leftmost path stopped

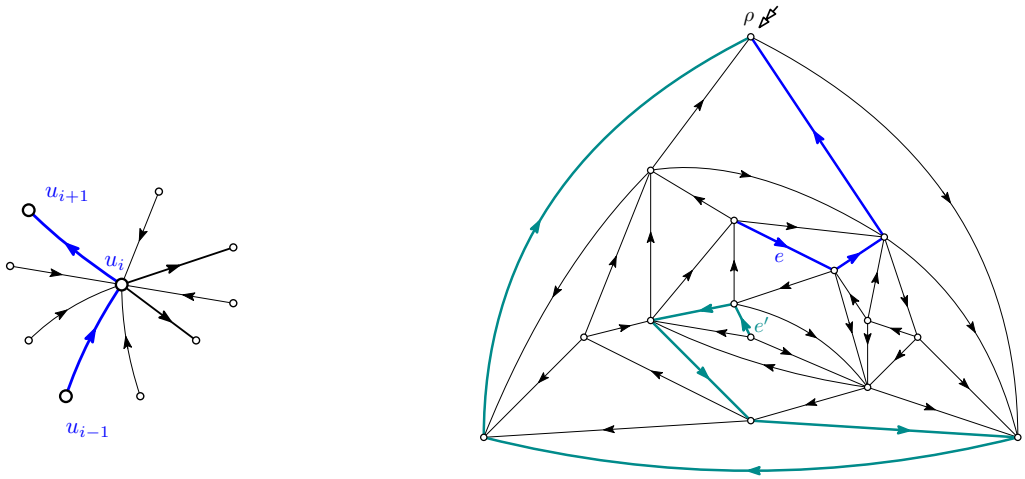

(a) Illustration of the local rule.

(b) Two examples of leftmost paths.

Figure 3.12. Illustration of the definition of leftmost paths. A simple triangulation endowed with its minimal α_3-orientation is represented on (b), together with two leftmost paths, started at e and e' respectively.

at its first visit to ρ_M is self-avoiding. In the following, we always consider that *leftmost paths are stopped at their first visit to* ρ_M. A study of leftmost paths and of the reformulation of the bijection given in the previous section allows us to prove the following result:

Lemma 3.2.6

Let M be a simple triangulation and let $v \in V(M)$ be a vertex which is not incident to the root face of M. By a slight abuse of notation, we identify v with its image in the validly-labeled tree T corresponding to M and denote by $\ell(v)$ its label in T. Then:

$$|LMP(v) - \ell(v)| \leq 2,$$

where $LMP(v)$ is the length of the shortest leftmost path among the three that start from one of the outgoing edges of v.

To prove Point (3), it hence remains to establish that – up to a $o(n^{1/4})$ correction – a leftmost path started at a vertex u is a geodesic path between u and ρ_M. Indeed, we prove the following result:

Theorem 3.2.7 (*Theorem 8.1 of [10]*)

Let M_n be uniformly random simple triangulation with n vertices. Then, with the same notation as above, for all $\epsilon > 0$,

$$\lim_{n\to\infty} \mathbf{P}\left\{\exists\, v \in V(M_n) : \mathrm{dist}_{M_n}(v, \rho_{M_N}) \notin [\ell(v) - \epsilon n^{1/4}, \ell(v) + 2]\right\} = 0\,.$$

Let me mention that leftmost paths were introduced well before our work, and similar constructions already appear in the original work of Schnyder [Sch89]. But the fact that leftmost paths of minimal orientations are close to being geodesics was quite a (welcome) surprise[6].

I now sketch the proof of Theorem 3.2.7. First, for any $v \in V(M_n)$, $LMP(v)$ is clearly an upper bound for $\mathrm{dist}_{M_n}(v, \rho_{M_N})$. Hence, Lemma 3.2.6 implies that $\mathrm{dist}_{M_n}(v, \rho_{M_N}) \leq \ell(v) + 2$ *deterministically*. To prove the lower bound, I adopt a slightly different and simpler presentation from the one of the original paper, and in particular do not introduce the so-called *winding number*.

[6] A very naive but illustrative way to find this result natural *a posteriori*, is that minimal orientations tend to spiral clockwise, so that the shortest oriented path to the root must turn left as much as possible !

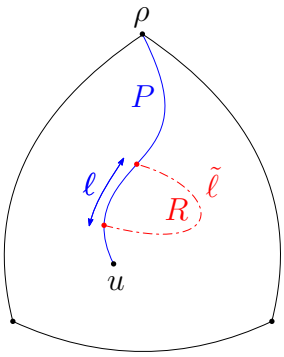

(a) Excursion of type (1): $\tilde{\ell} \geq \ell + 1$

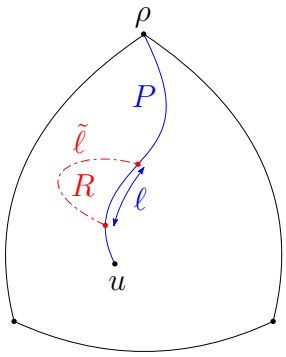

(b) Excursion of type (2): $\tilde{\ell} \geq \ell$.

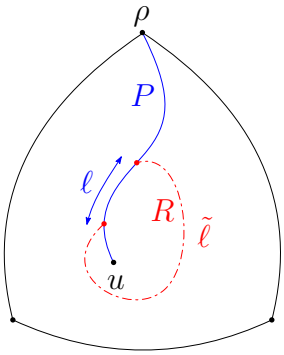

(c) Excursion of type (3): $\tilde{\ell} \geq \ell + 3$.

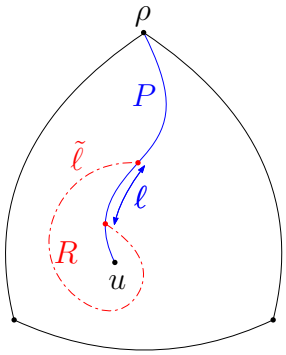

(d) Excursion of type (4): $\tilde{\ell} \geq \ell - 2$.

Figure 3.13. The different possible types for an excursion R away from P. For each type, we indicate a lower bound for the length $\tilde{\ell}$ of the excursion in term of the length ℓ of the corresponding subpath of P.

Let u be a vertex of M_n, let P be the shortest leftmost path starting from u and let Q be a geodesic path from u to ρ_M. We will compare the lengths of P and Q.

We start with a combinatorial analysis. The path Q can be decomposed into subpaths $R_1, R_2, \ldots$, such that some are subpaths of P and the others are called "excursions away from P". These excursions can be of 4 types, represented in Figure 3.13, depending on whether they leave P and return to P on its left or on its right. A counting argument (again based on Euler's formula, on the properties of the 3-orientation and on the definition of leftmost paths) gives some lower bounds for the lengths of these excursions, listed in Figure 3.13. In particular, these bounds ensure that a geodesic path cannot have excursions of type 1 and 3, that each excursion of type 2 can be replaced by the corresponding subpath of P without modifying the length of Q and that the only possible *shortcuts* are the excursions of type 4. However, each of these shortcuts is at worst only 2 edges shorter than the corresponding subpath of P.

We now proceed by contradiction and assume that $|Q| < |P| - 2\epsilon n^{1/4}$. The combinatorial analysis we just carried out implies then that Q has at least $\epsilon n^{1/4}$ excursions away from P of type 4. Furthermore, since Q is a geodesic path, it is in particular shorter than P, hence of order $\mathcal{O}(n^{1/4})$ (with high probability by Lemma 3.2.6 and Theorem 3.2.4). Since the sum of the lengths of its excursions of type 4 is a lower bound for the length of Q, it implies that a positive proportion of the $\epsilon n^{1/4}$ excursions of type 4 of Q has bounded length (again with probability tending to one). Let R be such an excursion. Then, concatenating R with the corresponding subpath of P forms a cycle of length at most $2|R| + 2$ that separates u from the root face. The convergence stated in Theorem 3.2.4 allows then to use properties of the Brownian snake to prove that there exists one such cycle that separates M into 2 macroscopic components. But, since the probability that a simple triangulation can be separated into two macroscopic components by a cycle of bounded length tends

to 0, this concludes the proof of Theorem 3.2.7.

□

3.3 Symmetrization of trees and scaling limit of odd-angulations

I present in this section the results of [12] obtained in collaboration with Louigi Addario-Berry. In this article, we establish an invariance principle for the scaling limit of *non-necessarily bipartite* regular critical Boltzmann maps, with bounded face degree[7]. In particular, we obtain the following result for the scaling limit of uniform p-angulations for $p \in 2\mathbb{N}+1$ and $p \geq 5$.

Theorem 3.3.1 (*Theorem 1 of [12]*)

Let $p \geq 5$ be an odd *integer and let (M_n) be a sequence of random maps, such that for any $n \geq 1$, M_n is a uniform p-angulation with n vertices. Then there exists a constant C_p such that, as n goes to infinity,*

$$\left(V(M_n), \left(\frac{C_p}{n}\right)^{1/4} \mathrm{dist}_{M_n}\right) \xrightarrow{(\mathrm{d})} (M, d^*),$$

for the Gromov–Hausdorff topology and where (M, d^*) is the Brownian map.

The main motivation for our work is again the conjecture that the Brownian map is a universal limiting object for many families of planar maps, and to address the missing values of p in the results of convergence of p-angulations established in [LG13]. Moreover, recall that a *bipartite* map is a map whose vertices can be partitioned into two sets, say B and W such that all edges in the map have one extremity in B and one extremity in W. It is easy to see that a planar map is bipartite if and only if all its faces have even degree. With the notable exception of [BJM14] (which does not control the degree of faces of the maps considered), all the results mentioned in Section 3.1.4 deal with either bipartite maps or with triangulations.

As with most results in this field, our work relies on a bijection between planar maps and labeled multitype trees: the Bouttier–Di Francesco–Guitter bijection [BDFG04] plays this role in our case. Again following the approach presented in Section 3.1.4, the only new result needed to prove Theorem 3.3.1 is that the encoding functions of multitype labeled trees associated to p-angulations by that bijection converge to the Brownian snake. We again follow the approach presented in Section 3.1.2. However, neither assumptions (A) or (B) hold in our setting. Our main result consists in relaxing Assumption (A) into the assumption (C) stated in the following theorem and satisfied in our setting:

Theorem 3.3.2 (*Follows directly from Theorem 2 of [12]*)

Let μ be a critical offspring distribution with finite variance and let (T_n) be a sequence of (monotype) labeled Galton-Watson trees distributed according to $\mathrm{LGW}(\mu, \nu)$ and satisfying the following assumption:

Assumption (C): *For any $k \in \mathbb{N}$, the distribution ν_k is* centered, *meaning that*

$$\sum_{i=1}^{k} \int_{\mathbb{R}} x \mathrm{d}\nu_k^i(x) = 0.$$

Then, there exist explicit constants $a, b \in \mathbb{R}_{>0}$ such that:

$$\left(\frac{a}{n^{1/2}} C_{\mathrm{T}_n}((2n-2)t), \frac{b}{n^{1/4}} Z_{\mathrm{T}_n}((2n-2)t)\right)_{0 \leq t \leq 1} \xrightarrow{(\mathrm{d})} (\mathbf{e}(t), Z(t))_{0 \leq t \leq 1}.$$

[7] Since introducing Boltzmann maps requires quite some terminology, I will only present the results obtained for p-angulations.

I must emphasize that to prove this theorem, we in fact obtain a bootstrapping principle stated in Theorem 3.3.5, which allows us to transfer the result obtained by Miermont (which holds under Assumption (A)) to obtain this scaling limit. Let me mention that our bootstrapping principle also holds for multitype labeled trees so that we also obtain as well a scaling limit for multitype labeled trees, again by extending the results of [Mie08a]. This result establishes in particular that the scaling limit of the random mobiles is the Brownian snake. Partial results in that direction were obtained in [Mie06], in particular he obtained the convergence of the rescaled profile of uniform p-angulations.

3.3.1 The Bouttier–Di Francesco–Guitter bijection

In this section, I describe the Bouttier–Di Francesco–Guitter bijection [BDFG04], roughly following the presentation given in [CLM13]. Let $\mathcal{M}^\bullet$ be the set of rooted planar maps with a pointed vertex.

Let $(M, e, v^\bullet)$ be an element of $\mathcal{M}^\bullet$, where M is a planar map, e its root edge and $v^\bullet$ its pointed vertex. Let e^- and e^+ be respectively the tail and the head of e. Three cases can occur: either $\mathrm{dist}_M(v^\bullet, e^-) = \mathrm{dist}_M(v^\bullet, e^+)$, $\mathrm{dist}_M(v^\bullet, e^-) = \mathrm{dist}_M(v^\bullet, e^+) + 1$ or $\mathrm{dist}_M(v^\bullet, e^-) = \mathrm{dist}_M(v^\bullet, e^+) - 1$. Depending on which case occurs, we say that M is respectively *null*, *negative* or *positive*. In the following, we focus only on the set $\mathcal{M}^+$ of positive maps, since the other cases can be treated similarly (we refer the reader to the original paper [BDFG04] or to [CLM13] for details).

I now introduce formally the class of decorated trees – called *positive mobiles* – which appear in the bijection with positive maps.

Definition 3.3.3

A positive mobile $\mathrm{t} = (t, d)$ *is a 4-type rooted plane labeled tree which satisfies the following constraints.*

(i) Vertices at even generations are of type 1 *or* 2 *and vertices at odd generations are of type* 3 *or* 4*. The root vertex is of type* 1*.*

(ii) Each child of a vertex of type 1 *is of type* 3*.*

(iii) Each vertex of type 2 *has exactly one child of type* 4 *and no other child.*

The labeling d *satisfies the following conditions:*

(1) Vertices of type 1 *and* 3 *are labeled by integers and vertices of type* 2 *and* 4 *by half-integers.*

(2) For every vertex u *of type* 3 *or* 4*, list its children as* $u_1, \dots, u_{k_t(u)}$*. Then, for every* $i = 0, \dots, k_t(u)$*,*

$$\begin{cases} \ell(u_{i+1}) \geq \ell(u_i) - 1 & \text{if } u_{i+1} \text{ is of type } 1, \\ \ell(u_{i+1}) \geq \ell(u_i) - 1/2 & \text{if } u_{i+1} \text{ is of type } 2. \end{cases}$$

where we use the convention that $u_{k_t(u)+1}$ *and* u_0 *both denote the parent of* u*.*

(3) For every vertex u *of type* 3 *or* 4*, we have* $\ell(u) = \ell(u_0)$*.*

We denote $\mathbb{T}^+$ *the set of positive mobiles and* $\mathbb{T}^+_n$ *the set of positive mobiles with* n *vertices of type* 1*.*

We now give the construction which maps an element of $\mathcal{M}^+$ to a rooted labeled 4-type tree and which is illustrated in Figure 3.14. First, label each vertex of M by $\ell_M(v) := \mathrm{dist}_M(v, v^\bullet)$. Then, for each edge of the map both extremities of which have the same label, say ℓ, add a "flag-vertex" f in the middle of the edge and label it $\ell_M(f) := \ell + 1/2$. Call the resulting augmented map M'. Next, add a "face-vertex" in each face of the map. Now, for each face of M', considering its vertices in clockwise order, each time a vertex v is immediately followed by a vertex w with smaller label (the introduction of flag-vertices ensures that any two adjacent vertices have different labels), draw an edge between v and the corresponding face-vertex. Erase all edges of M'.

The result of [BDFG04] ensures that the resulting map, denoted $\Phi(M)$, is in fact a spanning tree of the union of the set of face-vertices, the set of flag-vertices and the set of vertices $V(M)\backslash\{v^\bullet\}$. The tree $\Phi(M)$ inherits a planar embedding from M. To make it a rooted plane tree, we additionally root it at e^+, and choose the first child of e^+ to be the face-vertex associated to the face on the left

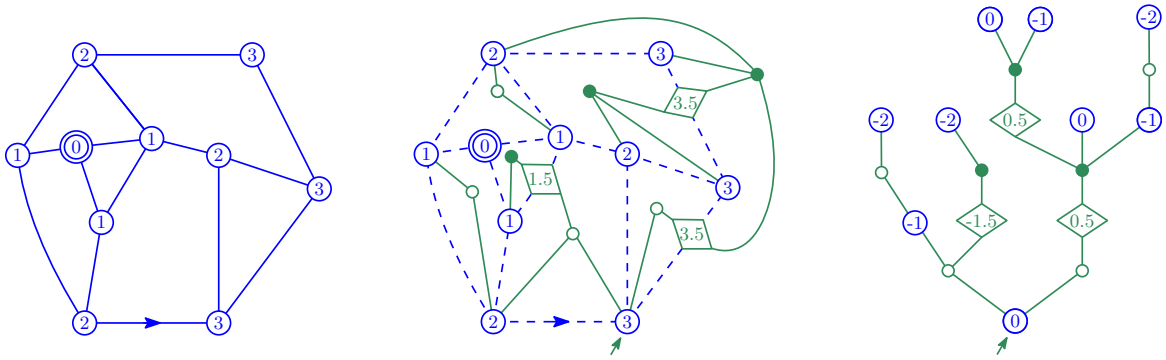

(a) The original map, (b) the construction of $\Phi(m)$, (c) and the resulting mobile.

Figure 3.14. An example of the Bouttier–Di Francesco–Guitter bijection. Circle and square labeled vertices correspond respectively to vertices of type 1 and 2. Empty and filled unlabeled vertices correspond respectively to vertices of type 3 and 4, and they inherit the label of their parents.

of (e^-, e^+); note that because M is positive, there always exists an edge in $\Phi(M)$ between e^+ and this face-vertex.

We assign types to the vertices of $\Phi(M)$ as follows. Vertices of M have type 1, and flag-vertices have type 2. Face-vertices have type 3 if their parent is of type 1 and have type 4 otherwise. This turns $\Phi(M)$ into a mobile, rooted at a vertex of type 1. For $v \in V(M) \setminus \{v^\bullet\}$ we denote the image of v in $\Phi(M)$ by $\Phi(v)$.

Label the vertices of $\Phi(M)$ as follows. For u of type 1 or 2, let $\ell(u) = \ell_M(u) - \ell_M(e^+)$, this makes sense since u is a vertex of M'. Having rooted $\Phi(M)$, we give vertices of type 3 and 4 the same label as their parent. We now use these vertex labels to turn $\Phi(M)$ into a rooted labeled tree by giving each edge (u, u_i) of $\Phi(M)$ the label $\ell(u_i) - \ell(u)$.

The properties of this construction which are essential to our work appear in the following theorem. Note that properties (i) and (ii) follow directly from the construction.

Theorem 3.3.4 (*Bouttier–Di Francesco–Guitter bijection, [BDFG04]*)

For each $n \geq 1$, Φ gives a bijection between $\mathcal{M}^+$ and $\mathbb{T}^+$.
For $(m, e, v^\bullet) \in \mathcal{M}^+$, write $\mathrm{t} = (t, d)$ for the image of $(m, e, v^\bullet)$ by Φ. Then
(i) Elements of $V(m)\backslash\{v^\bullet\}$ are in bijection with vertices of type 1 in t.
(ii) For all $v \in V(m)\backslash\{v^\bullet\}$, $d_m(v, v^\bullet) = \ell_{\mathrm{t}}(\Phi(v)) - \min_{x \in V(t)} \ell_{\mathrm{t}}(x) + 1$.

3.3.2 Convergence to the Brownian snake and symmetrization of trees

For the sake of clarity, I only state our result and sketch its proof for labeled *monotype* trees. The main difficulty to generalize the proof from monotype trees to multitype trees, is somehow to deal with the heavier formalism inherent to multitype trees! I also restrict my attention to Galton-Watson trees only, since this is enough to prove Theorem 3.3.1. I refer the reader to the publication [12] for the more general setting.

I first introduce some notions and definitions. Given a plane tree t, let $[t]$ be the set of plane trees which are isomorphic to t as rooted trees (but not necessarily as *plane* rooted trees). Write P_t for the set of vectors $\sigma = (\sigma_v, v \in V(t))$, where each σ_v is a permutation of $\{1, \dots, k_t(v)\}$. Such a vector σ uniquely specifies a tree $t' = \sigma(t) \in [t]$ as follows, see Figure 3.15. Visually, reorder the children of each node v according to the permutation σ_v. Formally, for each node $v = v_1 v_2 \dots v_k \in V(t)$, there is a corresponding node $\sigma(v) \in V(t')$ whose Ulam–Harris–Neveu label is

$$\sigma(v) = \sigma_\emptyset(v_1)\sigma_{v_1}(v_2)\dots\sigma_{v_1\dots v_{k-1}}(v_k)\,.$$

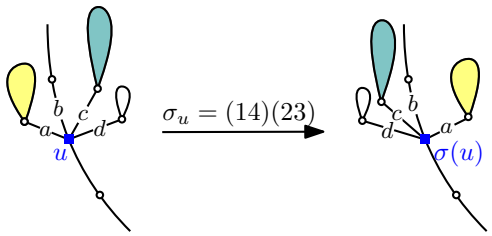

Figure 3.15. A local example to illustrate the construction of $\sigma(t)$. The tree t is represented on the left and $\sigma(t)$ on the right. Labels a, b, c and d represent the displacements along the edges.

If $\mathrm{t} = (t, \mathrm{d})$ is a labeled plane tree, we likewise define $[\mathrm{t}]$ and $\mathrm{t}' = \sigma(\mathrm{t}) \in [\mathrm{t}]$ by letting the labels follow their edges. Formally, if $e = uv \in e(t)$ then $d'(\sigma(u)\sigma(v)) = d(uv)$.

Fix a labeled plane tree (t, d) and let $\sigma = (\sigma_v, v \in V(t))$ be a uniformly random element of P_t. We call the random tree $\sigma(t, \mathrm{d})$ the *symmetrization* of t. This also makes sense for a random labeled tree (T, D); in this case, conditionally given (T, D), σ is a uniformly random element of P_T, and the symmetrization is the tree $\sigma(T, \mathrm{D})$. If ν is the law of the random labeled plane tree (T, D) then we write ν^{sym} for the law of the symmetrization of (T, D). We additionally write ν_n and ν_n^{sym} respectively for the law of the tree sampled according to ν and ν^{sym} and conditioned to be of size n. Then:

Theorem 3.3.5 (*Theorem 2 of [12]*)

For each $n \geq 1$ let $\mathrm{T}_n = (T_n, \mathrm{D}_n)$ be a random labeled Galton-Watson tree with law ν_n, and let $\mathrm{T}_n^{\mathrm{sym}}$ have law ν_n^{sym}. Suppose that there exist two positive constants $a, b \in \mathbb{R}_{>0}$, such that

$$\left(\frac{a}{n^{1/2}} C_{\mathrm{T}_n^{\mathrm{sym}}}\Big((2n-2)t\Big), \frac{b}{n^{1/4}} Z_{\mathrm{T}_n^{\mathrm{sym}}}\Big((2n-2)t\Big)\right)_{0 \leq t \leq 1} \xrightarrow{(\mathrm{d})} (\mathbf{e}(t), Z(t))_{0 \leq t \leq 1}$$

for the uniform topology. Then, the following convergence also holds for the uniform topology:

$$\left(\frac{a}{n^{1/2}} C_{\mathrm{T}_n}, \frac{b}{n^{1/4}} Z_{\mathrm{T}_n}\right) \xrightarrow{(\mathrm{d})} (\mathbf{e}, Z).$$

3.3.3 Sketch of the proof of Theorem 3.3.5

In brief, the proof proceeds as follows. It is classical (see for instance [Bil13]), that to prove convergence in distribution it suffices to prove convergence of finite-dimensional distributions (FDDs), stated in Proposition 3.3.6[8], plus tightness of the process, stated in Proposition 3.3.7[9].

Proposition 3.3.6

Let $\mathrm{T}_n = (T_n, D_n)$ be a family of random labeled trees satisfying the hypotheses of Theorem 3.3.5. Let $(X_i, i \geq 1)$ be independent Uniform$[0,1]$ random variables, independent of the trees T_n. Fix $k \geq 1$ and write $(X_i^{\uparrow}, 1 \leq i \leq k)$ for the increasing reordering of $X_1, \ldots, X_k$. Then

$$\left(\frac{a}{n^{1/2}} C_{\mathrm{T}_n}\Big((2n-2)X_i^{\uparrow}\Big), \frac{b}{n^{1/4}} Z_{\mathrm{T}_n}\Big((2n-2)X_i^{\uparrow}\Big), 1 \leq i \leq k\right) \xrightarrow{(\mathrm{d})} (\mathbf{e}(X_i^{\uparrow}), Z(X_i^{\uparrow}), 1 \leq i \leq k)$$

as $n \to \infty$.

[8] The result stated in Proposition 3.3.6 is about *random* FDDs rather than FDDs sampled at deterministic times. But, since the limiting processes are uniformly continuous, the corresponding result for deterministic FDDs can be deduced readily.

[9] The two processes C_{T_n} and $C_{\mathrm{T}_n^{\mathrm{sym}}}$ are equal in distribution, by definition of a Galton-Watson process. Hence, the convergence of $C_{\mathrm{T}_n^{\mathrm{sym}}}/n^{1/2}$ implies directly that $C_{\mathrm{T}_n}/n^{1/2}$ is tight. This is why it is enough to prove the tightness of $Z_{\mathrm{T}_n}/n^{1/4}$, as stated in Proposition 3.3.7.

Proposition 3.3.7

Under the hypotheses of Theorem 3.3.5, the family $(Z_{\mathrm{T}_n}/n^{1/4})$ *is tight. In other words, for all* $\delta > 0$, *there exists* $\alpha = \alpha(\delta)$ *such that*

$$\limsup_{n\to\infty} \mathbf{P}\left\{ \sup_{x,y\in[0,1],|x-y|\le\alpha} \left| Z_{\mathrm{T}_n}\Big((2n-2)x\Big) - Z_{\mathrm{T}_n}\Big((2n-2)y\Big)\right| > \delta n^{1/4} \right\} < \delta\,. \qquad (3.6)$$

We use some couplings between a tree and its symmetrization to prove these two propositions. In the rest of the section, I will stay at a very informal level and only give a rough sketch of the proofs.

Finite-dimensional distributions The proof of Proposition 3.3.6 relies on the definition of *partial symmetrization* of plane labeled trees. Informally, this partial symmetrization is defined as follows. Let t be a plane labeled tree, fix $k \in \mathbb{N}$ and let S be a set of k independent uniform vertices of t. Additionally, let $\sigma = (\sigma_v, v \in V(\mathrm{t}))$ be a uniformly random element of P_{t}. Denote $\mathrm{t}(\mathrm{S})$ the subtree of t spanned by its root vertex and by the vertices of S. Then, we perform symmetrization at every vertex of t, except at the branchpoints of $\mathrm{t}(\mathrm{S})$. At each branchpoint of $\mathrm{t}(\mathrm{S})$, we do not permute the subtrees but only permute the displacements between this vertex and its children, see Figure 3.16[10] . The tree obtained is denoted $\hat{t}$.

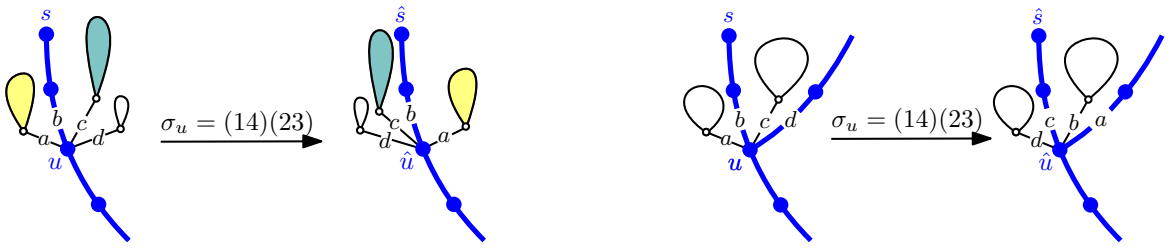

(a) Symmetrization outside the branchpoints.

(b) Symmetrization at a branch point.

Figure 3.16. Examples of the construction of $\hat{\mathrm{t}}$. In both figures, the tree t is on the left and $\hat{\mathrm{t}}$ on the right. Labels a, b, c and d represent the displacements along the edges. Branches of $t(\mathrm{S})$ are represented in bold blue.

For u a vertex of t, denote $\hat{u}$ its image in $\hat{t}$, i.e. if the Ulam–Harris–Neveu encoding of u is $u_1 \dots u_h$, then the Ulam–Harris–Neveu encoding of $\hat{u}$ is

$$\hat{u} = \tilde{\sigma}_\emptyset(u_1)\tilde{\sigma}_{u_1}(u_2)\dots\tilde{\sigma}_{u_1\dots u_{h-1}}(u_h), \text{ where } \tilde{\sigma}_v = \begin{cases} Id & \text{if } v \text{ is a branchpoint of } \mathrm{t}(S), \\ \sigma_v & \text{otherwise.} \end{cases}$$

Let now T_n be as in Proposition 3.3.6 and let S_n be a set of k independent uniform vertices of T_n. List the elements of S_n as $(s_1, \dots, s_k)$ in the order they are first encountered by the contour exploration of T_n. Then Proposition 3.3.6 is clearly equivalent to the following convergence:

$$\left(\frac{a}{n^{1/2}}|s_i|, \frac{b}{n^{1/4}}\ell_{\mathrm{T}_n}(s_i), 1 \le i \le k\right) \xrightarrow{(\mathrm{d})} (\mathbf{e}(X_i^{\uparrow}), Z(X_i^{\uparrow}), 1 \le i \le k) \text{ as } n \to \infty, \qquad (3.7)$$

where $|s|$ denotes the length of the Ulam-Harris-Neveu encoding of s.

Fix $i \in \{1, \dots, k\}$. By construction, we have that $|s_i| = |\hat{s}_i|$. Moreover, it follows from the partial symmetrization that the labels of s_i and $\hat{s}_i$ only differ by the difference of labels at the branchpoints

[10] Note, that the convention adopted in [12] for the displacements at the branchpoints in $\hat{t}$ is slightly different than here. Indeed, in [12], every displacement between a branchpoint and its children is set to 0.

of $\mathrm{t}(\mathrm{S})$, and this difference can easily be shown to be negligible in the scaling limit. It is hence enough to prove a result analogous to (**3.7**) when s_i and T_n are respectively replaced by $\hat{s}_i$ and $\hat{\mathrm{T}}_n$.

Observe now that the image of S_n in $\hat{\mathrm{T}}_n$ is a set of k independent uniform vertices of $\hat{\mathrm{T}}_n$, and the order in which the elements of $\hat{\mathrm{T}}_n$ are encountered by the contour exploration of $\hat{\mathrm{T}}_n$ is given by $(\hat{s}_1, \dots, \hat{s}_k)$. Moreover, by construction of the partial symmetrization, the law of $\hat{\mathrm{T}}_n$ is ν_n^{sym}. So that, by the assumption of Theorem 3.3.5, a result analogous to (**3.7**) is known to be true when s_i and T_n are respectively replaced by $\hat{s}_i$ and $\hat{\mathrm{T}}_n$, which concludes the proof. □

Tightness As for the convergence of FDDs, the proof of Proposition 3.3.7 relies on a coupling between the law of T_n and $\mathrm{T}_n^{\mathrm{sym}}$. This time, we simply consider the natural coupling used in the definition of symmetrization. However, we cannot deduce directly the tightness of $Z_{\mathrm{T}_n}/n^{1/4}$ from the tightness of $Z_{\mathrm{T}_n^{\mathrm{sym}}}/n^{1/4}$. Let indeed u and v be two vertices of T_n explored at times $\lfloor tn \rfloor$ and $\lfloor (t+\epsilon)n \rfloor$ in its contour exploration. Then, the coupling does not imply that the difference between the times at which $\sigma(u)$ and $\sigma(v)$ are explored in the contour exploration of $\sigma(\mathrm{T}_n)$ is also of order ϵn. This is illustrated in Figure 3.17.

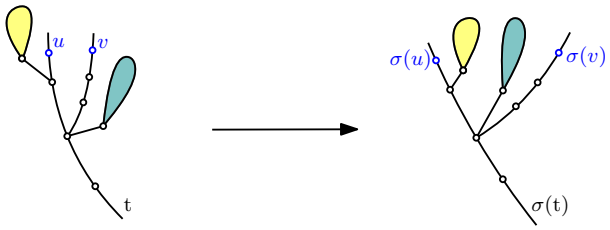

Figure 3.17. Example of the coupling between t and $\sigma(\mathrm{t})$. In t, v is explored shortly after u in the contour process, whereas in $\sigma(\mathrm{t})$, $\sigma(v)$ is explored a long time after $\sigma(u)$ in the contour process.

But, since $C_{\mathrm{T}_n}/n^{1/2}$ is tight, the distance (rescaled by $n^{1/2}$) in T_n between u and v is small. It is easy to see that the distance in T_n between u and v is equal to the distance in $\sigma(\mathrm{T}_n)$ between $\sigma(u)$ and $\sigma(v)$. So that the rescaled distance in $\sigma(\mathrm{T}_n)$ between $\sigma(u)$ and $\sigma(v)$ is also small.

Now, the Brownian snake is known to be a continuous function of the Brownian Continuum Random Tree, meaning that if $s, t \in [0,1]$ are such that $d_{\mathcal{T}_e}(s,t)$ is small then $|Z(s) - Z(t)|$ is also small. By the convergence for $(\mathrm{T}_n^{\mathrm{sym}})$ stated in Theorem 3.3.5, we can propagate this continuity property to the discrete setting to ensure that the difference of labels (rescaled by $n^{1/4}$) between $\sigma(u)$ and $\sigma(v)$ is small. By construction, the labels of u and $\sigma(u)$ and of v and $\sigma(v)$ are equal. This concludes the proof. □

3.3.4 A recipe by Timothy Budd to compute the scaling constant in Theorem 3.3.1

It is natural to ask whether the constants C_p appearing in Theorem 3.3.1 can be computed and if so, if they admit an explicit form. It is even more natural considering that the analogous constants C_p are known to admit the following very simple closed forms for $p = 3$ or p an even integer, see for instance [LG13, Theorem 1][11]:

$$C_3 = 3 \qquad \text{and} \qquad C_p = \frac{9}{2p}, \text{ for } p \text{ even.}$$

In [Mie06], Miermont outlines an algorithm to compute the scaling constant C_p. Since this algorithm requires the computations of eigenvectors of three 3×3 matrices, it rapidly leads to very heavy computations and becomes intractable for $p > 5$. But based on it and by quite an impressive

[11] It is important to note that in [LG13], n stands for the number of faces rather that the number of vertices, so that the constant must be adapted accordingly.

computation, Timothy Budd ([Buda] and [Budb, p.157]) managed to relate the constants C_p to a quantity which appears in the peeling exploration of the local limit of random maps. Since, to my knowledge, this formula does not appear in the literature, I thought it would be nice to include it here.

I now follow [Bud16, Section 8.2]. Consider first the family of functions $h_r^{(k)}$ defined as follows. For $k \in \mathbb{N}$, $l \in \mathbb{Z}$ and $r \in [-1,1]$,

$$h_r^{(k)}(l) = [y^{-l-1}] \frac{1}{(y-1)^{k+1/2}\sqrt{y+r}} = \left(\frac{-r}{4}\right)^{l-k} \binom{2l-2k}{l-k} {}_2F_1\left(\frac{1}{2}+k, k-l; \frac{1}{2}+k-l; -1/r\right),$$

where in the first expression for $h_r^{(k)}(l)$, we compute the development in powers of $1/y$ and in the second expression, ${}_2F_1$ denotes the ordinary hypergeometric function. Observe that $h_r^{(k)}(l) = 0$ for $l < k$ and that $h_r^{(k)}(k) = 1$.

Next, fix an odd integer p, and consider the following system of equations:

$$\nu_p(p-2) > 0, \quad \nu_p(k) = 0 \text{ for } k \geq -1 \text{ and } k \neq p-2,$$

and:

$$\sum_{l=-\infty}^{\infty} h_{r_p}^{(1)}(l+k)\nu_p(l) = h_{r_p}^{(1)}(k), \quad \text{for any } k > 0. \tag{3.8}$$

This system determines both a unique value for $r_p \in (-1,1)$ and a unique function $\nu_p : \mathbb{Z} \to \mathbb{R}$. Then, Budd proves the following[12]:

Proposition 3.3.8

For any odd integer p, the scaling constant C_p that appears in Theorem 3.3.1 is equal to:

$$C_p = \frac{48 \cdot \nu_p(-2)}{(1+r_p)^3 \cdot \nu_p(p-2) \cdot h_{r_p}^{(2)}(p-1)}.$$

Let me explain how this result gives an effective way to compute C_p. We only need to compute $\nu_p(p-2)$, $\nu_p(-2)$ and r_p. If we write (3.8) for $k \in \{1,2,3\}$, we obtain exactly 3 equations involving these 3 unknowns. We get that r_p is the unique solution in $(-1,1)$ of the following polynomial of degree $p-1$:

$$h_r^{(1)}(p) - \frac{1}{2}(3-r)h_r^{(1)}(p-1) = 0,$$

and the following expressions for $\nu_p(p-2)$ and $\nu(-2)$:

$$\nu_p(p-2) = \frac{1}{h_{r_p}^{(1)}(p-1)} \quad \text{and} \quad \nu_p(-2) = h_{r_p}^{(1)}(3) - h_{r_p}^{(1)}(p+1)\nu_p(p-2).$$

For $p=3$, we find $r_3 = 2\sqrt{3} = 3$, $\nu_3(1) = (3+\sqrt{3})/6$, $\nu_3(-2) = (2\sqrt{3}-3)/3$ and $C_3 = 3$ as expected. For $p > 3$, r_p can only be expressed by radicals and we cannot obtain a nice closed formula for C_p. We can however efficiently compute numerical approximations and obtain for instance that $C_5 \approx 1.301$, $C_7 \approx 0.827$, $C_9 \approx 0.606$, ...

3.4 Scaling limit of triangulations of polygons

I present in this section the publication [13] obtained in collaboration with Nina Holden and Xin Sun. In this article, we obtain the scaling limit of *triangulations of a p-gon* towards the Brownian disk,

[12] He obtains in fact a formula valid in the much more general setting of critical Boltzmann planar maps, but I restrict here my attention to p-angulations.

introduced by Bettinelli and Miermont [BM17] (following some earlier work by Bettinelli [Bet15b]). The Brownian disk is an analogue of the Brownian map but with the topology of the disk rather than of the sphere.

I will start by presenting the construction of the Brownian disk and the result of Bettinelli and Miermont. Then, I will state our result together with some combinatorial constructions underlying its proof.

3.4.1 Scaling limit of quadrangulations with a boundary, [BM17]

Scaling limit of critical Boltzmann maps In this section, I slightly change the randomness setting: instead of considering uniform maps with a fixed size, I consider maps sampled from a *critical Boltzmann distribution*.

For quadrangulations with a boundary, it amounts to the following. Consider the set $\mathcal{Q}^{(p)}$ of quadrangulations with a boundary of length p (as defined in Section 1.4.4), then assign to each element $q \in \mathcal{Q}^{(p)}$ a weight ρ^n, where n is the number of vertices of q and $\rho = 1/12$. It is well known that this defines a finite measure on $\mathcal{Q}^{(p)}$ for any p[13]. Then, the *critical Boltzmann distribution* $\mathrm{Bol}^{\square}(p)$ on $\mathcal{Q}^{(p)}$ is the probability distribution obtained after normalizing this measure.

The scaling limit $\mathrm{Bol}^{\square}(p)$ was studied by Bettinelli and Miermont, who prove, among other things, the following result:

Theorem 3.4.1 ([BM17])

Let M_p *be sampled from* $\mathrm{Bol}^{\square}(p)$. *Then, as* $p \to \infty$:

$$\left(\mathsf{M}_p, \left(\frac{3}{2p}\right)^{1/2} \mathrm{dist}_{\mathsf{M}_p}\right) \xrightarrow{(\mathrm{d})} BD_1,$$

for the Gromov–Hausdorff topology, where BD_1 *is the free Brownian disk with perimeter 1, defined in the rest of this section.*

Random real forests Theorem 3.4.1 relies on a generalization of Cori–Vauquelin–Schaeffer's bijection between quadrangulations with a boundary and labeled *cyclic forests* (as defined in Section 2.2.2). Hence, mimicking the approach presented in Section 3.1.2, the first step of the construction of the Brownian disk consists in studying the scaling limit of labeled forests to obtain an analogue of Theorem 3.1.2, with similar assumptions. I will not give a formal statement of convergence but will only describe the scaling limit obtained when studying the labeled cyclic forests obtained by Cori–Vauquelin–Schaeffer's bijection applied to critical Boltzmann quadrangulations.

Let $\mathbf{C} = (\mathbf{C}_s, s \in \mathbb{R}_{\geq 0})$ be a standard Brownian motion and for $y \geq 0$, set $\mathbf{T}_y := \inf\{t \geq 0 : \mathbf{C}_t \leq -y\}$. Define $\mathcal{A} := \mathbf{T}_1$. The random process $(\mathbf{C}_s, 0 \leq s \leq \mathcal{A})$ is then a standard Brownian motion killed at the first time it reaches -1. It will play an analogous role of the one played by the Brownian excursion in the construction of the Brownian map. Let me be slightly more explicit: in the discrete setting, the contour process of a forest is the concatenation of the contour processes of its trees, where the contours of two consecutive trees are separated by a down step, see Figure 3.18. In the continuum, $\mathbf{C}$ can hence be seen as the contour function of a real forest by saying that successive excursions of $\mathbf{C}$ above its current minimum encode a sequence of trees.

More precisely, for $0 \leq s \leq s' \leq \mathcal{A}$, let $\underline{\mathbf{C}}_{s,s'} = \inf\{\mathbf{C}_u : u \in [s, s']\}$ and

$$d_{\mathbf{C}}(s, s') = \mathbf{C}_s + \mathbf{C}_{s'} - 2\underline{\mathbf{C}}_{s,s'}. \tag{3.9}$$

Then, $d_{\mathbf{C}}$ defines a metric on $[0, \mathcal{A}]/\{d_{\mathbf{C}} = 0\}$, which I will still denote $d_{\mathbf{C}}$. The metric space $\mathcal{F}_{\mathbf{C}} = ([0, \mathcal{A}]/\{d_{\mathbf{C}} = 0\}, d_{\mathbf{C}})$ is the random real forest encoded by $\mathbf{C}$.

[13] Indeed, for any $p \in \mathbb{N}$, it is well known (and follows from the computation presented in Section 1.2) that the radius of convergence of the generating series $Q^{(p)}$ of $\mathcal{Q}^{(p)}$ is equal to ρ and that $Q^{(p)}(\rho) < \infty$.

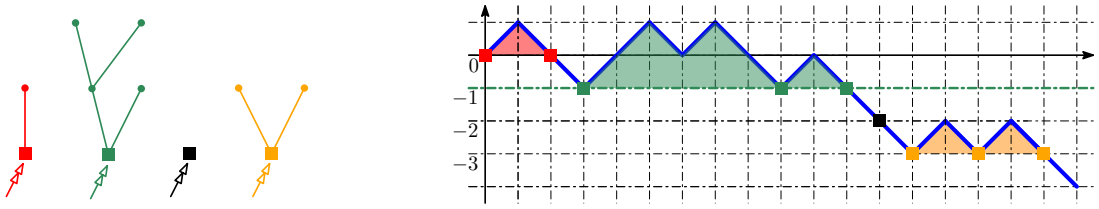

Figure 3.18. A (discrete) forest (left) with its contour (right). The roots of the trees are represented by squared vertices. Each excursion of the contour process above its current minimum is colored as the corresponding tree.

Random labeled real forests Some labels can then be attributed to $\mathcal{F}_{\mathbf{C}}$. Informally speaking, its floor (that is the set of roots of its trees) is labeled by a Brownian bridge with variance factor 3. Then, each tree is labeled by an independent Brownian snake, which is then shifted by the label of its root.

More precisely, conditionally given $\mathbf{C}$, let $\mathbf{\Lambda^0}$ be (the continuous modification of) a centered Gaussian process with covariance given by:

$$\mathrm{Cov}(\mathbf{\Lambda}^{\mathbf{0}}_s, \mathbf{\Lambda}^{\mathbf{0}}_{s'}) = \inf_{u\in[s,s']} (\mathbf{C}_u - \underline{\mathbf{C}}_u) \text{ for } s < s' \in [0, \mathcal{A}], \tag{3.10}$$

where $\underline{\mathbf{C}}_u := \inf_{0\le v\le u} \mathbf{C}_v$ is the past infimum of $\mathbf{C}$. In particular $\mathbf{\Lambda}^{\mathbf{0}}_s$ and $\mathbf{\Lambda}^{\mathbf{0}}_{s'}$ are independent if s and s' belong to two different trees of $\mathcal{F}_{\mathbf{C}}$. Moreover, recall the discussion just after Theorem 3.1.2, which states that the Brownian snake can be seen as a random process indexed by the Brownian CRT. Here, a similar statement holds and $\mathbf{\Lambda^0}$ can be seen as a random process indexed by the random forest encoded by $\mathbf{C}$. Indeed, let $s, s' \in [0, \mathcal{A}]$ be such that s and s' represent the same vertex of the forest, i.e. such that $d_{\mathbf{C}}(s, s') = 0$. Then, it follows from (3.10) that $\mathbf{\Lambda}^{\mathbf{0}}_s = \mathbf{\Lambda}^{\mathbf{0}}_{s'}$ almost surely.

Next, for $y \in [0, L]$, recall that T_y is the hitting time of $-y$ by $\mathbf{C}$. By definition of $\mathbf{\Lambda^0}$, we have that a.s., $\mathbf{\Lambda}^{\mathbf{0}}_{T_y} = 0$ for every $y \in [0, L]$. Informally speaking, it means that the label process defined by $\mathbf{\Lambda^0}$ gives label 0 to all the roots of the trees of the forest encoded by $\mathbf{C}$. To end the description of the limiting label process on the random forest, we now need to add the proper labels at the roots.

To this purpose, let $\mathbf{b}$ be a standard Brownian bridge of duration 1 independent of $(\mathbf{C}, \mathbf{\Lambda^0})_{[0,\mathcal{A}]}$ and with covariance given by

$$\mathrm{Cov}(\mathbf{b}_y, \mathbf{b}_{y'}) = y(1 - y') \text{ for } 0 \le y \le y' \le 1.$$

We define $\mathbf{\Lambda}$ by:

$$\mathbf{\Lambda}_s := \mathbf{\Lambda}^{\mathbf{0}}_s + \sqrt{3}\mathbf{b}_{\mathbf{T}^{-1}(s)} \text{ for } 0 \le s \le \mathcal{A}, \tag{3.11}$$

where $\mathbf{T}^{-1}(s) := -\underline{\mathbf{C}}_s$. Observe that, if s and s' belong to the same excursion of $\mathbf{C}$ above its current minimum, then by definition $\mathbf{T}^{-1}(s) = \mathbf{T}^{-1}(s')$. Hence, $\mathbf{\Lambda}_s - \mathbf{\Lambda}_{s'} = \mathbf{\Lambda}^{\mathbf{0}}_s - \mathbf{\Lambda}^{\mathbf{0}}_{s'}$, in other words the difference between $\mathbf{\Lambda}$ and $\mathbf{\Lambda^0}$ corresponds to an additive shift for vertices in the "same tree".

From the previous observation on $\mathbf{\Lambda^0}$, it follows that $\mathbf{\Lambda}_s = \mathbf{\Lambda}_{s'}$ if s and s' represent the same vertex of the forest. Hence, $\Big((\mathbf{C}_s, \mathbf{\Lambda}_s), 0 \le s \le \mathcal{A}\Big)$ can really be seen as the encoding of a real random labeled forest.

The Brownian disk Now, similarly to the construction given in Theorem 3.1.4, we can define a pseudo distance on $\mathcal{F}_{\mathbf{C}}$ in the following way. Let $\underline{\mathbf{\Lambda}}_{s,s'} = \inf\{\mathbf{\Lambda}_u : u \in [s, s']\}$ for $0 \le s \le s' \le \mathcal{A}$ and $\underline{\mathbf{\Lambda}}_{s,s'} = \underline{\mathbf{\Lambda}}_{s,\mathcal{A}} \wedge \underline{\mathbf{\Lambda}}_{0,s}$ for $0 \le s' < s \le \mathcal{A}$. Let

$$d_{\mathbf{\Lambda}}(s, s') = \mathbf{\Lambda}_s + \mathbf{\Lambda}_{s'} - 2\max\{\underline{\mathbf{\Lambda}}_{s,s'}, \underline{\mathbf{\Lambda}}_{s',s}\} \qquad \text{for} \qquad s, s' \in [0, \mathcal{A}]. \tag{3.12}$$

Next, let D^* be the largest pseudo-distance on $[0, \mathcal{A}]$ such that $D^* \le d_{\mathbf{\Lambda}}$, and such that for all $x, y \in [0, \mathcal{A}]$, if $d_{\mathbf{C}}(x, y) = 0$, then $D^*(x, y) = 0$. Then, let $M = [0, \mathcal{A}]/\{D^* = 0\}$ and let d^* be the push-forward of D^* to M. The *free Brownian disk with perimeter 1* is (the law of) $\mathrm{BD}_1 := (M, d^*)$.

3.4.2 The scaling limit of triangulations of a p-gon

In [13], we extend Theorem 3.4.1 to triangulations of a p-gon. We consider in fact three such families of triangulations. When loops and multiple edges are allowed, the triangulations are called *triangulations of type I* or general triangulations. *Triangulations of type II* or *loopless triangulations* are triangulations in which loops are not allowed but multiple edges are. Finally, *triangulations of type III* or *simple triangulations* are triangulations with neither loops nor multiple edges.[14]

For integers $n \geq p \geq 3$ and $i \in \{\mathrm{I}, \mathrm{II}, \mathrm{III}\}$, let $\Delta_i(p,n)$ be the set of type i triangulations of the p-gon with n vertices. Define $\Delta_i(p) = \cup_{n\geq p}\Delta_i(p,n)$. Set

$$\rho_{\mathrm{I}} = (12\sqrt{3})^{-1}, \qquad \rho_{\mathrm{II}} = 2/27, \qquad \text{and} \qquad \rho_{\mathrm{III}} = 27/256. \tag{3.13}$$

Given $i \in \{\mathrm{I}, \mathrm{II}, \mathrm{III}\}$, let $\mathrm{Bol}_i(p)$ be the critical Boltzmann distribution on $\Delta_i(p)$, defined similarly as $\mathrm{Bol}^{\square}(p)$. We call a sample drawn from $\mathrm{Bol}_i(p)$ a Boltzmann triangulation of type i with perimeter p. Our main result is the following theorem.

Theorem 3.4.2 (*Thorem 1 of [13]*)

Fix $i \in \{\mathrm{I}, \mathrm{II}, \mathrm{III}\}$. For $p \geq 3$, let M_p be sampled from $\mathrm{Bol}_i(p)$. Then:

$$\left(\mathsf{M}_p, \left(\frac{3}{2p}\right)^{1/2}\mathrm{dist}_{\mathsf{M}_p}\right) \xrightarrow{(\mathrm{d})} BD_1,$$

for the Gromov–Hausdorff topology and, where BD_1 is the free Brownian disk with perimeter 1.

It is interesting to note that the renormalization in this theorem does not depend on the type of triangulations and is in fact the same as in Theorem 3.4.1. In fact, the latter theorem is only a particular case of [BM17, Theorem 8], which states that the scaling limit (with the same normalization !) of many families of critical bipartite Boltzmann maps is the free Brownian disk of perimeter one.

3.4.3 Some ideas of proof

We first prove Theorem 3.4.2 for type III triangulations. By standard core decompositions studied in [BFSS01, ABW17], the results for type II and type I triangulations then follow effortlessly. I hence now focus on type III triangulations or simple triangulations.

First, we rely on the convergence of quadrangulations with a boundary to the Brownian disk, stated in Theorem 3.4.1. Then, Le Gall's argument for the convergence of planar maps (presented in Section 3.1.4) can be extended without difficulty to maps with a boundary. It hence remains to prove that random simple triangulations with a simple boundary can be encoded by some random labeled forests, that admit the same scaling limit as the ones that encode quadrangulations with a boundary and which are used to construct the brownian disk. To do so, we use the bijection between simple triangulations with a simple boundary and blossoming cyclic forests due to Poulalhon and Schaeffer [PS06], already presented in Section 2.2.2. This bijection is a variation of the bijection (also due to Poulalhon and Schaeffer) between simple triangulations and blossoming trees, which was instrumental in the work [10] presented in Section 3.2. We again reformulate this bijection into a bijection between simple triangulations with a simple boundary and *labeled cyclic forests* as illustrated in Figure 3.19.

To see how distances in the simple triangulation can be encoded by some functional of the blossoming forest, we adapt the techniques developed in [10] and presented in Section 3.2. In particular, we label the corner and vertices of the blossoming forest by the same local rule as the one pictured in Figure 3.11, see Figure 3.19 for an illustration of the bijection based on this labeling. It is easily seen that the vertex $v^\star$ with minimum label is incident to the outer face. And, we prove that the labels of the vertices give an approximation of their distance to $v^\star$. However, in the course of this proof, two new difficulties arise:

[14] Recall from Section 1.1.2 that triangulations of types I, II, and III are 1-connected, 2-connected, and 3-connected triangulations, respectively.

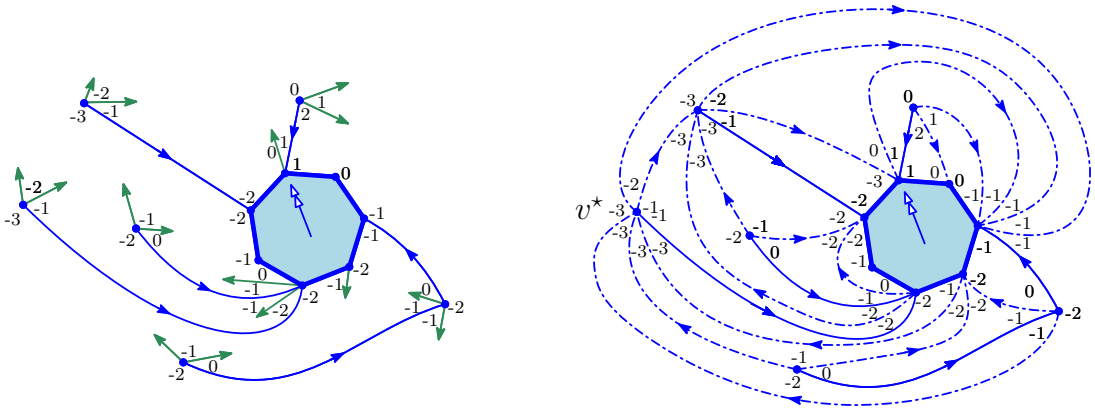

Figure 3.19. (a) A blossoming cyclic forest endowed with the labeling of its corners. (b) Its closure is a *plane* simple triangulation of the 7-gon endowed with its minimal pseudo-α_3-orientation. Note that the vertex with minimum label $v^\star$ is incident to the outer face.

Modified leftmost paths Because of the particular choice of the embedding (with the outer face not being the root face), leftmost paths are not as nice in triangulations of the p-gon. Leftmost paths are indeed no longer self-avoiding, and they do not necessarily reach $v^\star$. They can no longer be used as "almost-geodesic" paths from any vertex to $v^\star$. Fortunately, we can consider a variant of leftmost paths, the so-called *modified leftmost paths*, which reach $v^\star$ and are self-avoiding (when stopped at $v^\star$).

Triangulations with a random perimeter To prove that these modified leftmost paths are almost-geodesic, we adapt the proof sketched in Section 3.2.2. For P a modified leftmost path from u to $v^\star$ and Q a geodesic path from u to $v^\star$, we study the excursions of Q away from P. Compared to Figure 3.13, more cases have to be considered (depending on whether the excursion away from P separates the root face from the outer face or not), but this remains tractable *as long as Q does not contain a vertex incident to the root face*. Indeed, in a pseudo-orientation, the outdegrees of the vertices incident to the root face are not prescribed (only the sum of the outdegrees is fixed). Hence, the counting argument collapses for vertices incident to the boundary.

We hence study geodesics in the complement of the ball of radius 1 around the root face. It does in fact amount to studying the scaling limit of a simple triangulation with a *random perimeter*, see Figure 3.20. Thanks to results obtained in [BCK18], we can couple the original map and the triangulation with random perimeter and prove that geodesics in both maps behave similarly.

3.5 Ongoing work and perspectives

Scaling limit of planar *graphs* Now that the scaling limit of many natural families of planar maps is known to be the Brownian map, it is natural to turn one's attention to planar *graphs* instead of maps. A natural approach would be to show that the scaling limit of 3-connected planar maps is the Brownian map. Indeed, recall from Section 1.1.2 that, by a theorem of Whitney [Whi33], 3-connected planar graphs admit a unique planar embedding. It gives a straightforward bijection between 3-connected planar graphs and planar maps.

With Éric Fusy and Thomas Lehéricy, we started investigating the scaling limit of *cubic planar graphs*. Cubic 3-connected planar graphs are known to be in bijection by duality with simple triangulations. Our work relies on the recent article [CLG19], where Curien and Le Gall proved (among many other things) that random triangulations and their duals converge jointly (after normalization) to the

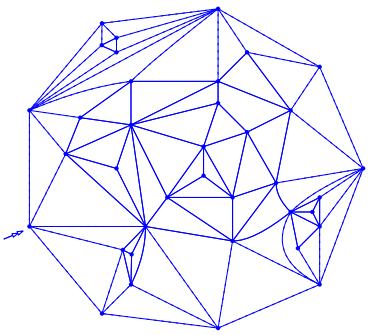

(a) A simple triangulation of a p-gon.

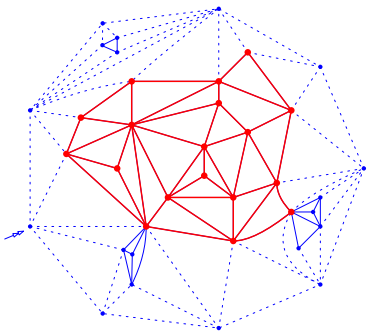

(b) The ball of radius one around the root face is represented by dashed edges.

Figure 3.20. In (b), there exists a unique macroscopic 3-connected component in the complement of the ball of radius one. This is a triangulation of a ℓ_p-gon (represented in fat and red edges), where ℓ_p is a random variable.

same instance of the Brownian map. We generalize their result to *simple* triangulations. Coupled with the scaling limit of simple triangulations obtained in [10], it gives a proof for the convergence of cubic 3-connected planar graphs. By standard core decompositions and another adaptation of an argument of [CLG19], we believe we can also prove that the scaling limit of cubic planar graphs is the Brownian map.

If this work is successful, we could then tackle the scaling limit of general planar graphs relying on the same approach. General 3-connected planar graphs are known to be in bijection, via Tutte's bijection, with irreducible quadrangulations (I recall that irreducible quadrangulations are quadrangulations in which every cycle of length 4 is the boundary of a face). Very recently, Lehéricy [Leh19] extended the results of [CLG19] to prove that quadrangulations and their images by Tutte's bijection converge jointly to the same instance of the Brownian map. It would remain to extend his result to irreducible quadrangulations and prove that the scaling limit of irreducible quadrangulations is the Brownian map.

These results hence appear to be within reach. They would be a major step forward in the understanding of metric properties of random planar graphs, which are still very ill-understood. In particular, only non-tight bounds are known for their diameter (see [CFGN09]).

Bootstrapping principle for non-continuous label processes: application to stable maps The proof for the invariance principle for labeled Galton-Watson trees obtained in Section 3.3 is quite robust but, so far, relies crucially on the fact that the limiting processes are continuous. However, some natural classes of trees (such as Galton-Watson trees with a critical offspring distribution with infinite variance) are encoded by processes whose scaling limits are not continuous.

In [LGM11], Le Gall and Miermont introduced a model of maps with large faces (called *stable maps*) which are mapped to such trees by the Bouttier–Di Francesco–Guitter bijection. They proved that the scaling limit of these maps (up to the extraction of a subsequence) is the so-called *stable map* (in [Mar18a], some similar results are obtained with slightly weaker assumptions).

This model is particularly interesting, since maps with large faces appear naturally in some models studied in statistical physics, such as the O(n) model (see for instance [BBG11]), percolation on random planar maps (see [BCM19]) or the Ising model (see also Chapter 4). Because results obtained in [LGM11] only hold for bipartite maps, it prevents them from being applied to some of the aforementioned physical models, which are often studied on triangulations. An extension of our bootstrapping principle to non-continuous limiting processes would lift this obstruction.

Chapter 4

Random triangulations with matter

In this chapter, I present my publications [11] and [4]. Here is a presentation of its different sections.

Section 4.1 I start with an introduction to the study of local limits of random maps with and without matter. I state the main results of [11] and present the (conjectured or established) connections between local limits of random planar maps and the Liouville Quantum Gravity.

Section 4.2 I present in this section the main ingredients behind the proofs of the results obtained in [11] about the local limit of triangulations endowed with an Ising model. The first part is very combinatorial and consists in a refinement of results obtained by Bernardi and Bousquet-Mélou in [BBM11]. The second part is more probabilistic and is dedicated to the analysis of the behavior of the degree of the root vertex in a random triangulation sampled from an Ising-weighted distribution.

Section 4.3 In this very last section, I describe briefly the results obtained in [4] as well as some ongoing work and perspectives.

4.1 Local limit of random planar maps with and without matter

4.1.1 Local limit of random planar maps

Benjamini-Schramm distance and local topology In this chapter, I study the *local limit* of some family of random planar maps. As in Chapter 3, planar maps are seen as metric spaces, but rather than investigating their scaling limit, I am interested in a non-rescaled notion of convergence. Instead of looking at the whole map, the local limit point of view only focuses on a finite neighborhood around the root vertex.

More formally, for M a rooted planar map and $r \in \mathbb{N}$, let $B_r(M)$ denote the map made of all the faces of M with at least one vertex at distance less than r from the root vertex, see Figure 4.1. Then, following Benjamini and Schramm [BS01], we equip the set of rooted planar maps with the local distance d_{loc} defined as follows. For M_1 and M_2 two rooted planar maps, we set:

$$d_{\mathrm{loc}}(M_1, M_2) = (1 + \sup\{R \geq 0 : B_R(M_1) = B_R(M_2)\})^{-1}. \tag{4.1}$$

Denote $\mathcal{M}_f$ the set of finite rooted maps, then the closure $(\mathcal{M}, d_{\mathrm{loc}})$ of the metric space $(\mathcal{M}_f, d_{\mathrm{loc}})$ is a Polish space and elements of $\mathcal{M} \setminus \mathcal{M}_f$ are called infinite maps. The topology induced by d_{loc} is called the *local topology*.

An infinite map $M \in \mathcal{M}$ is said to be *one-ended* if and only if, for any $R \geq 0$, only one of the connected components of $M \setminus B_R(M)$ is infinite.

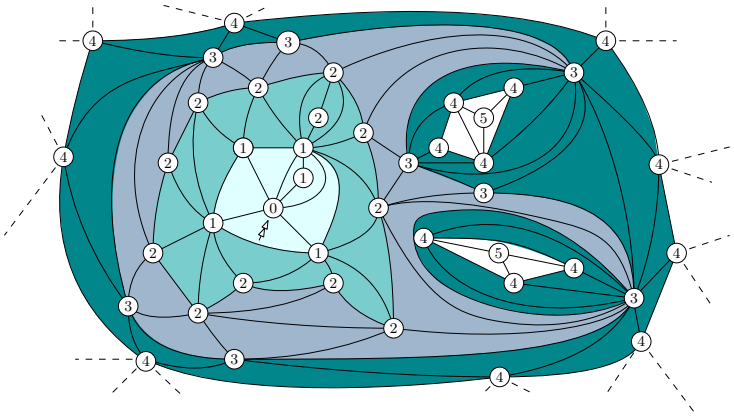

Figure 4.1. Vertices are labeled by their distance to the root vertex. The balls of radius 1, 2, 3 and 4 centered at the root of the triangulation are represented in various shades of blue.

Uniform Infinite Planar Triangulation In 2003, Angel and Schramm [AS03] proved that uniform triangulations converge for the local topology. More precisely, they proved that there exists a probability distribution supported on infinite one-ended triangulations, called the *UIPT* or *Uniform Infinite Planar Triangulation*, such that if Δ_n is a uniform rooted triangulation with n vertices[1], then for any integer $r \geq 1$:

$$B_r(\Delta_n) \xrightarrow{(\mathrm{d})} B_r(\Delta_\infty), \text{ where } \Delta_\infty \sim \mathrm{UIPT}.$$

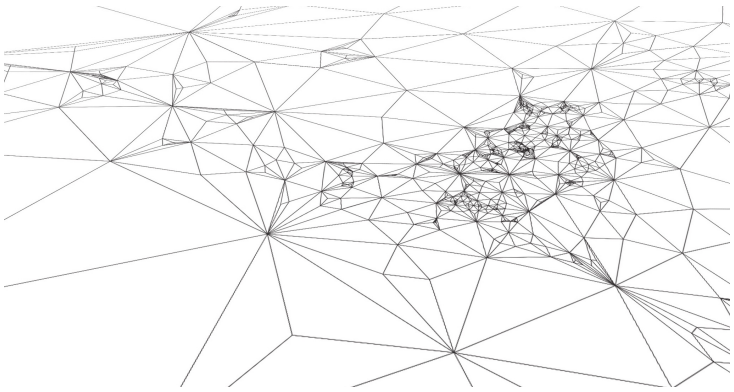

Figure 4.2. A simulation of the (simple) UIPT, due to Igor Kortchemski.

Similar results (but with quite different proofs) were then obtained for quadrangulations by Chassaing and Durhuus [CD06] and Krikun [Kri05], by Björnberg and Stefánsson [BS14] for Boltzmann bipartite maps and by Stephenson [Ste18] for Boltzmann general maps.

Since the result of Angel and Schramm, the local limit of random maps has become an active area of research. The UIPT is now a well-understood object. Among the many available results, let me cite in particular that the simple random walk on the UIPT is known to be recurrent [GGN13], and that precise estimates about the volume and the perimeter of the balls of radius r are available [Ang03, CLG17].

All the results cited above deal with models of maps that fall in the same "universality class", identified in the physics literature as the class of "pure 2d quantum gravity": the generating series admit the same critical exponent and the volume of the r-balls of the local limits of several of those models of random maps are known to grow as r^4. We say that the *volume growth exponent* of these models is 4. The fact that all these models share the same volume growth exponent is reminiscent of

[1] In [AS03], the result is in fact established for uniform loopless or simple triangulations but it was later extended to uniform general triangulations in [Ste18].

the fact that they all admit the Brownian map as their scaling limit, see Section 3.1.4 and references therein. In particular, we expect the local limit of the uniform distribution on any "reasonable families of planar maps" to also have a volume growth exponent equal to 4.

4.1.2 Escaping pure gravity: triangulations endowed with a critical Ising model

To escape this pure gravity behavior, it is now well understood that one should "couple gravity with matter", that is, consider models of random maps endowed with a statistical physics model. From a combinatorial point of view, evidence for the existence of other universality classes was first given by constructing models, like tree-rooted maps or triangulations endowed with Ising configurations, whose generating series exhibit a different singular behavior than regular maps.

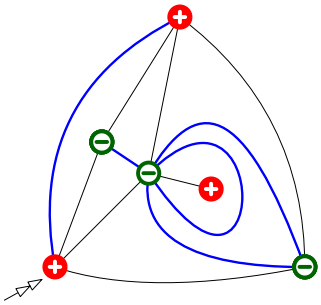

Figure 4.3. Example of a triangulation endowed with a spin configuration with 5 monochromatic edges represented by fat blue edges.

Let me define precisely the Ising model on triangulations. Let T be a rooted triangulation. A *spin configuration* on T is an application $\sigma : V(T) \to \{\oplus, \ominus\}$. An edge $\{u, v\}$ of T is called *monochromatic* if $\sigma(u) = \sigma(v)$ and *frustrated* otherwise. The number of monochromatic edges of (T, σ) is denoted $m(T, \sigma)$. For $\nu > 0$, the *ν–Ising–weighted generating series of triangulations* is defined as[2]:

$$Z(\nu, t) = \sum_{T \in \mathcal{T}_f} t^{|T|} \sum_{\sigma : V(T) \to \{\oplus, \ominus\}} \nu^{m(T,\sigma)},$$

where $\mathcal{T}_f$ denotes the set of finite rooted triangulations and $|T|$ is the number of edges of T.

For $k \geq 0$, write $[t^k]Z(\nu, t)$ for the coefficient of t^k in Z (note that since we consider triangulations, $[t^k]Z(\nu, t) \neq 0$ if and only if k is a multiple of 3). Then, the asymptotic behavior of $[t^{3n}]Z(\nu, t)$ was fully characterized in [BBM11] (see also [BK87] for equivalent results obtained in the physics literature):

Theorem 4.1.1 (*Claim 24 of [BBM11]*)

Set $\nu_c := 1 + 1/\sqrt{7}$. Then, for any $\nu > 0$, there exist two positive constants k_ν and ρ_ν, such that:

$$[t^{3n}]Z(\nu, t) \sim \begin{cases} k_{\nu_c} \cdot \rho_{\nu_c}^{-n}\, n^{-7/3} & \text{if } \nu = \nu_c, \\ k_\nu \cdot \rho_\nu^{-n}\, n^{-5/2} & \text{if } \nu \neq \nu_c. \end{cases} \tag{4.2}$$

Observe that except for $\nu = 1+1/\sqrt{7}$, the coefficients of $Z(\nu, t)$ exhibit the same asymptotic behavior (with a polynomial correction in $n^{-5/2}$) as the coefficients of the generating series of triangulations (without matter) and more generally as the coefficients of the generating series of all the "reasonable families of planar maps", see Section 3.1.4.

[2] Note that upon setting $\nu = \exp(-2\beta)$, it corresponds exactly to the classical definition of the Ising model without exterior magnetic field, where the interaction between each pair of neighboring vertices is equal to 1, and with β as inverse temperature. In particular, the model is *anti-ferromagnetic* for $0 < \nu < 1$ and *ferromagnetic* for $\nu > 1$. The case $\nu = 1$ corresponds to uniform triangulations.

The fact that this model of Ising–weighted maps exhibits a phase transition at $\nu = 1 + 1/\sqrt{7}$ first appeared in [BK87]. In this paper, Boulatov and Kazakov initiated the study of Ising models on random triangulations (following initial work by Kazakov about Ising models on random quadrangulations [Kaz86]). They established the existence of a phase transition, and gave the critical value of the model and the corresponding critical exponents. Their proof is based on the expression of the generating series of the model as a matrix integral and the use of orthogonal polynomial methods. Their result was later rederived via bijections with blossoming trees by Bousquet-Mélou and Schaeffer [BMS02] and with mobiles by Bouttier, Di Francesco and Guitter [BDFG07].

Since triangulations endowed with a critical Ising model do not belong combinatorially to the same universality class as triangulations, their local limit is a natural candidate for a model of maps not belonging to the same universality class as the UIPT. That was our main motivation with Laurent Ménard and Gilles Schaeffer to investigate the local limit of Ising–weighted triangulations in the article [11]. More precisely, for $n \in \mathbb{N}$ and $\nu > 0$, let $\mathbb{P}_n^\nu$ be the probability distribution supported on elements of $\mathcal{T}_f$ with $3n$ edges, such that for $T \in \mathcal{T}_f$ and $\sigma : V(T) \to \{\ominus, \oplus\}$:

$$\mathbb{P}_n^\nu(T, \sigma) \propto \nu^{m(T,\sigma)} \mathbf{1}_{\{|T|=3n\}}. \tag{4.3}$$

Then, our main result (whose proof will be sketched in Section 4.2) is the following theorem:

Theorem 4.1.2 (*Theorem 1 of [11]*)

For any $\nu > 0$, there exists a probability distribution $\mathbb{P}_\infty^\nu$ supported on infinite one-ended triangulations endowed with a spin configuration, such that:

$$\mathbb{P}_n^\nu \xrightarrow{(\mathrm{d})} \mathbb{P}_\infty^\nu, \text{ for the local topology.}$$

We call a random triangulation distributed according to this limiting law the Infinite Ising Planar Triangulation with parameter ν *or* ν-IIPT.

The ν_c-IIPT is called the *critical IIPT*. So far not much is known about it. Even if it is believed to belong to a different class of universality than the UIPT, it is not even clear that their distribution are mutually singular (see also the discussion at the end of the following section). However, these two models share at least some common features. We indeed managed to prove that:

Theorem 4.1.3 (*Theorem 2 of [11]*)

The simple random walk on the critical IIPT is almost surely recurrent.

We expect this result to hold also on the non-critical IIPT, but were unfortunately not able to prove it in full generality, see the discussion on that matter in Section 4.2.4.

4.1.3 Maps with matter and link with Liouville Quantum Gravity

I conclude this introduction by describing the links (conjectured or established) between models of decorated maps and Liouville Quantum Gravity. In Section 3.1.5, I discussed the work of Miller and Sheffield [MS15, MS16a, MS16b], who established that $\sqrt{8/3}$-LQG is equivalent to the Brownian map. It is widely believed that the scaling limit of most models of decorated maps is the γ-LQG for an appropriate value of the parameter γ. In particular, the critical Ising model should converge to the $\sqrt{3}$-LQG.

Apart from the value $\gamma = \sqrt{8/3}$, such a result seems out of reach for the moment. However – building on the so-called mating-of-trees approach initiated by Sheffield [She16b] and which has led to various local convergence results for models of decorated maps (see e.g. [Che17, GM17, BLR17]) – Gwynne, Holden and Sun [GHS20] obtained remarkable results. They proved that the volume growth of some of these models (including spanning-tree decorated maps, maps endowed with a bipolar orientation, and triangulations decorated by a Schnyder wood), is equal to d_γ, where d_γ is the "fractal dimension" of the conjectured limiting γ-LQG.

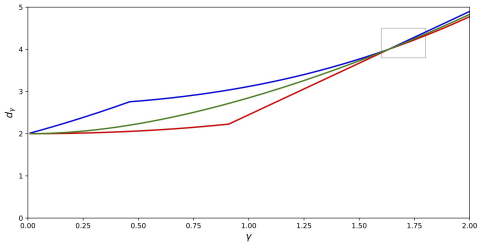

(a) Ding and Gwynne's bounds and Watabiki's prediction.

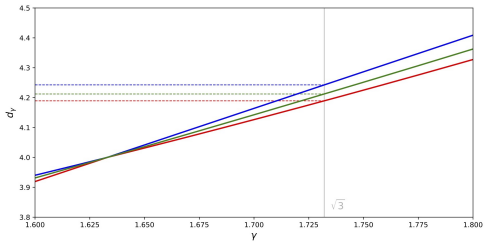

(b) A zoom for values of γ closed to $\sqrt{3}$.

Figure 4.4. Comparison of Ding and Gwynne's bounds (represented in blue and red) and of Watabiki's prediction (in green). The point where the three curves meet corresponds to $\gamma = \sqrt{8/3}$. In (b), I zoom around $\sqrt{3}$, which is the conjectured value of γ for the critical Ising model.

The value of d_γ is only known in the pure gravity case and $d_{\sqrt{8/3}} = 4$. For other values of γ, only bounds are available. As of today, the best ones have been established by Ding and Goswami [DG17] for γ near 0 and by Ding and Gwynne [DG20] for other values of γ. Except when γ is close to 0, these bounds are compatible with Watabiki's famous prediction which states that (see Figure 4.4):

$$d_\gamma^{Wat} = 1 + \frac{\gamma^2}{4} + \frac{1}{4}\sqrt{(4+\gamma^2)^2 + 16\gamma^2}.$$

As far as I understand, the Ising model does not fall into the scope of this mating-of-trees approach and so far, we are not able to derive information on the volume growth of balls in the IIPT. For $\gamma = \sqrt{3}$, Watabiki's prediction gives $d_{\sqrt{3}}^{Wat} = \dfrac{7+\sqrt{97}}{4} \approx 4.212$ and the bounds of Ding and Gwynne give:

$$4.189 \approx \frac{7+\sqrt{31}}{3} \leq d_{\sqrt{3}} \leq 3\sqrt{2} \approx 4.243.$$

If we believe in the connection between the critical IIPT and $\sqrt{3}$−LQG, this is hence a strong indication that its volume growth should be bigger than 4, and hence, that the critical IIPT and the UIPT should be mutually singular.

4.2 Convergence of Ising-weighted triangulations, [11]

In this section, I sketch the proofs of some of the results obtained in [11]. To prove Theorem 4.1.2, we follow the original proof of Angel and Schramm [AS03]. We first obtained some enumerative results about Ising-weighted triangulations refining Theorem 4.1.1, which I present in Section 4.2.1. Then we prove that, for any $\nu > 0$, the family of probability measures $(\mathbb{P}_n^\nu)$ is tight (see Section 4.2.2) and that the limits of all converging subsequences of $(\mathbb{P}_n^\nu)$ have the same finite-dimensional distributions (see Section 4.2.3). Lastly, I will conclude in Section 4.2.4 with some ideas underlying the proof of Theorem 4.1.3.

4.2.1 Enumeration of Ising-weighted triangulations

Asymptotic behavior for any fixed boundary condition Before sketching the proof of Theorem 4.1.2, I present some of the enumerative results crucial for the proof. Roughly speaking, we need a result analogous to Theorem 4.1.1 but for the generating series of Ising-weighted triangulations with simple boundary and with every possible boundary condition.

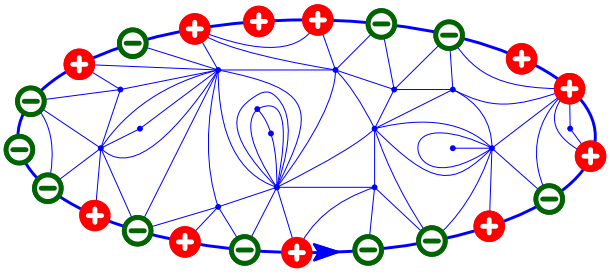

Figure 4.5. A triangulations of the 22-gon with boundary condition given by $\omega = \ominus\ominus\oplus\ominus\oplus\oplus\oplus\ominus\ominus\oplus\oplus\oplus\ominus\oplus\ominus\ominus\ominus\oplus\ominus\oplus\ominus\oplus$.

More formally, let p be a fixed integer and $\omega = \omega_1 \cdots \omega_p$ be a word of length p on the alphabet $\{\oplus, \ominus\}$. We write $\mathcal{T}_f^\omega$ for the set of triangulations of the p-gon endowed with a spin configuration such that the word on $\{\oplus, \ominus\}$ obtained by listing the spins of the vertices incident to the root face, starting with the head of the root edge, is equal to ω (see Figure 4.5). Moreover, we denote Z_ω the generating series of $\mathcal{T}_f^\omega$ defined by:

$$Z_\omega(\nu, t) = \sum_{(T,\sigma)\in\mathcal{T}_f^\omega} t^{|E(T)|}\nu^{m(T,\sigma)}.$$

Then, we obtain the following refinement of Theorem 4.1.1.

Theorem 4.2.1 (*Theorem 6 of [11]*)

For any $\omega \in \{\oplus, \ominus\}^+$ and for any $\nu > 0$, there exists $\kappa_\omega(\nu)$ such that, as $n \to \infty$,

$$[t^{3n-|\omega|}]Z_\omega(t) \sim \begin{cases} \kappa_\omega(\nu) \cdot t_\nu^{-3n}\, n^{-5/2} & \text{if } \nu \neq \nu_c, \\ \kappa_\omega(\nu_c) \cdot t_{\nu_c}^{-3n}\, n^{-7/3} & \text{if } \nu = \nu_c. \end{cases} \tag{4.4}$$

To prove this theorem, the first step is to write an equation *à la* Tutte (see Section 1.2) for Z_ω. From this equation, a proof by induction ensures that *it is enough to establish the result for $\omega = \oplus^k$, for any $k \geq 0$.*

Positive boundary condition and Tutte's invariant method We hence restrict our attention to $Z^+ := \sum_{k\geq 1} Z_{\oplus^k} x^k$. We again try and write a Tutte-like equation. However, a closed equation for Z^+ cannot be obtained directly. Indeed, when exploring the face on the left of the root edge, the newly explored vertex can have spin $\ominus$ as illustrated on Figure 4.6.

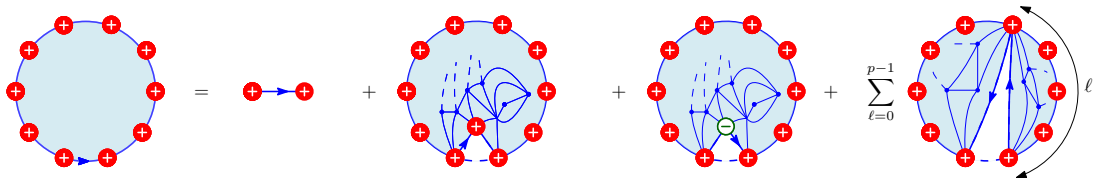

Figure 4.6. For Z^+, the deletion of the root edge does not give a closed equation.

To solve this issue, we also consider the generating series $Z^{+,-}(x, y)$ of triangulations with boundary conditions of the form $\oplus^p\ominus^q$ with $p, q \in \mathbb{Z}_{>0}$, the variable x being the variable for the number of $\oplus$ and the variable y being the variable for the number of $\ominus$. In other words,

$$Z^{+,-}(x, y) := \sum_{p,q\geq 1} \sum_{(T,\sigma)\in\mathcal{T}_f^{\oplus^p\ominus^q}} t^{|T|}\nu^{m(T,\sigma)}\, x^p y^q.$$

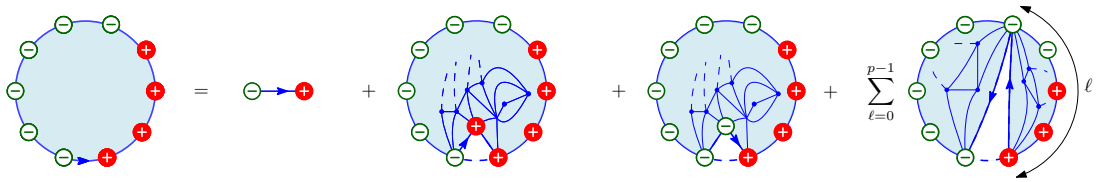

Figure 4.7. Tutte-like equations for $Z^{+,-}$, obtained after deletion of the root edge.

The generating series Z^+ and $Z^{+,-}$ are then solutions of a closed system of equations. We can indeed check that (up to a suitable choice of rooting convention) deleting the edge $\ominus\oplus$ of a triangulation enumerated by $Z^{+,-}$ can only produce triangulations with eithr the same type of boundary condition or with monochromatic boundary conditions (which are hence enumerated by Z^+), see Figure 4.7. But, the syste of equations we obtain has now two catalytic variables.

Fortunately, we can rely on Tutte's invariant method (introduced by Tutte, see for instance [Tut95], and generalized and popularized by Bernardi and Bousquet-Mélou [BBM11]) to eliminate one of these catalytic variables.

I spare the reader the presentation of this method, which is quite technical and refer to Section 2 of [11] for details. The important point is that, via this method, we obtain an algebraic equation for $Z^+(x)$, which only depends on $Z_\oplus$ and $Z_{\oplus^3}$. Thanks to explicit expressions for the latter series computed in [BBM11], we obtain the following *rationality scheme*:

Theorem 4.2.2 (*Theorem 23 of [BBM11] for $p = 1, 2, 3$, Proposition 12 of [11], for $p \geq 4$*)

Define $U \equiv U(\nu, t)$ as the unique power series in t^3 having constant term 0 and satisfying

$$t^3 = U\frac{\Big((1+\nu)U-2\Big)\Big(8\nu(\nu+1)^2U^3-(11\nu+13)(\nu+1)U^2+2(\nu+3)(2\nu+1)U-4\nu\Big)}{32\nu^3(1-2U)^2}. \tag{4.5}$$

Then, each series $Z_{\oplus^p}$ is a rational function of ν and U. More precisely there exist polynomials R_p^ν whose coefficients are rational in ν, such that, for all $p \geq 1$:

$$t^{3p} \cdot t^p Z_{\oplus^p} = \frac{R_p^\nu(U)}{(1-2U)^{3p}}.$$

From this theorem, the asymptotic behavior of coefficients of $t^p Z_{\oplus^p}$ follows quasi-automatically from the general approach of [FS09, Chap. VII.7], even if the parameter ν complicates the analysis. An important point which drastically simplifies the analysis is that U is a power series with *non-negative* coefficients. This was only claimed in [BBM11] and interestingly enough, our proof of this statement deeply relies on a *combinatorial interpretation* of U as the generating series of blossoming trees (as introduced in [BMS02]) and on the generic bijective framework described in Section 2.2.

4.2.2 Degree of the root vertex and tightness of $(\mathbb{P}_n^\nu)$

To prove that $(\mathbb{P}_n^\nu)$ is tight, we adapt the argument of [AS03]. Most of their arguments extend to triangulations with spins effortlessly. The only new needed result is stated in the following lemma.

Lemma 4.2.3 (*Lemma 15 of [11]*)

For $n \in \mathbb{N}$ and $\nu > 0$, write X_n^ν for the degree of the root vertex of a triangulation sampled from $\mathbb{P}_n^\nu$. Then, for any $\nu > 0$, the sequence of random variables (X_n^ν) is tight, i.e. for any $\epsilon > 0$, there exists $K > 0$ such that:

$$\mathbb{P}_n^\nu(X_n^\nu > K) < \epsilon \quad \text{for } n \text{ sufficiently large.}$$

The proof of this lemma relies on a double counting argument by considering rooted triangulations with a marked edge. We define $\overline{\mathbb{P}}_n^\nu$ as the law of a random triangulation sampled from $\mathbb{P}_n^\nu$ with a marked uniform edge. Denote ρ the root vertex and e the marked edge of a triangulation sampled according to $\overline{\mathbb{P}}_n^\nu$. We have:

$$\overline{\mathbb{P}}_n^\nu(\rho \in e) \geq \frac{1}{6n}\mathbb{E}_n^\nu[\deg(\rho)] = \frac{1}{6n}\mathbb{E}[X_n^\nu], \tag{4.6}$$

since an edge incident to the root vertex can contribute to its degree by at most 2 (exactly by 2 if it is a loop, and by 1 otherwise).

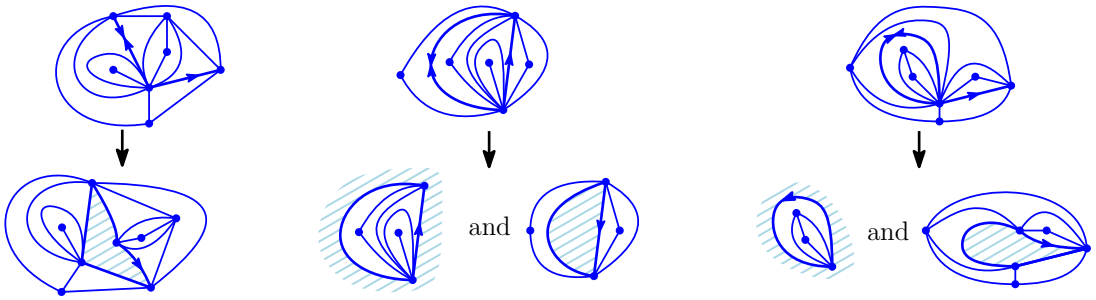

Figure 4.8. Some of the possibilities that may arise in the course of the proof of Lemma 4.2.3. The simple and double arrows represent respectively the root edge and the marked edge and the face outside of the boundary is dashed. Two possibilities can occur when neither the marked edge nor the root edge are loops (represented on the left and in the middle). The figure on the right illustrates one of the possibilities that can occur when the marked edge is a loop.

Now, by duplicating and opening the marked edge and the root edge (see Figure 4.8), we can see that there is an injection from the set of triangulations with a marked edge incident to the root vertex into the set of triangulations with a boundary (and no marked edge) and the set of pairs of triangulations with a boundary (and no marked edge). Thanks to the enumerative results obtained in Theorem 4.2.1, we easily obtain in this way an upper bound for $\overline{\mathbb{P}}_n^\nu(\rho \in e)$.

Together with (**4.6**), this yields an upper bound for $\mathbb{E}[X_n^\nu]$ independent of n. It concludes the proof of Lemma 4.2.3 by Markov's inequality. □

Before moving to the section about finite dimensional-distributions, let me mention that this proof is completely different from the original proof of the analogue result in [AS03]. For reasons that I will describe more precisely in Section 4.2.4, some difficulties appeared when considering triangulations with loops and with a spin configuration, that we were unfortunately unable to overcome[3].

But, our proof seems much more robust than the original one: indeed, in [AS03], as a by product of their proof they obtain exponential moments for the degree of the root vertex, which is much stronger that the requisite tightness. Our (much more elementary) proof gives only tightness and we are confident that it might be easily adapted to many other models of maps.

[3]However, we managed to apply the method of [AS03] to study random Ising-weighted Boltzmann triangulations for $\nu = \nu_c$. It allowed us to obtain exponential bounds on the degree of their root, which was instrumental in the proof of Theorem 4.1.3 (see Section 4.2.4).

4.2.3 Convergence of finite-dimensional distributions

To state the result of convergence of finite-dimensional distributions for random triangulations, I first need to introduce some additional terminology. A *triangulation with holes* is a rooted planar map such that all its faces are triangles, except possibly some marked faces. Moreover the boundary of those marked faces have to be simple cycles, which do not share edges. In particular, a triangulation of the p-gon is a triangulation with holes, whose only hole is its root face. The set of triangulations with holes is denoted $\mathcal{T}_h$.

For $T, T' \in \mathcal{T}_h$, we say that T is included in T' and write $T \subset T'$, if T' can be obtained from T by gluing in its holes some further triangulations with holes[4]. A nice property of triangulations with holes is their *rigidity*: two different ways of filling the holes of a given element of $\mathcal{T}_h$ will produce two different elements of $\mathcal{T}_h$, see also [AS03, Definition 4.7].

Recall the definition of balls given in Section 4.1.1 and illustrated in Figure 4.1. It follows from the definition that, for any fixed $R \in \mathbb{N}$ and any $T \in \mathcal{T}_f$, the ball $B_R(T)$ is a triangulation with holes. Hence, for any $\Delta \in \mathcal{T}_h$, if $B_R(T) = \Delta$, there exists a unique way to fill the holes of Δ to recover T.

From this observation, it is easy to write a formula for $\mathbb{P}_n^\nu(T : B_R(T) = \Delta)$ by summing over all the possible ways to fill the holes of Δ. For instance, assume that Δ is a triangulation endowed with a spin configuration and with only one hole such that there exist R and n for which $\mathbb{P}_n^\nu(B_R(T) = \Delta) \neq 0$. Write $\omega = \omega_1 \dots \omega_p$ for the sequence of spins around the unique hole of Δ, then:

$$\mathbb{P}_n^\nu(B_R(T) = \Delta) = \frac{\nu^{m(\Delta)-m(\omega)}[t^{3n-(|\Delta|-|\omega|)}]Z_\omega(\nu,t)}{[t^{3n}]Z(\nu,t)},$$

where $m(\omega) = |\{i \in \{1,\dots,p\}, \text{ such that } \omega_i = \omega_{i+1 (\mathrm{mod}\, p)}\}|$. Building up on this idea and following the same approach as in [AS03], we can prove the following proposition which concludes the proof of Theorem 4.1.2:

Proposition 4.2.4 (*Direct consequence of Proposition 21 of [11]*)

For every triangulation with holes Δ and any $R \in \mathbb{N}$, there exists $p_{\Delta,R} \in \mathbb{R}_+$ such that for any subsequential limit $\mathbb{P}^\nu$ of $(\mathbb{P}_n^\nu)_{n\geq 1}$, we have:

$$\mathbb{P}^\nu(T : B_R(T) = \Delta) = p_{\Delta,R}.$$

Additionally, $\mathbb{P}^\nu$ is supported on infinite one-ended triangulations.

4.2.4 Recurrence of the simple random walk

Thanks to a general result by Gurel-Gurevich and Nachmias [GGN13], the proof of Theorem 4.1.3 amounts to establishing the following result:

Proposition 4.2.5 (*Proposition 30 of [11]*)

Recall that $X_n^{\nu_c}$ is the degree of the root vertex of a triangulation sampled according to $\mathbb{P}_n^{\nu_c}$. Then, the distribution of $X_n^{\nu_c}$ has exponential tails; in other words, there exist two constants $c > 0$ and $\lambda \in (0,1)$, such that, for every n and every $k \geq 1$,

$$\mathbb{P}_n^{\nu_c}\left(X_n^{\nu_c} \geq k\right) \leq c\,\lambda^k.$$

Let me first mention that the proof of this result relies on the tightness result obtained in Lemma 4.2.3 and does not constitute an alternative proof of this lemma. Indeed, we first prove that the degree

[4] We assume that each hole has a distinguished marked oriented edge (selected in a deterministic but arbitrary way) such that there is a canonical way to glue a rooted triangulation in a hole by merging the root edge with the marked edge.

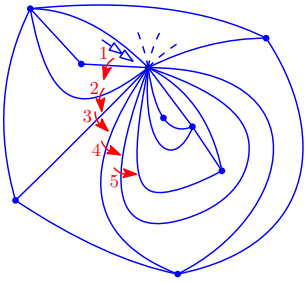

(a) The first steps of exploration,

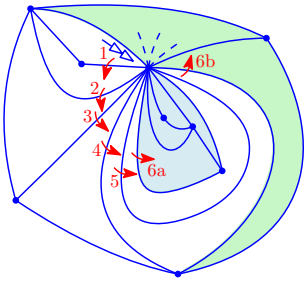

(b) when a loop is encountered, the exploration splits.

Figure 4.9. Successive exploration of the edges incident to the root are represented in (a). After a loop, the exploration splits to explore the two remaining faces colored in blue and green in (b).

of the root of a random *Boltzmann* Ising-weighted triangulation has exponential tails, and can then deduce Proposition 4.2.5 thanks to properties established for the limiting object defined in Theorem 4.1.2.

Roughly speaking, the proof is based on an iterative exploration of the faces incident to the root vertex, as depicted in Figure 4.9(a) and directly inspired from [AS03]. However, we have to deal with two additional difficulties. The first one is of course the presence of spins, which lead to many more possible boundary conditions. The second one is the presence of loops, which implies that the exploration process can split, see Figure 4.9(b). Such an issue already appeared in [CLG19, Proposition 30] (in which a result similar to Proposition 4.2.5 is obtained for Boltzmann triangulations without spins). We managed however to prove that the degree of the root vertex is stochastically dominated by a subcritical branching process[5] with 5 types, which gives the result. □

We strongly believe the result of Proposition 4.2.5 to be true for every value of $\nu \geq 0.3$[6]. Numerical computations suggest that the branching process we are considering is subcritical when ν lies between 0.3 and 2.07, but we were not able to give a generic proof of this result. For $\nu \geq 2.08$, the branching process becomes supercritical. However, by considering a domination by a branching process with more types, it would probably be possible to increase the range of ν for which such a process is subcritical.

4.3 Perspectives and ongoing works

Study of the clusters and scaling limit of the super-critical IIPT The clusters of a map endowed with a spin configuration are the connected components of the map obtained after deleting all the non-monochromatic edges (i.e. the frustrated edges). At the discrete level, the Ising model is closely related via cluster interfaces to the $O(n)$ model. The latter model has been studied on triangulations or bipartite Boltzmann maps via a gasket decomposition approach in a series of papers [BBG11, BBG12a, BBG12b, BBD16, Bud18, CCM17], revealing a remarkable connection with the stable maps of [LGM11]. In particular this approach allows to identify a dense phase, a dilute phase and a generic phase for the loop configurations.

Thanks to the new enumerative results obtained in [11], we may be able to study the clusters of the ν-IIPT, which would shed some additional light on the connection between cluster interfaces and stable maps.

Let me also mention that, in a recent work, Chen and Turunen [CT20] considered random triangulations with spins on their faces, at a critical parameter similar to our ν_c and with Dobrushin

[5] Indeed the spectral radius of its offspring matrix is approximately equal to 0.98985, phew!

[6] In particular, for $\nu = 1$, the result is known to be true by [CLG19] and the limit when ν tends to infinity corresponds also to uniform triangulations. For values of ν close to 0, this is however not clear anymore. The model becomes indeed degenerate, as it would correspond to "bipartite triangulations", which do not exist !

boundary conditions (i.e. with a boundary formed by two monochromatic arcs). They show that their model has a local limit in distribution when the two components of the Dobrushin boundary tend to infinity one after the other. They obtained some results about the interface between the two components. It would be interesting to see if we can export their results to obtain some information about the boundary of the cluster of the root in our model.

For $\nu > \nu_c$, we started to investigate the clusters and we have a reasonable sketch of proof that there exists almost surely an infinite monochromatic cluster in the IIPT. If this cluster is "dense enough", it would imply that the Gromov-Hausdorff distance between this cluster and the super-critical IIPT is small. Hence we could deduce the convergence of the latter by studying the giant cluster, which is a priori much simpler.

Bijective combinatorics for Eulerian maps with prescribed face degrees The study of the Ising model on random maps is strongly related to the enumeration of Eulerian maps (or dually of bipartite maps). On the one hand, when ν is equal to 0, the support of the probability distribution induced by the Ising model is the set of bipartite maps. On the other hand, the generating series of the Ising model and of Eulerian maps differ from one another by a simple change of variables. In particular, the bijections obtained in [BMS02] and [BDFG07] deal respectively with bipartite maps and Eulerian maps and exploit this connection to retrieve the value of ν_c, see for instance [BDFG07, Section 7] for more details on this connection.

Together with Jérémie Bouttier, we studied the combinatorics of Eulerian maps, via the approach of "slices" introduced in [BG12] (see also [Bou19] for a thorough reinterpretation of the "mobiles bijection" in terms of slices). We first obtained in [4] a combinatorial proof of the generating series of Eulerian triangulations with two marked vertices at a fixed distance (the so-called *2-point function*). Then, we generalized previous results obtained in [BG12] and proved that the 2-point function of planar constellations (a subfamily of Eulerian maps where all black faces have degree p and all white faces have degree multiple of p) can be expressed as a quotient of some Hankel determinants. In the case of Eulerian triangulations, we were able to compute these determinants by a bijective proof. For other models of constellations, some enumeration formulas were guessed by Di Francesco [DF05] and it is still an open problem to find bijective proofs of these formulas.

Secondly, and more recently, we investigated the remarkable rational parameterizations obtained by Eynard [Eyn11, Chapter 8] for the generating series of maps endowed with an Ising model. Using again the slice decomposition, we are able to interpret bijectively these formulas for Eulerian maps with monochromatic boundary conditions. This is still a work in progress, in particular we would like to extend those first results to the case of Dobrushin boundary conditions, for which very nice formulas are also available.

Bijections and the Ising model As mentioned in Section 4.1.2 and recalled just above, there exist some bijections between bipartite maps and decorated trees, both with blossoming trees [BMS02] and with mobiles [BDFG07]. We realized very recently that the rational parameterization obtained in a purely computational way in [BBM11] is in fact directly linked to the generating series of the blossoming trees introduced in [BMS02]. Together with the generic framework developed in [7], which can capture that bijection as a special case, it could be a source of inspiration to guess some rational parameterizations for Ising models on different families of maps.

Another perspective of research in this direction would be to obtain a bijection of the "mating of trees" type for the critical Ising model on some model of maps to be determined. Having such a bijection would be extremely nice, because it would allow us to apply techniques developed in [GHS20] to obtain some bounds about the volume growth of maps endowed with a critical Ising model. Various intuitions from theoretical physics suggest that, if such a bijection exists, it is natural to expect that it would be between the so-called *Gessel walks* (those are walks in the quadrant $\mathbb{N}^2$, starting and ending at the origin $(0,0)$ and taking their steps in $\{E, NE, W, SW\}$) and some families of maps, see [GHS20, Section 4]. Gessel's walks are known to be enumerated by a simple hypergeometric

function, see [KKZ09, BKR17, BM16], but it is even hard to guess what would be the right family of maps to consider.

I am particularly pleased to conclude this habilitation on this very nice open problem, which gives a convincing illustration – if further illustration were still necessary – of how theoretical physics, combinatorics and probability theory are inextricably related.

Bibliography

[AB13] J. Ambjørn and T. Budd. Trees and spatial topology change in causal dynamical triangulations. *J. Phys. A*, 46(31):315201, 2013.

[Abr16] C. Abraham. Rescaled bipartite planar maps converge to the Brownian map. *Ann. Inst.Henri Poincaré*, 52(2):575–595, 2016.

[ABW17] L. Addario-Berry and Y. Wen. Joint convergence of random quadrangulations and their cores. *Ann. Inst. Henri Poincaré Probab. Stat.*, 53(4):1890–1920, 2017.

[Alb08] M. Albenque. *Tresses, animaux, cartes : à l'interaction entre combinatoire et probabilités*. PhD thesis, Université Paris Diderot, 2008.

[Ald93] D. Aldous. The continuum random tree III. *Ann. Probab.*, 21(1):248–289, 1993.

[Ang03] O. Angel. Growth and percolation on the uniform infinite planar triangulation. *Geom. Funct. Anal.*, 13(5):935–974, 2003.

[Arq85] D. Arquès. Une relation fonctionnelle nouvelle sur les cartes planaires pointées. *J. Combin. Theory Ser. B*, 39(1):27–42, 1985.

[Arq87] D. Arquès. Relations fonctionnelles et dénombrement des cartes pointées sur le tore. *J. Combin. Theory Ser. B*, 43(3):253–274, 1987.

[AS03] O. Angel and O. Schramm. Uniform infinite planar triangulations. *Comm. Math. Phys.*, 241(2-3):191–213, 2003.

[BBD16] G. Borot, J. Bouttier, and B. Duplantier. Nesting statistics in the O(n) loop model on random planar maps. *arXiv preprint arXiv:1605.02239*, 2016.

[BBG11] G. Borot, J. Bouttier, and E. Guitter. A recursive approach to the O(n) model on random maps via nested loops. *J. Phys. A*, 45(4):045002, 2011.

[BBG12a] G. Borot, J. Bouttier, and E. Guitter. Loop models on random maps via nested loops: the case of domain symmetry breaking and application to the Potts model. *J. Phys. A*, 45(49):494017, 2012.

[BBG12b] G. Borot, J. Bouttier, and E. Guitter. More on the O(n) model on random maps via nested loops: loops with bending energy. *J. Phys. A*, 45(27):275206, 2012.

[BBM11] O. Bernardi and M. Bousquet-Mélou. Counting colored planar maps: algebraicity results. *J. Combin. Theory Ser. B*, 101(5):315–377, 2011.

[BBMDP17] N. Bonichon, M. Bousquet-Mélou, P. Dorbec, and C Pennarun. On the number of planar Eulerian orientations. *Electron. J. Combin.*, 65:59–91, 2017.

[BC86] E.A. Bender and E.R. Canfield. The asymptotic number of rooted maps on a surface. *J. Combin. Theory Ser. A*, 43(2):244–257, 1986.

[BC91] E.A. Bender and E.R. Canfield. The number of rooted maps on an orientable surface. *J. Combin. Theory Ser. B*, 53(2):293–299, 1991.

[BC11] O. Bernardi and G. Chapuy. A bijection for covered maps, or a shortcut between Harer-Zagier's and Jackson's formulas. *J. Comb. Theory, Ser. A*, 118(6):1718–1748, 2011.

[BCF14] O. Bernardi, G. Collet, and É. Fusy. On the distance-profile of random rooted plane graphs. In *AofA'2014*, pages 37–48, 2014.

[BCK18] J. Bertoin, N. Curien, and I. Kortchemski. Random planar maps and growth-fragmentations. *Ann. Probab.*, 46(1):207–260, 2018.

[BCM19] O. Bernardi, N. Curien, and G. Miermont. A Boltzmann approach to percolation on random triangulations. *Canad. J. Math.*, 71(1):1–43, 2019.

[BCR93] E. Bender, E. Canfield, and L. Richmond. The asymptotic number of rooted maps on a surface.: II. enumeration by vertices and faces. *J. Combin. Theory Ser. A*, 63(2):318–329, 1993.

[BDFG02a] J. Bouttier, Ph. Di Francesco, and E. Guitter. Census of planar maps: from the one--matrix model solution to a combinatorial proof. *Nuclear Phys. B*, 645(3):477–499, 2002.

[BDFG02b] J. Bouttier, Ph. Di Francesco, and E. Guitter. Counting colored random triangulations. *Nuclear Phys. B*, 641(3):519–532, 2002.

[BDFG04] J. Bouttier, Ph. Di Francesco, and E. Guitter. Planar maps as labeled mobiles. *Electron. J. Combin.*, 11(1):R69, 2004.

[BDFG07] J. Bouttier, Ph. Di Francesco, and E. Guitter. Blocked edges on Eulerian maps and mobiles: Application to spanning trees, hard particles and the Ising model. *J. Phys. A*, 40:7411–7440, 2007.

[Ber07] O. Bernardi. Bijective counting of tree-rooted maps and shuffles of parenthesis systems. *Electron. J. Combin.*, 14(1):9, 2007.

[Ber17] N. Berestycki. An elementary approach to Gaussian multiplicative chaos. *Electron. Commun. Probab.*, 22, 2017.

[Bet15a] J. Bettinelli. A bijection for nonorientable general maps. *arXiv preprint arXiv:1512.02208*, 2015.

[Bet15b] J. Bettinelli. Scaling limit of random planar quadrangulations with a boundary. *Ann. Inst. Henri Poincaré Probab. Stat.*, 51(2):432–477, 2015.

[BF12a] O. Bernardi and É. Fusy. A bijection for triangulations, quadrangulations, pentagulations, etc. *J. Combin. Theory Ser. A*, 119(1):218–244, 2012.

[BF12b] O. Bernardi and É. Fusy. Unified bijections for maps with prescribed degrees and girth. *J. Combin. Theory Ser. A*, 119(6):1351–1387, 2012.

[BFG14] J. Bouttier, É. Fusy, and E. Guitter. On the two-point function of general planar maps and hypermaps. *Ann. Inst.Henri Poincaré*, 1:265–306, 2014.

[BFSS01] C. Banderier, Ph. Flajolet, G. Schaeffer, and M. Soria. Random maps, coalescing saddles, singularity analysis, and Airy phenomena. *Random Structures Algorithms*, 19(3-4):194–246, 2001. Analysis of algorithms (Krynica Morska, 2000).

[BG10] J. Bouttier and E. Guitter. Distance statistics in quadrangulations with no multiple edges and the geometry of minbus. *J. Phys. A*, 43(20):205207, 2010.

[BG12] J. Bouttier and E. Guitter. Planar maps and continued fractions. *Comm. Math. Phys.*, 309(3):623–662, 2012.

[BHL19] V. Beffara, C. B. Huynh, and B. Lévêque. Scaling limits for random triangulations on the torus. *arXiv preprint arXiv:1905.01873*, 2019.

[Bil13] P. Billingsley. *Convergence of probability measures*. John Wiley and Sons, 2013.

[BJM14] J. Bettinelli, E. Jacob, and G. Miermont. The scaling limit of uniform random plane maps, via the Ambjørn–Budd bijection. *Electron. J. Probab.*, 19, 2014.

[BK87] D. Boulatov and V. Kazakov. The Ising model on a random planar lattice: the structure of the phase transition and the exact critical exponents. *Phys. Lett. B*, 186(3-4):379–384, 1987.

[BKR17] A. Bostan, I. Kurkova, and K. Raschel. A human proof of Gessel's lattice path conjecture. *Trans. Amer. Math. Soc.*, 369(2):1365–1393, 2017.

[BLG13] J. Beltran and J.-F. Le Gall. Quadrangulations with no pendant vertices. *Bernoulli*, 19(4):1150–1175, 2013.

[BLR17] N. Berestycki, B. Laslier, and G. Ray. Critical exponents on Fortuin-Kasteleyn weighted planar maps. *Comm. Math. Phys.*, 355(2):427–462, 2017.

[BM11] M. Bousquet-Mélou. Counting planar maps, coloured or uncoloured. *London Math. Soc. Lecture Note Ser.*, 392:1–50, 2011.

[BM16] M. Bousquet-Mélou. An elementary solution of Gessel's walks in the quadrant. *Adv. Math.*, 303:1171–1189, 2016.

[BM17] J. Bettinelli and G. Miermont. Compact Brownian surfaces I. Brownian disks. *Probab. Theory Related Fields*, 167:555–614, 2017.

[BMEP] M. Bousquet-Mélou and A. Elvey Price. The generating function of planar Eulerian orientations. *J. Combin. Theory Ser. A*.

[BMFR19] M. Bousquet-Mélou, É. Fusy, and K. Raschel. Plane bipolar orientations and quadrant walks. *arXiv preprint arXiv:1905.04256*, 2019.

[BMJ06] M. Bousquet-Mélou and A. Jehanne. Planar maps and algebraic series: a generalization of the quadratic method. *J. Combin. Theory Ser. B*, 96:623–672, 2006.

[BMS02] M. Bousquet-Mélou and G. Schaeffer. The degree distribution in bipartite planar maps: applications to the Ising model. *arXiv preprint math/0211070*, 2002.

[Bou19] J. Bouttier. *Carte planaires et partitions aléatoires*. Habilitation à diriger des recherches en mathématiques, Université Paris Sud, 2019.

[Bro64] W.G. Brown. Enumeration of triangulations of the disk. *Proc. Lond. Math. Soc.*, 3(4):746–768, 1964.

[BS01] I. Benjamini and O. Schramm. Recurrence of distributional limits of finite planar graphs. *Electron. J. Probab.*, 6:no. 23, 13 pp. (electronic), 2001.

[BS14] J. Björnberg and S. Stefánsson. Recurrence of bipartite planar maps. *Electron. J. Probab.*, 19, 2014.

[Buda] T. Budd. personal communication.

[Budb] T. Budd. Scaling constants and the lazy peeling of infinite Boltzmann planar maps. Slides of a talk given at the Newton Institute, Cambridge, available at https://hef.ru.nl/~tbudd/docs/cambridge-talk.pdf.

[Bud16] T. Budd. The peeling process of infinite Boltzmann planar maps. *Electron. J. Combin.*, 23(1):P1–28, 2016.

[Bud18] T. Budd. The peeling process on random planar maps coupled to an O(n) loop model (with an appendix by Linxiao Chen). *arXiv preprint arXiv:1809.02012*, 2018.

[CCM17] L. Chen, N. Curien, and P. Maillard. The perimeter cascade in critical Boltzmann quadrangulations decorated by an O(n) loop model. *arXiv preprint arXiv:1702.06916*, 2017.

[CD06] Ph. Chassaing and B. Durhuus. Local limit of labeled trees and expected volume growth in a random quadrangulation. *Ann. Probab.*, pages 879–917, 2006.

[CD17] G. Chapuy and M. Dołęga. A bijection for rooted maps on general surfaces. *J. Comb. Theory, Ser. A*, 145(3):252–307, J. 2017.

[CFGN09] G. Chapuy, É Fusy, O. Giménez, and M. Noy. On the diameter of random planar graphs. In *Discrete Math. Theor. Comput. Sci.*, pages 65–78, 2009.

[Cha09] G. Chapuy. Asymptotic enumeration of constellations and related families of maps on orientable surfaces. *Comb. Probab. Comput.*, 18(4):477–516, 2009.

[Cha18] G. Chapuy. *Rencontre autour de la combinatoire des cartes*. Habilitation à diriger des recherches en informatique, Université Paris Diderot, 2018.

[Che17] L. Chen. Basic properties of the infinite critical-FK random map. *Ann. Inst. Henri Poincaré D*, 4(3):245–271, 2017.

[CLG17] N. Curien and J.-F. Le Gall. Scaling limits for the peeling process on random maps. *Ann. Inst. Henri Poincaré Probab. Stat.*, 53(1):322–357, 2017.

[CLG19] N. Curien and J.-F. Le Gall. First-passage percolation and local modifications of distances in random triangulations. *Ann. Sci. Éc. Norm. Supér*, 52:31–701, 2019.

[CLM13] N. Curien, J.-F. Le Gall, and G. Miermont. The Brownian cactus I . Scaling limits of discrete cactuses. *Ann. Inst.Henri Poincaré*, 49(2):340–373, 2013.

[CMS09] G. Chapuy, M. Marcus, and G. Schaeffer. A bijection for rooted maps on orientable surfaces. *SIAM J. Discrete Math.*, 23(3):1587–1611, 2009.

[CS04] Ph. Chassaing and G. Schaeffer. Random planar lattices and Integrated SuperBrownian Excursion. *Probab. Theory Related Fields*, 128:161–212, 2004.

[CT20] L. Chen and J. Turunen. Critical Ising model on random triangulations of the disk: enumeration and local limits. *Comm. Math. Phys.*, 374(3):1577–1643, 2020.

[CV81] R. Cori and B. Vauquelin. Planar maps are well labeled trees. *Canad. J. Math.*, 33(5):1023–1042, 1981.

[DF05] Ph. Di Francesco. Geodesic distance in planar graphs: An integrable approach. *The RamanuJ. Journal*, 10(2):153–186, 2005.

[DG17] J. Ding and S. Goswami. First passage percolation on the exponential of two-dimensional branching random walk. *Electron. Commun. Probab.*, 22, 2017.

[DG20] J. Ding and E. Gwynne. The fractal dimension of Liouville quantum gravity: universality, monotonicity, and bounds. *Comm. Math. Phys.*, 374(3):1877–1934, 2020.

[DGL17] V. Despré, D. Gonçalves, and B. Lévêque. Encoding toroidal triangulations. *Discrete Comput. Geom.*, 57(3):507–544, 2017.

[DKRV16] F. David, A. Kupiainen, R. Rhodes, and V. Vargas. Liouville quantum gravity on the Riemann sphere. *Comm. Math. Phys.*, 342(3):869–907, 2016.

[DMS14] B. Duplantier, J. Miller, and S. Sheffield. Liouville quantum gravity as a mating of trees. *arXiv preprint arXiv:1409.7055*, 2014.

[DS11] B. Duplantier and S. Sheffield. Liouville quantum gravity and KPZ. *Invent. Math.*, 185:333–393, 2011.

[EPG18] A. Elvey Price and A. Guttmann. Counting planar Eulerian orientations. *European J. Combin.*, 71:73–98, 2018.

[Eyn11] B. Eynard. Counting surfaces. In *Prog. Math. Phys.*, volume 70. Springer, 2011.

[Fel04] S. Felsner. Lattice structures from planar graphs. *Electron. J. Combin.*, 11(1):15, 2004.

[FPS08] É. Fusy, D. Poulalhon, and G. Schaeffer. Dissections, orientations, and trees with applications to optimal mesh encoding and random sampling. *ACM Trans. Algorithms*, 4(2):19, 2008.

[FS09] Ph. Flajolet and R. Sedgewick. *Analytic combinatorics*. Cambridge University Press, Cambridge, 2009.

[Fus07] É. Fusy. *Combinatoire des cartes planaires et applications algorithmiques*. PhD thesis, École Polytechnique, 2007.

[Gar12] C. Garban. Quantum gravity and the KPZ formula. In *Séminaire Bourbaki*, volume 64, 2011-2012.

[GGN13] O. Gurel-Gurevich and A. Nachmias. Recurrence of planar graph limits. *Ann. Math.*, pages 761–781, 2013.

[GHS19] E. Gwynne, N. Holden, and X. Sun. Mating of trees for random planar maps and Liouville quantum gravity: a survey. *arXiv preprint arXiv:1910.04713*, 2019.

[GHS20] E. Gwynne, N. Holden, and X. Sun. A mating-of-trees approach to graph distances in random planar maps. *Probab. Theory Related Fields*, pages 1–60, 2020.

[GM17] E. Gwynne and J. Miller. Scaling limit of the uniform infinite half-plane quadrangulation in the Gromov-Hausdorff-Prokhorov-uniform topology. *Electron. J. Probab.*, 22:Paper No. 84, 47, 2017.

[HS19] N. Holden and X. Sun. Convergence of uniform triangulations under the Cardy embedding. *arXiv preprint arXiv:1905.13207*, 2019.

[JM05] S. Janson and J.-F. Marckert. Convergence of discrete snakes. *J. Theoret. Probab.*, 18(3):615–645, 2005.

[Kah85] J.-P. Kahane. Sur le chaos multiplicatif. *Ann. Sci. Math. Québec*, 9(2):105–150, 1985.

[Kaz86] V. Kazakov. Ising model on a dynamical planar random lattice: exact solution. *Phys. Lett. A*, 119(3):140–144, 1986.

[KKZ09] M. Kauers, C. Koutschan, and D. Zeilberger. Proof of Ira Gessel's lattice path conjecture. *Proc. Natl. Acad. Sci. USA*, 106(28):11502–11505, 2009.

[KMSW19] R. Kenyon, J. Miller, S. Sheffield, and D. Wilson. Bipolar orientations on planar maps and SLE(12). *Ann. Probab.*, 47(3):1240–1269, 2019.

[Kri05] M. Krikun. Local structure of random quadrangulations. *arXiv preprint math/0512304*, 2005.

[Leh19] T. Lehéricy. First-passage percolation in random planar maps and Tutte's bijection. *arXiv preprint arXiv:1906.10079*, 2019.

[Lep19] M. Lepoutre. Blossoming bijection for higher-genus maps. *J. Combin. Theory Ser. A*, 165:187–224, 2019.

[LG99] J.-F. Le Gall. *Spatial branching processes, random snakes and partial differential equations*. Springer Science & Business Media, 1999.

[LG05] J.-F. Le Gall. Random trees and applications. *Probability surveys*, 2:245–311, 2005.

[LG07] J.-F. Le Gall. The topological structure of scaling limits of large planar maps. *Invent. Math.*, 169(3):621–670, 2007.

[LG10] J.-F. Le Gall. Geodesics in large planar maps and in the Brownian map. *Acta Math.*, 205(2):287–360, 2010.

[LG13] J.-F. Le Gall. Uniqueness and universality of the Brownian map. *Ann. Probab.*, 41(4):2880–2960, 2013.

[LGM11] J.-F. Le Gall and G. Miermont. Scaling limits of random planar maps with large faces. *Ann. Probab.*, 39(1):1–69, 2011.

[LGP08] J.-F. Le Gall and F. Paulin. Scaling limits of bipartite planar maps are homeomorphic to the 2-sphere. *Geom. Funct. Anal.*, 18(3):893–918, 2008.

[LSW17] Y. Li, X. Sun, and S. Watson. Schnyder woods, SLE(16), and Liouville quantum gravity. *arXiv preprint arXiv:1705.03573*, 2017.

[LZ04] S.K. Lando and A.K. Zvonkin. *Graphs on surfaces and their applications. Appendix by Don B. Zagier.* Springer, 2004.

[Mar08] J.-F. Marckert. The lineage process in Galton–Watson trees and globally centered discrete snakes. *Ann. Appl. Probab.*, 18(1):209–244, 2008.

[Mar18a] C. Marzouk. On scaling limits of planar maps with stable face-degrees. *ALEA*, 15:1089–1122, 2018.

[Mar18b] C. Marzouk. Scaling limits of random bipartite planar maps with a prescribed degree sequence. *Random Structures Algorithms*, 53(3):448–503, 2018.

[Mie] G. Miermont. Aspects of random maps. Lecture notes of the 2014 Saint-Flour Probability Summer School. Preliminary draft.

[Mie06] G. Miermont. An invariance principle for random planar maps. *Discrete Math. Theor. Comput. Sci*, 2006.

[Mie08a] G. Miermont. Invariance principles for spatial multitype Galton-Watson trees. *Ann. Inst.Henri Poincaré*, 44(6):1128–1161, 2008.

[Mie08b] G. Miermont. On the sphericity of scaling limits of random planar quadrangulations. *Electron. Commun. Probab*, 13:248–257, 2008.

[Mie09] G. Miermont. Tessellations of random maps of arbitrary genus. *Ann. Sci. Éc. Norm. Supér.*, 42(5):725–781, 2009.

[Mie13] G. Miermont. The Brownian map is the scaling limit of uniform random plane quadrangulations. *Acta Math.*, 210:319 – 401, 2013.

[Mil] J. Miller. Liouville quantum gravity as a metric space and a scaling limit. Talk given at the ICM 2018, available at https://www.youtube.com/watch?v=kprG46AJ9xQ.

[MM06] J.-F. Marckert and A. Mokkadem. Limit of normalized quadrangulations: the Brownian map. *Ann. Probab.*, 34(6):2144–2202, 2006.

[MS15] J. Miller and S. Sheffield. Liouville quantum gravity and the Brownian map I: The QLE(8/3, 0) metric. *arXiv preprint arXiv:1507.00719*, 2015.

[MS16a] J. Miller and S. Sheffield. Liouville quantum gravity and the Brownian map II: geodesics and continuity of the embedding. *arXiv preprint arXiv:1605.03563*, 2016.

[MS16b] J. Miller and S. Sheffield. Liouville quantum gravity and the Brownian map III: the conformal structure is determined. *arXiv preprint arXiv:1608.05391*, 2016.

[MT01] B. Mohar and C. Thomassen. *Graphs on surfaces*, volume 2. Johns Hopkins University Press Baltimore, 2001.

[Pol81] A. M. Polyakov. Quantum geometry of bosonic strings. *Phys. Lett. B*, 103(3):207–210, 1981.

[Pro02] J. Propp. Lattice structure for orientations of graphs. *arXiv preprint math/0209005*, 2002.

[PS06] D. Poulalhon and G. Schaeffer. Optimal coding and sampling of triangulations. *Algorithmica*, 46(3):505–527, 2006.

[Sch89] W. Schnyder. Planar graphs and poset dimension. *Order*, 5:323–343, 1989.

[Sch97] G. Schaeffer. Bijective census and random generation of Eulerian planar maps with prescribed vertex degrees. *Electron. J. Combin.*, 4(1):20, 1997.

[Sch98] G. Schaeffer. *Conjugaison d'arbres et cartes combinatoires aléatoires*. PhD thesis, Université Bordeaux I, 1998.

[Sch11] O. Schramm. Conformally invariant scaling limits: an overview and a collection of problems. In *Selected Works of Oded Schramm*, pages 1161–1191. Springer, 2011.

[Sch15] G. Schaeffer. Planar maps. In M. Bóna, editor, *Handbook of Enumerative Combinatorics*, volume 87, chapter 5. CRC Press, 2015.

[She16a] S. Sheffield. Conformal weldings of random surfaces: SLE and the quantum gravity zipper. *Ann. Probab.*, 44(5):3474–3545, 2016.

[She16b] S. Sheffield. Quantum gravity and inventory accumulation. *Ann. Probab.*, 44(6):3804–3848, 2016.

[Sta11] R.P. Stanley. *Enumerative combinatorics*, volume 1. Cambridge Studies in Advanced Mathematics, 2011.

[Ste05] K. Stephenson. *Introduction to circle packing*. Cambridge Univ. Press, 2005.

[Ste18] R. Stephenson. Local convergence of large critical multi-type Galton–Watson trees and applications to random maps. *J. Theoret. Probab.*, 31(1):159–205, 2018.

[Tut62a] W.T. Tutte. A census of planar triangulations. *Canad. J. Math.*, 14:21–38, 1962.

[Tut62b] W.T. Tutte. A census of slicings. *Canad. J. Math.*, 14:708–722, 1962.

[Tut63] W.T. Tutte. A census of planar maps. *Canad. J. Math.*, 15:249–271, 1963.

[Tut95] W.T. Tutte. Chromatic sums revisited. *Aequationes Math.*, 50(1-2):95–134, 1995.

[Var17] V. Vargas. Lecture notes on Liouville theory and the DOZZ formula. *arXiv preprint arXiv:1712.00829*, 2017.

[Whi33] H. Whitney. 2-isomorphic graphs. *Amer. J. Math.*, 55(1):245–254, 1933.

[WL72a] T. Walsh and A. Lehman. Counting rooted maps by genus. I. *J. Combin. Theory Ser. B*, 13(3):192–218, 1972.

[WL72b] T. Walsh and A. Lehman. Counting rooted maps by genus II. *J. Combin. Theory Ser. B*, 13(2):122–141, 1972.